Australia's National Science Agency

Australian Government

National Water Grid®

Floodplain inundation mapping and modelling for the Victoria catchment

A technical report from the CSIRO Victoria River Water Resource Assessment for the National Water Grid

Fazlul Karim, Shaun Kim, Catherine Ticehurst, Justin Hughes, Steve Marvanek, Matt Gibbs, Ang Yang, Bill Wang, Cuan Petheram

ISBN 978-1-4863-2099-8 (print)

ISBN 978-1-4863-2100-1 (online)

Citation

Karim F, Kim S, Ticehurst C, Hughes J, Marvanek S, Gibbs M, Yang A, Wang B and Petheram C (2024) Floodplain inundation mapping and modelling for the Victoria catchment. A technical report from the CSIRO Victoria River Water Resource Assessment for the National Water Grid. CSIRO, Australia.

Copyright

Important disclaimer

CSIRO Victoria River Water Resource Assessment acknowledgements

This report was funded through the National Water Grid's Science Program, which sits within the Australian Government's Department of Climate Change, Energy, the Environment and Water.

Aspects of the Assessment have been undertaken in conjunction with the NT Government.

The Assessment was guided by two committees:

i. The Assessment's Governance Committee: CRC for Northern Australia/James Cook University; CSIRO; National Water Grid (Department of Climate Change, Energy, the Environment and Water); Northern Land Council; NT Department of Environment, Parks and Water Security; NT Department of Industry, Tourism and Trade; Office of Northern Australia; Queensland Department of Agriculture and Fisheries; Queensland Department of Regional Development, Manufacturing and Water

ii. The Assessment's joint Roper and Victoria River catchments Steering Committee: Amateur Fishermen's Association of the NT; Austrade; Centrefarm; CSIRO; National Water Grid (Department of Climate Change, Energy, the Environment and Water); Northern Land Council; NT Cattlemen's Association; NT Department of Environment, Parks and Water Security; NT Department of Industry, Tourism and Trade; NT Farmers; NT Seafood Council; Office of Northern Australia; Parks Australia; Regional Development Australia; Roper Gulf Regional Council Shire; Watertrust

Responsibility for the Assessment's content lies with CSIRO. The Assessment's committees did not have an opportunity to review the Assessment results or outputs prior to their release.

This report was reviewed by Dr Zaved Khan and Mr Mahdi Montazeri of CSIRO.

Acknowledgement of Country

CSIRO acknowledges the Traditional Owners of the lands, seas and waters of the area that we live and work on across Australia. We acknowledge their continuing connection to their culture and pay our respects to their elders past and present.

Photo

Jasper Gorge escarpment. Source: CSIRO

Director's foreword

Sustainable development and regional economic prosperity are priorities for the Australian and Northern Territory (NT) governments. However, more comprehensive information on land and water resources across northern Australia is required to complement local information held by Indigenous Peoples and other landholders.

Knowledge of the scale, nature, location and distribution of likely environmental, social, cultural and economic opportunities and the risks of any proposed developments is critical to sustainable development. Especially where resource use is contested, this knowledge informs the consultation and planning that underpin the resource security required to unlock investment, while at the same time protecting the environment and cultural values.

In 2021, the Australian Government commissioned CSIRO to complete the Victoria River Water Resource Assessment. In response, CSIRO accessed expertise and collaborations from across Australia to generate data and provide insight to support consideration of the use of land and water resources in the Victoria catchment. The Assessment focuses mainly on the potential for agricultural development, and the opportunities and constraints that development could experience. It also considers climate change impacts and a range of future development pathways without being prescriptive of what they might be. The detailed information provided on land and water resources, their potential uses and the consequences of those uses are carefully designed to be relevant to a wide range of regional-scale planning considerations by Indigenous Peoples, landholders, citizens, investors, local government, and the Australian and NT governments. By fostering shared understanding of the opportunities and the risks among this wide array of stakeholders and decision makers, better informed conversations about future options will be possible.

Importantly, the Assessment does not recommend one development over another, nor assume any particular development pathway, nor even assume that water resource development will occur. It provides a range of possibilities and the information required to interpret them (including risks that may attend any opportunities), consistent with regional values and aspirations.

All data and reports produced by the Assessment will be publicly available.

Chris Chilcott

Project Director

The Victoria River Water Resource Assessment Team

Project Director	Chris Chilcott
Project Leaders	Cuan Petheram, Ian Watson
Project Support	Caroline Bruce, Seonaid Philip
Communications	Emily Brown, Chanel Koeleman, Jo Ashley, Nathan Dyer

Activities

Agriculture and socio-economics	Tony Webster, Caroline Bruce, Kaylene Camuti[1], Matt Curnock, Jenny Hayward, Simon Irvin, Shokhrukh Jalilov, Diane Jarvis[1], Adam Liedloff, Stephen McFallan, Yvette Oliver, Di Prestwidge[2], Tiemen Rhebergen, Robert Speed[3], Chris Stokes, Thomas Vanderbyl[3], John Virtue[4]
Climate	David McJannet, Lynn Seo
Ecology	Danial Stratford, Rik Buckworth, Pascal Castellazzi, Bayley Costin, Roy Aijun Deng, Ruan Gannon, Steve Gao, Sophie Gilbey, Rob Kenyon, Shelly Lachish, Simon Linke, Heather McGinness, Linda Merrin, Katie Motson[5], Rocio Ponce Reyes, Nathan Waltham[5]
Groundwater hydrology	Andrew R. Taylor, Karen Barry, Russell Crosbie, Geoff Hodgson, Anthony Knapton[6], Shane Mule, Jodie Pritchard, Steven Tickell[7], Axel Suckow
Indigenous water values, rights, interests and development goals	Marcus Barber/Kirsty Wissing, Peta Braedon, Kristina Fisher, Petina Pert
Land suitability	Ian Watson, Jenet Austin, Bart Edmeades[7], Linda Gregory, Jason Hill[7], Seonaid Philip, Ross Searle, Uta Stockmann, Mark Thomas, Francis Wait[7], Peter L. Wilson, Peter R. Wilson, Peter Zund
Surface water hydrology	Justin Hughes, Matt Gibbs, Fazlul Karim, Steve Marvanek, Catherine Ticehurst, Biao Wang
Surface water storage	Cuan Petheram, Giulio Altamura[8], Fred Baynes[9], Kev Devlin[4], Nick Hombsch[8], Peter Hyde[8], Lee Rogers, Ang Yang

Note: Assessment team as at September, 2024. All contributors are affiliated with CSIRO unless indicated otherwise. Activity Leaders are underlined. For the Indigenous water values, rights, interests and development goals activity, Marcus Barber was Activity Leader for the project duration except August 2022 – July 2023 when Kirsty Wissing (a CSIRO employee at the time) undertook this role.

[1]James Cook University; [2]DBP Consulting; [3]Badu Advisory Pty Ltd; [4]Independent contractor; [5] Centre for Tropical Water and Aquatic Ecosystem Research. James Cook University; [6]CloudGMS; [7]NT Department of Environment, Parks and Water Security; [8]Rider Levett Bucknall; [9]Baynes Geologic

Shortened forms

SHORT FORM	FULL FORM
AEP	annual exceedance probability
AGDC	Australian Geoscience Data Cube
AHD	Australian Height Datum
AR6	Sixth Assessment Report
ASCII	American Standard Code for Information Interchange
AWRA-L	Australian Water Resources Assessment – Landscape model
AWRA-R	Australian Water Resources Assessment – River model
BRDF	Bidirectional Reflectance Distribution Function
CMIP	Coupled Model Intercomparison Project
CPU	central processing unit
DCFR	diversion commencement flow requirement
DEA	Digital Earth Australia
DEM	digital elevation model
DOI	digital object identifier
ERP	equivalent Riemann problem
ESA	European Space Agency
ETM	Enhanced Thematic Mapper
ETS	Equitable Threat Score
FABDEM	Forests And Buildings removed Copernicus DEM
FAR	False Alarm Ratio
FB	Frequency Bias
FFA	flood frequency analysis
GCM	global climate model
GCM-PS	global climate model – pattern scaling
GPU	graphics processing unit
HAND	Height Above Nearest Drainage
HDF	hierarchical data format
IDL	Interactive Data Language
IPCC	Intergovernmental Panel on Climate Change
LiDAR	Light Detection and Ranging
LP DAAC	Land Processes Distributed Active Archive Center
mAHD	elevation in metres relative to the AHD
MGA	Map Grid of Australia
MODIS	Moderate Resolution Imaging Spectroradiometer

SHORT FORM	FULL FORM
NBAR	Nadir BRDF-Adjusted Reflectance
NCI	National Computing Infrastructure
NDWI	Normalized Difference Water Index
OLI	Operational Land Imager
OWL	Open Water Likelihood
PE	potential evaporation
POD	Probability Of Detection
PS	pattern scaling
RCP	Representative Concentration Pathway
SAR	Synthetic Aperture Radar
SARA	Sentinel Australasia Regional Access
SILO	Scientific Information for Land Owners
SRTM	Shuttle Radar Topography Mission
SSP	Shared Socioeconomic Pathway
TM	Thematic Mapper
URBS	Unified River Basin Simulator
USGS	United States Geological Survey

Units

UNITS	DESCRIPTION
cm	centimetre
GL	gigalitre
km	kilometre
m	metre
ML/d	megalitres per day
GL/d	gigalitres per day
mm	millimetre
s	second

Preface

Sustainable development and regional economic prosperity are priorities for the Australian and NT governments and science can play its role. Acknowledging the need for continued research, the NT Government (2023) announced a Territory Water Plan priority action to accelerate the existing water science program 'to support best practice water resource management and sustainable development.'

Governments are actively seeking to diversify regional economies, considering a range of factors. For very remote areas like the Victoria catchment (Preface Figure 1-1), the land, water and other environmental resources or assets will be key in determining how sustainable regional development might occur. Primary questions in any consideration of sustainable regional development relate to the nature and the scale of opportunities, and their risks.

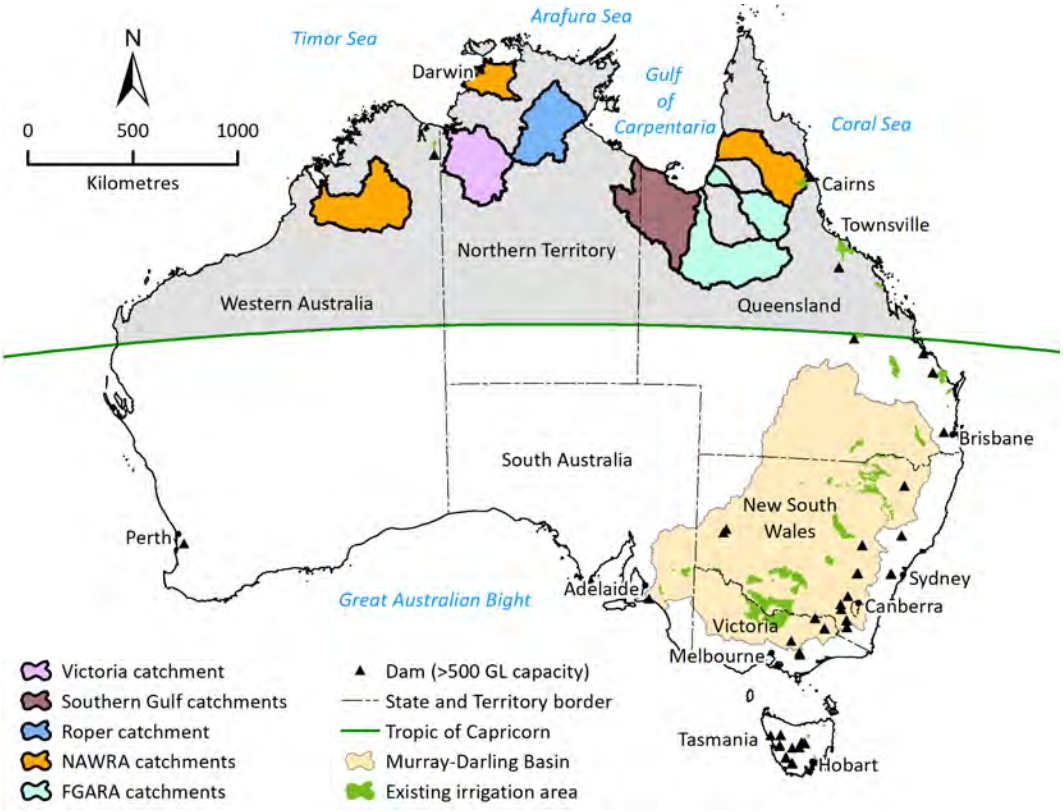

Preface Figure 1-1 Map of Australia showing Assessment area (Victoria catchment and other recent CSIRO Assessments

FGARA = Flinders and Gilbert Agricultural Resource Assessment; NAWRA = Northern Australia Water Resource Assessment.

How people perceive those risks is critical, especially in the context of areas such as the Victoria catchment, where approximately 75% of the population is Indigenous (compared to 3.2% for Australia as a whole) and where many Indigenous Peoples still live on the same lands they have inhabited for tens of thousands of years. About 31% of the Victoria catchment is owned by Indigenous Peoples as inalienable freehold.

Access to reliable information about resources enables informed discussion and good decision making. Such information includes the amount and type of a resource or asset, where it is found (including in relation to complementary resources), what commercial uses it might have, how the resource changes within a year and across years, the underlying socio-economic context and the possible impacts of development.

Most of northern Australia's land and water resources have not been mapped in sufficient detail to provide the level of information required for reliable resource allocation, to mitigate investment or environmental risks, or to build policy settings that can support good judgments. The Victoria River Water Resource Assessment aims to partly address this gap by providing data to better inform decisions on private investment and government expenditure, to account for intersections between existing and potential resource users, and to ensure that net development benefits are maximised.

The Assessment differs somewhat from many resource assessments in that it considers a wide range of resources or assets, rather than being a single mapping exercise of, say, soils. It provides a lot of contextual information about the socio-economic profile of the catchment, and the economic possibilities and environmental impacts of development. Further, it considers many of the different resource and asset types in an integrated way, rather than separately. The Assessment has agricultural developments as its primary focus, but it also considers opportunities for and intersections between other types of water-dependent development.

The Assessment was designed to inform consideration of development, not to enable any particular development to occur. The outcome of no change in land use or water resource development is also valid. As such, the Assessment informs – but does not seek to replace – existing planning, regulatory or approval processes. Importantly, the Assessment does not assume a given policy or regulatory environment. Policy and regulations can change, so this flexibility enables the results to be applied to the widest range of uses for the longest possible time frame.

It was not the intention of – and nor was it possible for – the Assessment to generate new information on all topics related to water and irrigation development in northern Australia. Topics not directly examined in the Assessment are discussed with reference to and in the context of the existing literature.

CSIRO has strong organisational commitments to reconciliation with Australia's Indigenous Peoples and to conducting ethical research with the free, prior and informed consent of human participants. The Assessment consulted with Indigenous representative organisations and Traditional Owner groups from the catchment to aid their understanding and potential engagement with its fieldwork requirements. The Assessment conducted significant fieldwork in the catchment, including with Traditional Owners through the activity focused on Indigenous values, rights, interests and development goals. CSIRO created new scientific knowledge about the catchment through direct fieldwork, by synthesising new material from existing information, and by remotely sensed data and numerical modelling.

Functionally, the Assessment adopted an activities-based approach (reflected in the content and structure of the outputs and products), comprising activity groups, each contributing its part to create a cohesive picture of regional development opportunities, costs and benefits, but also risks. Preface Figure 1-2 illustrates the high-level links between the activities and the general flow of information in the Assessment.

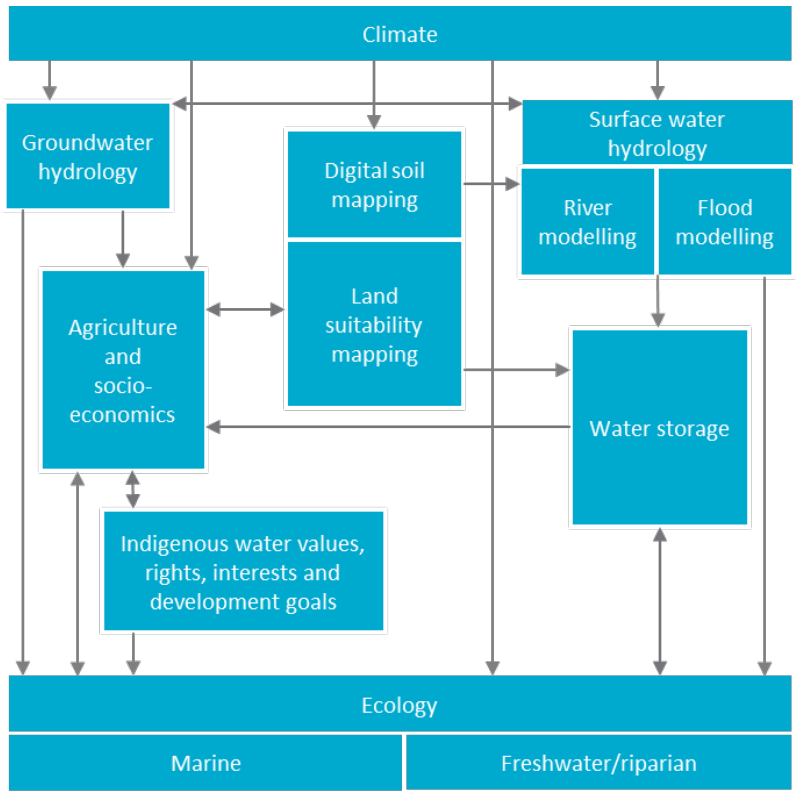

Preface Figure 1-2 Schematic of the high-level linkages between the eight activity groups and the general flow of information in the Assessment

Assessment reporting structure

Development opportunities and their impacts are frequently highly interdependent and, consequently, so is the research undertaken through this Assessment. While each report may be read as a stand-alone document, the suite of reports for each Assessment most reliably informs discussion and decisions concerning regional development when read as a whole.

The Assessment has produced a series of cascading reports and information products:

- Technical reports present scientific work with sufficient detail for technical and scientific experts to reproduce the work. Each of the activities (Preface Figure 1-2) has one or more corresponding technical reports.
- A catchment report, which synthesises key material from the technical reports, providing well-informed (but not necessarily scientifically trained) users with the information required to inform decisions about the opportunities, costs and benefits, but also risks associated with irrigated agriculture and other development options.
- A summary report provides a shorter summary and narrative for a general public audience in plain English.
- A summary fact sheet provides key findings for a general public audience in the shortest possible format.

The Assessment has also developed online information products to enable users to better access information that is not readily available in print format. All of these reports, information tools and data products are available online at https://www.csiro.au/victoriariver. The webpages give users access to a communications suite including fact sheets, multimedia content, FAQs, reports and links to related sites, particularly about other research in northern Australia.

Executive summary

This report focuses on flooding characteristics of the catchment of the Victoria River in the NT. The impact of flooding on agricultural production can be significant, potentially leading to the loss of livestock, fodder, and topsoil, and damage to crops and infrastructure. However, flooding is generally favourable to floodplain wetlands and coastal ecosystems. For example, flood pulses create opportunities for offstream wetlands to connect with the main river channels, allowing the exchange of water, sediments, organic matter and biota.

This report provides an overview of inundation duration and depth across the floodplains of the major rivers in the Victoria catchment. It also details the hydrodynamic modelling tools utilised to assess flood inundation. This includes information on data acquisition, model configuration, and the evaluation process, and a comparison of the model results with satellite-based flood inundation maps and water levels at gauging sites.

Hydrodynamic models offer several advantages over satellite-based approaches and conceptual node-link river system models when it comes to evaluating flood inundation. Hydrodynamic models enable the assessment of not only the extent of inundation but also water depth and velocity, with the ability to analyse these factors at very fine time intervals, often in the order of seconds. Furthermore, satellite-based approaches primarily focus on analysing historical flood events, whereas hydrodynamic models can be used to assess how flood characteristics might change under future climate and development scenarios.

The outputs derived from the hydrodynamic modelling play a crucial role, including:

- identifying areas prone to flooding under historical climates and the current level of development, commonly known as the baseline scenario
- estimating changes in inundation area under projected future climate and hypothetical development scenarios
- estimating changes in inundation depth and duration across the floodplain under future climate and development scenarios.

Hydrodynamic model configuration and calibration

In the Assessment, a two-dimensional flexible-mesh hydrodynamic model, MIKE 21 Flow Model FM, was used to simulate floodplain hydraulics (e.g. depth, velocity) and inundation dynamics across the floodplains of the Angalarri, Baines and Victoria rivers.

The boundary conditions were derived from the daily discharge from a calibrated river system model called the Australian Water Resources Assessment – River model (AWRA-R), the hourly tide gauge information, and Sacramento rainfall-runoff model simulations. Flood inundation maps for individual flood events from 2000 to 2023 were created using Moderate Resolution Imaging Spectroradiometer (MODIS), Sentinel and Landsat imagery. These maps were used to calibrate the hydrodynamic model. The hydrodynamic model was configured for the middle and downstream reaches of the Victoria River and its two major tributaries, the West Baines and Angalarri rivers.

The model domain includes areas downstream of Amanbidji in the West Baines River and downstream of Dashwood Crossing in the Victoria River and encompasses an area of 16,730 km^2.

High-resolution Light Detection and Ranging (LiDAR) data (5 m) was acquired for most of the floodplains along the West Baines and Angalarri rivers and the downstream reaches of the Victoria River as part of the Assessment. For the remainder of the model domain, where floods are less frequent, a 30 m Forest And Buildings removed Copernicus digital elevation model (FABDEM) was used for land topography. The highest resolution publicly available topographic data covering the entire Victoria catchment includes 1-second (i.e. approximately 30 m) SRTM (Shuttle Radar Topography Mission) digital elevation model (DEM) and 1-second FABDEM. These two global DEMs were compared, with the FABDEM being chosen due to its superior vertical accuracy in the Assessment area. The final combined DEM was created by resampling the FABDEM to 5 m, to match the original LiDAR resolution. The area covered by LiDAR is 6956 km^2, which is approximately 41.6% of the hydrodynamic model domain.

The hydrodynamic model was calibrated for the 2001 (annual exceedance probability (AEP) of 1 in 2), 2014 (AEP of 1 in 5), 2016 (AEP of 1 in 10), 2021 (AEP of 1 in 3) and 2023 (AEP of 1 in 18) flood events. The model was calibrated primarily by adjusting the roughness coefficient and the infiltration rate. While a good match was attained for the flood peaks, there were differences in the rising and falling limbs of the flood hydrograph. The model demonstrated reasonable simulation of spatial inundation patterns when compared with the Landsat, MODIS and Sentinel water maps. Overall, the model performed better for large floods, followed by medium-sized events, and then small events. There are some limitations to the model, and a lack of good-quality satellite imagery restricts rigorous calibration of the model results. Moreover, there are uncertainties in the river model simulations that were used to specify the inflow boundaries of the hydrodynamic model.

The calibrated hydrodynamic models were utilised to investigate flood characteristics under future climate and development scenarios. Due to the extensive computation time required, a limited number of simulations were conducted to explore the impact of future climate and hypothetical developments.

Flood characteristics

Intense seasonal rain from monsoonal bursts and tropical cyclones from December to March create flooding in parts of the Victoria catchment and inundate large areas of the floodplains on each side of the Victoria River and its two major tributaries, the Baines and Angalarri rivers. This is an unregulated catchment, and its overbank flow is generally governed by the topography of the floodplain. Flooding is widespread at the junction of the Victoria and Baines rivers, downstream of Timber Creek. In the last 70 years (1953 to 2023), there have been 80 floods ranging from small to large in the catchment. While floods can occur in any month from November to April, the majority of the past floods have occurred during the wet-season months of January, February and March.

Additional observations of flooding under the historical climate are as follows:

- Flood peaks typically take approximately 2 to 3 days to travel from Dashwood Crossing to Timber Creek, with a mean speed of 3.4 km/hour.

- For flood events with an AEP of 1 in 2, 1 in 5 and 1 in 10, the peak discharge at Coolibah Homestead on the Victoria River is 1850, 3210 and 5120 m^3/s, respectively (i.e. 159.8, 277.3 and 442.4 GL/day, respectively).
- Between 1953 and 2023 (70 years), events with all discharge greater than or equal to an AEP of 1 in 1 occurred during all months from November to April, with approximately 87% of historical floods occurring between January and March.
- Of the ten flood events that had the largest peak discharge at Coolibah on the Victoria River, six events occurred during March, three in February and one in December.
- The maximum areas inundated for events with an AEP of 1 in 2, 1 in 3, 1 in 5, 1 in 10 and 1 in 18 were 225, 322, 1191, 1297 and 1562 km^2, respectively.

Scenario analysis

A limited number of simulations were conducted to investigate the effects of future climate and development on inundation duration and depth. Three dam sites with a total capacity of 1367 GL and six water harvesting sites with a total annual maximum withdrawal of 680 GL were implemented in the model for impact assessment.

The model results revealed that the impacts of future projected wet (Scenario Cwet) and dry (Scenario Cdry) climates on floodplain inundation are more pronounced than the modelled impacts of water resource development. The increase in floodplain inundation under Cwet was larger than the decrease under Cdry, which is consistent with the changes in modelled streamflow under Cdry and Cwet scenarios.

The inclusion of three hypothetical dams resulted in a 7.4% decrease in the inundated area downstream for an event with an AEP of 1 in 3, and a 10% decrease for an event with an AEP of 1 in 18. The larger relative impact found for the event that occurred in 2023 (AEP of 1 in 18) is due to the different antecedent conditions at the beginning of each event, and the fact that the two events differed in the intensity and duration.

Water harvesting (680 GL annual irrigation target) resulted in a 6.4% decrease in inundation area and very minor changes to inundation duration for an event with an AEP of 1 in 3. For the event with an AEP of 1 in 18, the decrease in inundation area was only 2.4% and change in inundation duration was minimal. As expected, the impact was larger for the smaller flood event because the same amount of water were extracted for both flood events.

Hydrodynamic models are computationally demanding and therefore only a limited number of events can be analysed. In addition, the characteristics and timing (particularly antecedent effects) of chosen events can influence the apparent response to various scenarios. To counter this, a flood area emulator was derived using river model daily flows that could predict flooded area across the entire 133-year time series. Using the emulator, the annual maximum flooded area was calculated for various scenarios. The mean annual maximum flooded area across 133 years of simulation was 413 km^2 under Scenario A (Baseline). This was reduced to 302 km^2 under the three instream dams scenario, while the water harvesting scenario with an irrigation target of 680 GL was associated with a very small reduction in the annual maximum flooded area, to 408 km^2.

Contents

Figures

Tables

1 Introduction

Floods are the most frequent, and often most damaging, type of natural disaster, resulting in loss of life and damages to property and critical infrastructure (Kron, 2015; Wang and Gao, 2022; Yu et al., 2022). The changes in climate and land use (including rapid urbanisation) that have occurred in recent times have caused flood events to become even more frequent and disastrous (Arnell and Gosling, 2016; Dottori et al., 2018; Tabari, 2020). In Australia, floods are one of the costliest types of natural disasters (Rice et al., 2022; Ulubasoglu et al., 2019).

While floods are generally perceived as natural disasters, they can provide many environmental and ecological benefits (Opperman et al., 2009; Tockner et al., 2008). Floodplain inundation contributes to species diversity and relative abundance, aquatic biota growth (Phelps et al., 2015), groundwater recharge (Doble et al., 2012) and soil fertility (Ogden and Thoms, 2002). During floods, there is an exchange of water, sediments, chemicals, organic matter, and biota between the main river channels and their floodplains (Bunn et al., 2006; Thoms, 2003; Tockner et al., 2010). Since the Flood Pulse Concept first appeared in the scientific literature (Junk et al., 1989), the importance of floodplain inundation for these exchanges and for the productivity of diverse aquatic biota in river–floodplain systems has been emphasised in many studies (Bayley, 1991; Gallardo et al., 2009; Heiler et al., 1995; Middleton, 2002). However, our knowledge of the frequency and duration of floodplain inundation and the associated connectivity between water bodies and the ecological functioning of many of the world's largest floodplain systems is very limited. To date, the published knowledge is insufficient to adequately inform water management for biodiversity protection or adaptation to future climates (Arthington et al., 2015; Beighley et al., 2009).

Despite centuries of human activities that have altered river floodplains worldwide, remnant permanent water bodies still exist on the floodplains, but they are diminishing at increasing rates (Bayley, 1995; Tockner et al., 2008). An important requirement for the management of floodplain water bodies, including the management of wetlands of historical, cultural, economic and other biodiversity values, is knowledge of the extent, frequency and duration of floodplain inundation and of the hydrological connectivity between them. This is essential in deriving strategies for maintaining, or even enhancing to an optimal level, the biophysical exchanges between rivers and floodplains. The catchment of the Victoria River Assessment area has large floodplains in its middle and lower reaches, and they support a larger number of offstream wetlands with high ecological, cultural and biodiversity values. Therefore, it is important to quantify the inundation dynamics (in terms of extent, frequency and duration) and the hydrological connectivity between the offstream wetlands and the main channel (or several channels) under the historical climate, and to assess how the inundation and connectivity could be affected under future climate and development.

However, the quantification of floodplain inundation dynamics and hydrological connectivity between water bodies remains a great challenge. A number of studies have used a combination of remotely sensed inundated area and concurrent river flow data to predict the impact of river flow on flooded area (e.g. Frazier and Page, 2009; Overton, 2005; Peake et al., 2011; Townsend and

Walsh, 1998). The same approach has also been used to quantify how river flow affects the number of inundated wetlands (e.g. Frazier et al., 2003; Shaikh et al., 2001). However, this approach is not dynamic. It cannot produce a continuous time series of predicted inundation extent, and it cannot predict the duration of wetland connectivity. Inundation extent and the duration of wetland connectivity can have an important influence on wetland ecology. With the development of computational methods and computer technology, hydrodynamic modelling has become popular for the study of floodplain hydraulics and for quantifying the time course of flood inundation with high spatial and temporal resolution (Nicholas and Mitchell, 2003; Schumann et al., 2009). By combining these modelling techniques with high-resolution topography data, the duration, frequency and timing of wetland connectivity can be quantified (Karim et al., 2012, 2015). Previous studies have used a combination of hydrological and hydrodynamic models using simplified one-dimensional (e.g. Beighley et al., 2009; Chormanski et al., 2009) to more complex two-dimensional (Tuteja and Shaikh, 2009) modelling. In this Assessment, a two-dimensional flexible-mesh hydrodynamic module (MIKE 21 Flow Model FM, hereafter referred to as MIKE 21 FM) has been used with advanced model configuring and a flexible-mesh modelling tool to simulate floodplain inundation.

1.1 Objectives

The Victoria River Water Resource Assessment flood modelling activity seeks to answer the following questions:

- What areas on the floodplains are susceptible to flooding under the historical climate scenario?
- What would the extent, duration and frequency of floodplain inundation be under the historical climate scenario?
- What changes could be expected in inundation dynamics under the future climate and development scenarios?
- What changes could be expected in hydrological connectivity between floodplain water bodies due to flow regime change under the future climate and development scenarios?

This report describes the configuration and calibration of the MIKE 21 FM and scenario modelling for the future climate and water infrastructure development scenarios.

1.2 Previous flood studies in the Victoria catchment

Past flood modelling for the Victoria catchment has been very limited. A flood study for the Victoria River near Coolibah was undertaken by the Department of Lands, Planning and the Environment of the NT Government to assess flood immunity levels and to obtain the hydraulic information required to design a bridge on the Victoria River for the Department of Defence (Paiva, 1997). That study employed the Hydrologic Engineering Center River Analysis System (HEC-RAS) model, which is a one-dimensional hydraulic model (US Army Corps of Engineers, 2016).

1.3 Overview of flood modelling frameworks used in the Assessment

Hydrodynamic models are considered to be very useful tools for detailed flood inundation modelling, and they have been utilised for several decades (Bulti and Abebe, 2020; Liu et al., 2015; Teng et al., 2017). Based on the complexity of the river–floodplain network and the availability of input data for model configuration, one can select one-dimensional, two-dimensional or coupled one- and two-dimensional models (Horritt and Bates, 2002; Teng et al., 2017). However, it is extremely difficult to represent complex floodplain features using one-dimensional models because of the one-directional representation of the river–floodplain system. Two-dimensional models avoid much of the conceptualisation required to build an accurate one-dimensional model by using gridded topography data (Pinos and Timbe, 2019). Nonetheless, the application of traditional fixed-grid two-dimensional models is not always sufficient to reproduce river conveyance. This is because model grids are not aligned with the riverbanks, and in many cases the lowest points in the river are not adequately represented in the model (Bomers et al., 2019; Teng et al., 2017). More recently, flexible-mesh (also called irregular grid) models have been found to be superior to regular-grid models in terms of accuracy and computational time (Kim et al., 2014; Mackay et al., 2015; Pinos and Timbe, 2019). The use of a flexible-mesh model can overcome many of the limitations of regular-grid models, as they allow complex floodway geometries to be modelled with precision. They do not require the remainder of the floodplain to be modelled at the same spatial resolution, since they allow the computational mesh to be aligned and refined to suit the geometry of the floodplain (Mackay et al., 2015; Symonds et al., 2016).

The hydrodynamic models need to be calibrated against historical streamflow and inundation data before they can be applied with a degree of confidence. Traditionally, flood models are calibrated by comparing instream water heights (commonly gauge records) with floodplain inundation (commonly water marks on trees, buildings and electric poles). However, for relatively remote and sparsely populated catchments, it is often not possible to collect the field data that are necessary to robustly calibrate the model. This serves as a major constraint in the use of hydrodynamic models in remote and data-sparse areas. In recent years, there have been major advances in flood inundation mapping using satellite and airborne remote sensing. While the satellite imagery–based approaches have some limitations, including spatial and temporal resolutions, these techniques provide very useful data for hydrodynamic model calibration. In the Assessment, a combination of field-based observed stage heights and satellite-based inundation maps were used to calibrate the hydrodynamic model. Figure 1-1 shows the general steps in configuring and calibrating the two-dimensional hydrodynamic model (MIKE 21 FM) and scenario modelling for the future climate and dam impact assessment.

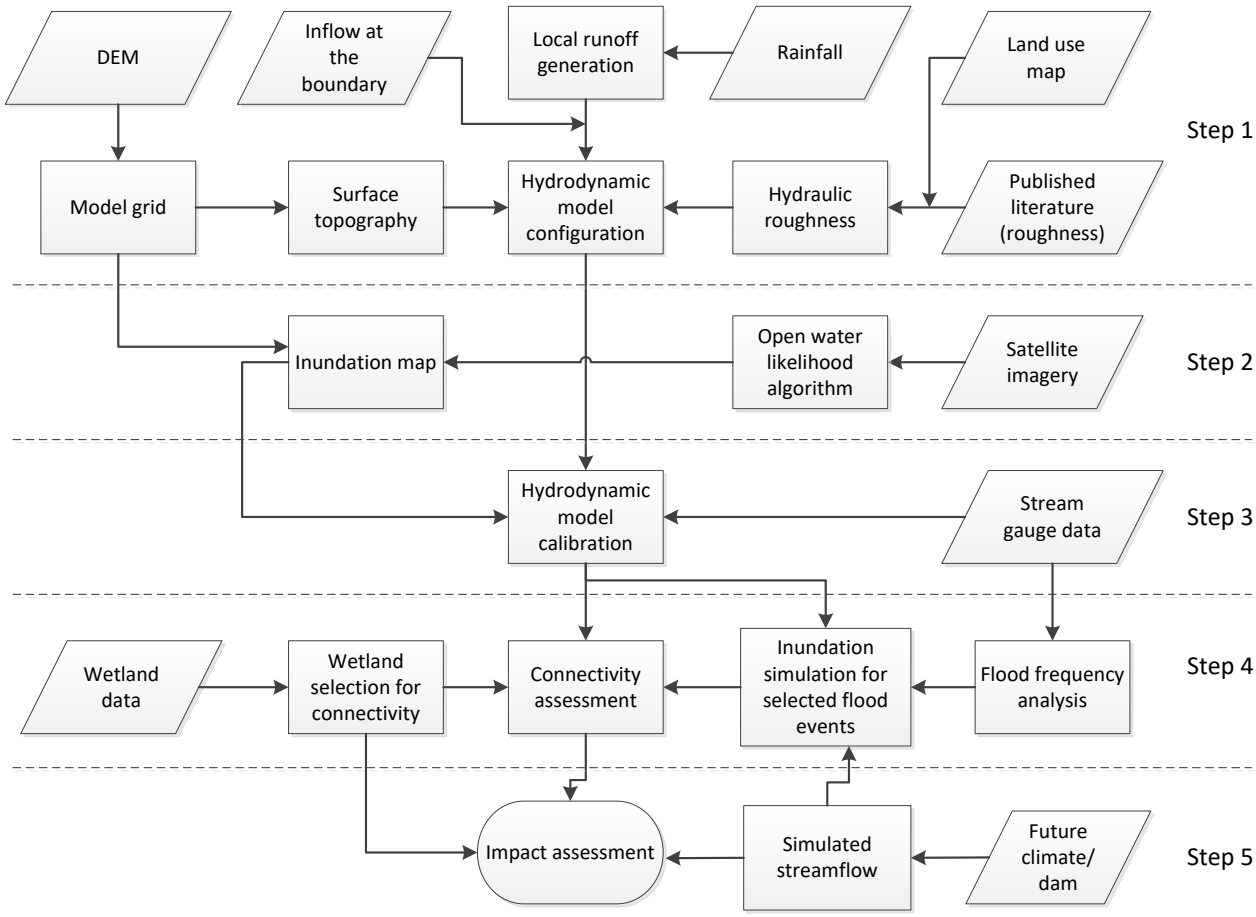

Figure 1-1 Flowchart illustrating the method used to calibrate a hydrodynamic model (MIKE 21 FM) and scenario modelling for future climate and dam impact assessment

DEM = digital elevation model.

1.4 Report overview and structure

This report has been prepared to:

- document the methods that were used to calibrate the MIKE FLOOD hydrodynamic models for the Assessment area
- report on the assessment of hydrodynamic model performance relative to satellite-based flood inundation mapping
- report on potential flood inundation extent under the historical climate and current level of development scenario
- report on potential changes to flood inundation and wetland connectivity under future climate and development scenarios.

This report is structured as follows. Chapter 2 describes the inundation mapping approach using satellite data and provides a summary of long-term inundation extent for the Assessment area. Chapter 3 describes the hydrodynamic modelling approach, including the rationale for the selection of the MIKE 21 FM model, its input/output data requirements and the model calibration algorithm. Chapter 4 describes the hydrodynamic model configuration and the calibration of hydrodynamic model parameters for the Victoria catchment. Chapter 5 provides the results and

discussion on the impacts of future climate and infrastructure scenarios on floodplain inundation. Chapter 6 summarises the key findings of the Assessment.

1.5 Key terminology and concepts

1.5.1 WATER YEAR AND WET AND DRY SEASONS

Northern Australia has a highly seasonal climate, with most rain falling from December to March. Unless otherwise specified, the Assessment defines the wet season as the 6-month period from 1 November to 30 April, and the dry season as the 6-month period from 1 May to 31 October.

All results in the Assessment are reported over the water year, defined as the period 1 September to 31 August, unless otherwise specified. This allows each individual wet season to be counted in a single 12-month period, rather than being split over two calendar years (i.e. counted as two separate seasons). This is more realistic for reporting climate statistics from a hydrological and agricultural assessment viewpoint.

1.5.2 SCENARIO DEFINITIONS

The Assessment considered four scenarios, reflecting combinations of different levels of development and historical and future climates, much like those used in the Northern Australia Sustainable Yields projects (CSIRO, 2009a, 2009b, 2009c), the Flinders and Gilbert Agricultural Resource Assessment (Petheram et al., 2013a, 2013b) and the Northern Australia Water Resource Assessments (Petheram et al., 2018a, 2018b, 2018c):

Scenario A – historical climate and current development

Scenario B – historical climate and future development

Scenario C – future climate and current development

Scenario D – future climate and future development.

SCENARIO A

Scenario A is a historical climate scenario. The historical climate series is defined as the observed climate (rainfall, temperature and potential evaporation for the water years from 1 September 1890 to 31 August 2022). All baseline results presented in this report has been calculated from data for this period unless specified otherwise. Justification for use of this period is provided in the companion technical report on climate (McJannet et al., 2023).

Scenario A is assumed to have no surface water or groundwater development. Scenario A was used as the baseline against which assessments of relative change were made. Scenario A could be assumed to yield the most conservative results. Historical tidal data were used to specify downstream boundary conditions for the flood modelling.

SCENARIO B

Scenario B is a historical climate and future development scenario. Scenario B used the same historical climate series as Scenario A. However, river inflow, groundwater recharge and flow, and agricultural productivity were modified to reflect potential future development. Potential development options were devised to assess the responses of the hydrological, ecological and

economic systems. Modifications ranged from small incremental increases in surface water and groundwater extraction through to extraction volumes representative of the likely physical limits of the Victoria catchment (i.e. considering the co-location of agriculture-suitable soil and water).

SCENARIO C

Scenario C is a future climate scenario with current levels of surface water and ground development, assessed at approximately the year 2060. Future climate impacts on water resources were explored within a sensitivity analysis framework by applying percentage changes in rainfall and potential evaporation (PE) to modify the 133-year historical climate series (as in Scenario A). The percentage change values adopted were informed by projected changes in rainfall and PE under Shared Socioeconomic Pathways (SSPs) 2-4.5 and 5-8.5. SSP2-4.5 is broadly considered representative of a likely projection, given current global commitments to reducing emissions, and SSP5-8.5 is representative of an (unlikely) upper bound (IPCC, 2022).

SCENARIO D

Scenario D is a future climate and future development scenario. It used the same future climate series as Scenario C, but river inflow, groundwater recharge and flow, and agricultural productivity were modified to reflect potential future development, as in Scenario B.

Therefore, in this report, the climate data for scenarios A and B are the same (based on historical observations from 1 September 1890 to 31 August 2022), and the climate data for scenarios C and D are the same (the above historical data scaled to reflect a plausible range of future climates).

1.5.3 HYPOTHETICAL DEVELOPMENT TERMINOLOGY

The development of the surface water resources for irrigated agriculture in the highly seasonal streamflow regime prevailing in the Victoria catchment is likely to require some degree of storage and river regulation. To explore how flood characteristics may change under hypothetical development scenarios, a series of simulation experiments were devised for different water storages and extractions.

Water harvesting – an operation in which water is pumped or diverted from a river into an offstream storage, assuming no instream structures.

Offstream storages – usually fully enclosed circular or rectangular earthfill embankment structures situated close to major watercourses or rivers to minimise the cost of pumping.

Large engineered instream dam – a barrier across a river for storing water in the created reservoir, usually constructed from earth, rock or concrete materials. In the Victoria catchment, most hypothetical dams were assumed to be concrete gravity dams with a central spillway (see companion technical report on water storage (Yang et al., 2024)).

Annual diversion commencement flow requirement (DCFR) – the cumulative flow that must pass the most downstream node (81100000) during a water year (1 September to 31 August) before pumping can commence. It is usually implemented as a strategy to mitigate the ecological impact of water harvesting.

Pump start threshold – a daily flow rate threshold above which pumping of water can commence. It is usually implemented as a strategy to mitigate the ecological impact of water harvesting.

Pump capacity – the capacity of the pumps expressed as the number of days it would take to pump the entire node irrigation target.

Reach irrigation volumetric target – the maximum volume of water extracted in a river reach over a water year. Note, the end use is not necessarily limited to irrigation. Users could also be involved in aquaculture, mining, urban or industrial activities.

System irrigation volumetric target – the maximum volume of water extracted across the entire study area over a water year. Note, the end use is not necessarily limited to irrigation. Users could also be involved in aquaculture, mining, urban or industrial activities.

Transparent flow – a strategy to mitigate the ecological impacts of large instream dams by allowing all reservoir inflows below a flow threshold to pass through the dam.

2 Floodplain inundation mapping

Spatial maps of water in the landscape were derived from satellite imagery for dates coinciding with flood events. They were useful in calibrating and post-auditing the hydrodynamic models used to simulate flood events for the floodplain of the Victoria catchment. These maps were produced using satellite imagery from the optical sensors of Moderate Resolution Imaging Spectroradiometer (MODIS), Landsat and Sentinel-2, and from the radar sensor of Sentinel-1. However, frequent cloud occurrence across northern Australia during the wet season limits the optical remote-sensing opportunities for capturing inundation extents over the different rivers and floodplains in the hydrodynamic model domain, particularly during flood peaks. Refer to the technical report on Earth observation methods, Sims et al. (2016), for further details on the satellite data, processing methods, and calibration of the products.

2.1 Satellite imagery acquisition and pre-processing

MODIS satellite data were used for producing daily maps of surface water. The MODIS sensor is an optical/infrared sensor from the National Aeronautics and Space Administration. There are two MODIS sensors currently orbiting the Earth (TERRA since 2000 and AQUA since 2002), although they are approaching their end of life. They acquire daytime images of Australia at around 10 am (TERRA) and 2 pm (AQUA). MODIS surface reflectance data are available from early 2000 until the present from the United States Geological Survey (USGS) Land Processes Distributed Active Archive Center (LP DAAC) (https://lpdaac.usgs.gov) as gridded tiles, and they are also stored at CSIRO for the whole of Australia. These data are available in hierarchical data format (HDF), in a sinusoidal projection, with a pixel size of 0.004697 degrees (~500 m). It was planned that daily images of surface reflectance from both the TERRA MODIS sensor (MOD09GA1) and the AQUA MODIS sensor (MOD09GA) would be used, together with an 8-day composite product (based on cloud-free, good-quality images from TERRA – MOD09A1). In the end, data from the AQUA sensor were not used, due to a detector failure in Band 6 (Gladkova et al., 2012) that resulted in a striped pattern in the data.

Landsat data, where available, are also useful for mapping surface water. These data are at a much finer spatial resolution (30-m pixels) than MODIS data, which are better suited to identifying narrow or small water features. However, Landsat images are only available every 8 to 16 days at best (depending on the number of operating sensors). The frequency is often further reduced due to cloud cover and missing data. Landsat 5 data (Thematic Mapper or TM), Landsat 7 data (Enhanced Thematic Mapper or ETM), and Landsat 8 and Landsat 9 data (Operational Land Imager or OLI) are available from Digital Earth Australia (DEA) from 1987 until the present. DEA provides consistent pre-processing, organisation and analytics of Landsat data for the Australian continent (Dhu et al., 2017). This processing involves corrections for illumination and observation angles, the Bidirectional Reflectance Distribution Function (BRDF, which influences relative pixel brightness across large scene areas) and atmospheric conditions. Refer to the companion technical report on Earth observation methods, Sims et al. (2016), for further details on Landsat data processing.

The European Space Agency (ESA) operates the Sentinel-2 satellites. Sentinel-2 has two operating sensors (2A since 2015 and 2B since 2017), and its data has a spatial resolution of 10 m to 20 m and a temporal frequency of 5 days. Sentinel-2A and 2B are optical remote-sensing instruments, so cloud cover reduces the amount of usable data for identifying inundation. These data are available from DEA (https://www.ga.gov.au/scientific-topics/dea) in a similar analysis-ready format to the Landsat data.

To help overcome the negative impact of frequent cloud cover during flood events, the ESA's Sentinel-1 Synthetic Aperture Radar (SAR) sensors were also used. Sentinel-1 SAR operates in the microwave wavelength range, so is not affected by cloud cover (although heavy rain can influence its return signal). Sentinel-1A (launched in 2014) and Sentinel-1B (operating from 2016 until 2022) have a pixel size of 10 m and a temporal frequency of (generally) 12 days within Australia. These data are currently available through the Sentinel Australasia Regional Access (SARA) hub (https://copernicus.nci.org.au/sara.client/#/home) as a level 1 product in their native radar coordinates.

2.2 Inundation mapping using MODIS

The Open Water Likelihood (OWL) algorithm (Guerschman et al., 2011) was used for mapping open surface water with MODIS imagery at a 500 m pixel resolution. The OWL was developed using empirical statistical modelling and calculates the fraction of water within a MODIS pixel. A cloud mask was applied using the MODIS state band associated with each product, which contains information on cloud and cloud-shadow locations. Refer to the companion technical report on Earth observation methods, Sims et al. (2016), for further details on the MODIS OWL algorithm. Using Python code, the daily MODIS OWL water maps (from TERRA – MOD) and the 8-day MODIS OWL water maps (also from TERRA – MOD) for the Assessment area were extracted from the Australia-wide products.

A limitation of MODIS mapping of surface water is that it is not of sufficient detail for mapping narrow water features of less than 1 pixel in width (~500 m). This problem is even more exaggerated when the narrow river channel is covered by vegetation along the banks or floating vegetation, which effectively obscures the water from the sensor.

2.2.1 EVENT MAPS

The daily MODIS maps were extracted for the Victoria hydrodynamic model domain for flood events used for inundation modelling. The years 2001, 2006, 2014, 2016, 2021 and 2023 were considered for inundation modelling. The MODIS OWL water maps were converted into a map of water and non-water pixels, and a threshold was used to stratify each MODIS map into water/non-water grids. Ticehurst et al. (2015) showed that, in the Flinders catchment, a 10% threshold resulted in the best match when comparing MODIS and Landsat inundation maps. Thus, all pixels above the OWL threshold of 10% were mapped as water, and the images were reprojected onto the geographic latitude/longitude coordinate system (coordinate system code EPSG:4326), before conversion to a GeoTIFF format for use with the hydrodynamic models. To help reduce the commission errors throughout the Victoria catchment, the Height Above Nearest Drainage (HAND)

algorithm (Nobre et al., 2011) was used to identify areas that were unlikely to flood. Pixels for which the HAND value was above 40 were masked as nulls.

2.2.2 SUMMARY MAPS

Summary maps were also produced for the flood events processed for the hydrodynamic model domain (Figure 2-1). These summary maps used composites of the MOD09A1 MODIS OWL water maps to show maximum inundation extent, and the percentage of clear observations (i.e. observations without clouds and/or nulls).

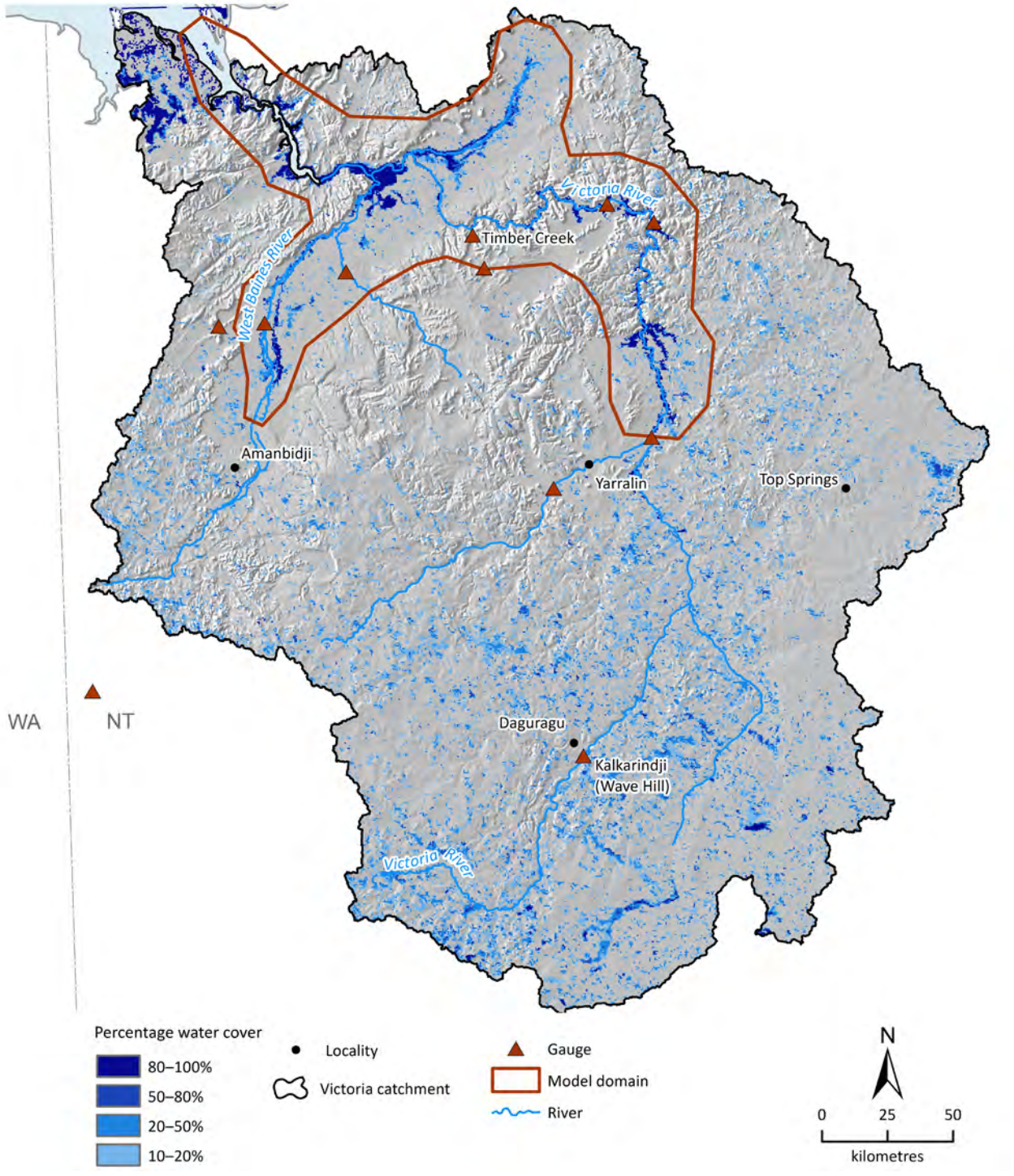

Figure 2-1 MODIS satellite–based flood inundation map of the Victoria catchment

Data captured using MODIS satellite imagery. This figure illustrates the maximum percentage of MODIS pixel inundation between 2000 and 2023.

2.3 Inundation mapping using Landsat imagery

2.3.1 ALGORITHM USED

Landsat 5 TM, 7 ETM, 8 OLI and 9 OLI data were extracted from DEA. For mapping flood inundation, the Normalized Difference Water Index $(NDWI)_{Xu}$ (Xu, 2006) – an index based on the green and mid infrared wavelengths – was used. Water was separated from other features using a threshold of $NDWI_{Xu} \geq 0$, which is consistent with Xu (2006), and balanced errors of omission and commission in the Victoria catchment. Masking of cloud cover was undertaken by extracting the pixel quality band ('fmask') available with each Nadir BRDF-Adjusted Reflectance (NBAR) product. As for the MODIS water maps, to reduce the commission errors that were detected throughout the catchment, the HAND algorithm (with a threshold of 40) was applied to mask pixels in steep terrain.

2.3.2 EVENT MAPS

Landsat water maps were selected for the same hydrodynamic model domain and flood events as the MODIS data. These were examined to find those images least affected by cloud cover, which greatly limited the number of available images, given that deep clouds and sustained rain prevail during the wet season across northern Australia, and the infrequent satellite overpass. These images were then converted to the geographic latitude/longitude (EPSG:4326) coordinate system and GeoTIFF format for use with the hydrodynamic models.

2.4 Inundation mapping using Sentinel-2

2.4.1 ALGORITHM USED

All Sentinel-2 imagery available during the flood event dates were extracted from DEA. The $NDWI_{Xu}$ was used to separate water from non-water, and the same threshold as used for Landsat was used for the Sentinel-2 imagery. The 'fmask' band was used to mask pixels affected by cloud or cloud shadow. The HAND algorithm (with a threshold of 40) was applied to mask pixels in steep terrain.

2.4.2 EVENT MAPS

Sentinel-2 water maps were selected for the same hydrodynamic model domain and flood events as the MODIS data. These were examined to find those images least affected by cloud cover, which greatly limited the number of available images, given that deep clouds and sustained rain prevail during the wet season across northern Australia. The Fmask quality band for Sentinel-2 does not always detect clouds, so images affected by significant remnant clouds were removed. The remaining images were then converted to the geographic latitude/longitude (EPSG:4326) coordinate system and GeoTIFF format for use with the hydrodynamic models.

2.5 Inundation mapping using Sentinel-1

2.5.1 ALGORITHM USED

Sentinel-1 backscatter data for the flood events were processed to normalised radar backscatter, an analysis-ready format, and filtered to reduce speckle effects. The radar backscatter was converted from intensity to decibels for better contrast between water and land. A low backscatter threshold was used to identify surface water. This threshold was calculated using the Otsu algorithm (Otsu, 1979) over areas with greater than 10% permanent surface water. The differences in backscatter between a dry image and the flooded images were used to identify flooded areas not detected by the low backscatter. The threshold was manually selected. To reduce commission errors, small 'clumps' of pixels (up to 50 pixels in size) that were misclassified as water bodies were removed using a sieve filter. The HAND algorithm was applied to mask pixels in steep terrain.

2.5.2 EVENT MAPS

Sentinel-1 images for four dates were processed to water maps. However, only one image showed evidence of flooding. These images were provided in the geographic latitude/longitude (EPSG:4326) coordinate system and GeoTIFF format for use with the hydrodynamic model.

2.6 Combined summary maps

There were a limited number of images identifying flooding in the Landsat, Sentinel-2 and Sentinel-1 images. However, because they were of a similar spatial resolution and quality, these images were able to be combined to produce a summary map. Those water maps produced for the flood events used in the hydrodynamic modelling were combined to delineate the maximum flooding extent, and to calculate the percentage of observations in which a pixel was identified as inundated (Figure 2-2).

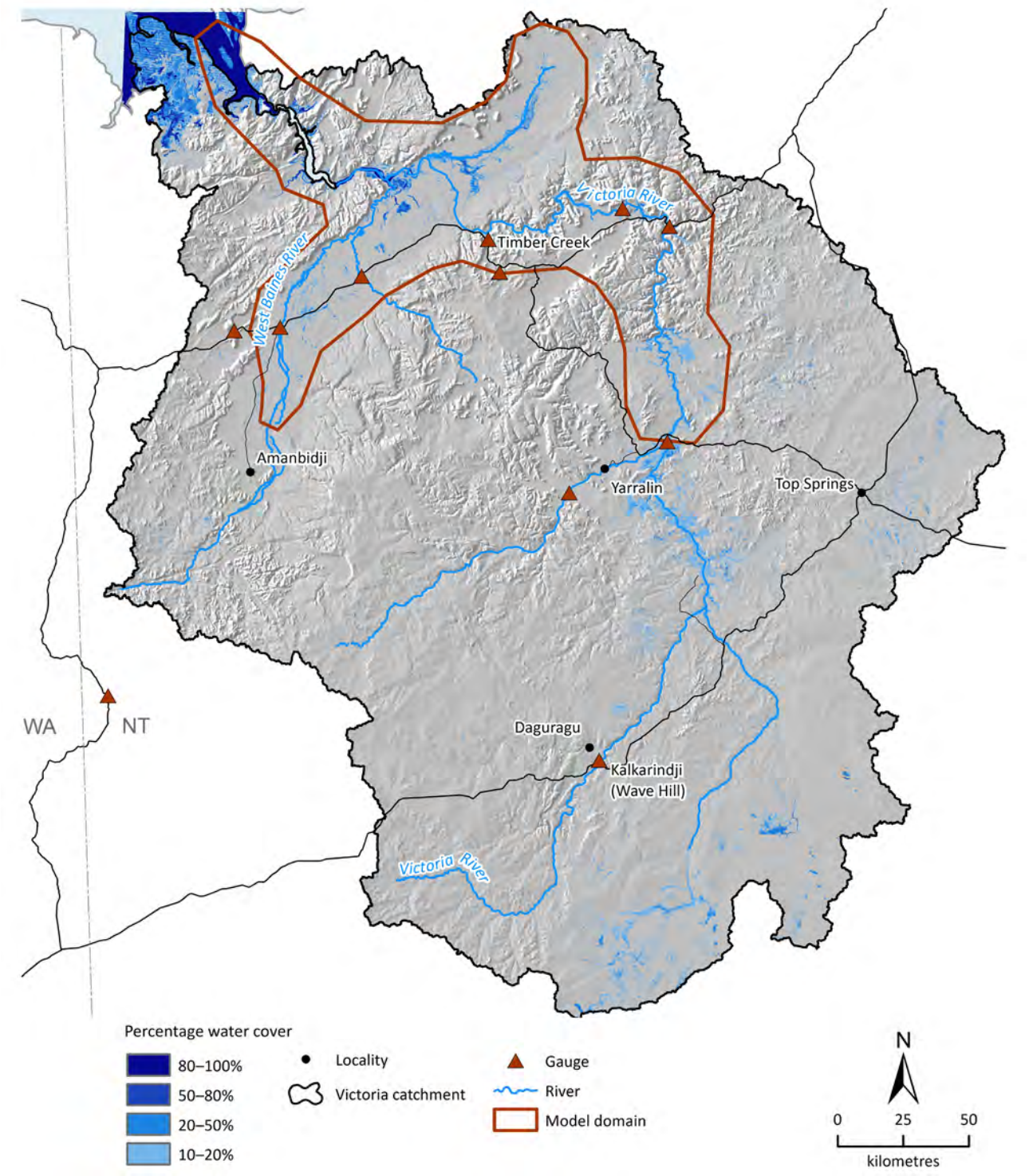

Figure 2-2 Combined Landsat, Sentinel-2 and Sentinel-1 satellite–based flood inundation map of the Victoria catchment

Data captured using Landsat, Sentinel-2 and Sentinel-1 satellite imagery. This figure illustrates the percentage of clear observations in which a pixel was inundated during the flood events used in the hydrodynamic modelling.

2.7 Summary

Flood inundation maps were produced using MODIS, Landsat, Sentinel-2 and Sentinel-1 imagery for the Victoria catchment. MODIS surface reflectance data are available since 2000 for the whole of Australia. Daily images of surface reflectance from the TERRA sensor (MOD09GA), and 8-day composite images of surface reflectance from the TERRA MODIS sensor (MOD09A1) were used in the analysis. Landsat data are available from DEA from 1987 until the present in a consistent analysis-ready format. Sentinel-2 data are available from DEA from 2015 until the present.

The OWL algorithm was used for mapping open surface water with MODIS imagery at a 500 m pixel resolution. The OWL algorithm was developed using empirical statistical modelling and calculates the fraction of water within a MODIS pixel. The daily MODIS OWL water maps were extracted for the Victoria catchment hydrodynamic model domain, and a series of flood maps were produced for selected flood days for hydrodynamic model calibration.

Sentinel-1 data, which are not affected by cloud cover, were also used to identify flooding, based on low radar backscatter. However, only one image was acquired at the right time to capture flooding.

The NDWI algorithm was used for mapping flood inundation based on Landsat and Sentinel-2 imagery. Water was separated from other features using a threshold of NDWI ≥ 0, which balances errors of omission and commission in the Victoria catchment. Similarly, for MODIS, a set of event-based and summary maps were produced using the combined Landsat, Sentinel-2 and Sentinel-1 data.

Water maps generated from satellite imagery are particularly useful for encompassing large areas at a reasonable temporal frequency. While MODIS can provide daily water maps, it is of a poorer spatial resolution (~500 m) compared with Landsat (30 m pixels), Sentinel-2 (10–20 m pixels) and Sentinel-1 (10 m pixels). In addition, surface water of less than 1 pixel in width (~500 m) cannot be mapped, particularly if there is vegetation along the riverbanks. In general, it was found that in northern Australia's wet–dry tropical/monsoonal climate, MODIS produces better flood maps for large floodplains and/or big flood events. Care must be taken when interpreting the MODIS water maps, due to artefacts in the imagery and confusion with dark soils, dark rocks, residual cloud and topographic shadow. Unusual water features appearing in only one image need to be treated with caution, and a flood-likelihood mask would be of great benefit in interpretation of the data.

The Landsat and Sentinel-2 water maps are very useful for detecting fine water features. However, the temporal frequency of the imagery made it difficult to analyse flood events, as the flood peak was often missed due to either the timing of satellite overpass or cloud cover. As for MODIS, the Landsat and Sentinel-2 water maps will be affected by the difficulty of detecting water under flooded vegetation, and by confusion with dark features (e.g. residual cloud and topographic shadow).

The maximum percentage water cover based on MODIS imagery is higher than that determined from Landsat/Sentinel-2/Sentinel-1 imagery. The reason for this is that MODIS OWL water maps can identify wet soil as water (Sims et al., 2016). Another reason for the difference could be that MODIS has a much higher temporal frequency (daily) than Landsat (every 16 days), Sentinel-2 (every 5 days), and Sentinel-1 (every 12 days), which means that these sensors will fail to coincide with as many flood events as MODIS, especially as there can be high cloud cover in this catchment.

3 Floodplain inundation modelling

3.1 Hydrodynamic models

Two-dimensional hydrodynamic models (e.g. MIKE 21 FM, TUFLOW, LISFLOOD-FP) are commonly used to simulate flood levels and inundation extent in a river–floodplain system (Kumar et al., 2023; Kvocka et al., 2015; Neal et al., 2012). The main strengths of the hydrodynamic models are that they produce floodplain hydraulics that can be used to estimate inundation extent and duration, and depth and frequency of wetting and drying at desired spatial (e.g. 5 to 10 m-grid) and temporal (e.g. hourly) scales (Horritt and Bates, 2002). Based on the modelling objectives and the availability of input data, either a two-dimensional regular-grid model (DHI, 2012) or a two-dimensional flexible-grid model (DHI, 2016) can be selected. Technical considerations include the size of the hydrodynamic model domain, irregularity in the land topography, the availability of topography data, and the complexity of the hydraulic regime. These two-dimensional models can be coupled with one-dimensional river models, which allows finer-scale representation of the highly dynamic river processes with river cross-sections.

For the Assessment, a two-dimensional flexible-mesh model (MIKE 21 FM) was selected for the Victoria catchment, primarily based on the availability of fine-scale laser altimetry (LiDAR) data. A brief description of the MIKE 21 FM model is presented in the following sections.

3.1.1 TWO-DIMENSIONAL HYDRODYNAMIC MODEL – MIKE 21 FM

The hydrodynamic module of the MIKE 21 FM is based on the two-dimensional incompressible Reynolds-averaged Navier–Stokes equations (DHI, 2016). The model simulates the water level and velocity flux in response to a variety of forcing functions in floodplains, lakes, estuaries, bays and coastal areas. The boundary conditions in MIKE 21 FM can vary in both time and space. Point sources and sinks can also be incorporated into the model. The model has been widely used across the world, including in Australia, for flood inundation modelling (Teng et al., 2017). The main strength of the MIKE 21 FM model is its ability to simulate wetting and drying of a floodplain during a flood event, and the large number of computational cells that it can handle (in the range of millions). Model input includes river bathymetry, floodplain topography, land surface roughness (constant or spatially variable), inflow and outflow conditions, eddy viscosity and radiation stresses. Rainfall, evaporation and surface infiltration can also be incorporated in MIKE 21 FM. The model output includes time series of water depth, velocity and discharge for the entire computational domain and user-specified time intervals. In the Assessment, we have used a triangular mesh of varying size, and the modelling domain was divided into three subzones based on mesh size. The flexible-mesh model is preferable over the classic MIKE 21 FM regular-grid model, because it allows selection of a very small grid at the area of interest and also the alignment of model grids to the river banks.

3.1.2 SOLVING GOVERNING EQUATIONS AND HARDWARE REQUIREMENTS

The primitive variables of the governing equations are discretised using an element-centred finite-volume method. The spatial domain is discretised into non-overlapping elements, which can be either triangular or quadrilateral (DHI, 2016). The finite-volume method sets up an equivalent Riemann problem (ERP) across each element interface and solves it to determine the variable fluxes between the elements. The technique used in MIKE 21 FM produces an exact solution to an approximate Riemann problem. The approach treats the problem as one-dimensional in the direction perpendicular to each element interface. MIKE 21 FM has two options for obtaining time integration accuracy: a first-order explicit Euler method (referred to as the lower temporal order scheme) and a second-order Runge–Kutta method (referred to as the higher temporal order scheme). There are also two options for obtaining spatial integration, with the second-order (higher-order) accuracy being achieved through a variable gradient reconstruction technique prior to the ERP formulation (DHI, 2016). The model can be simulated on either a central processing unit (CPU) or a graphics processing unit (GPU) machine. In the present Assessment, the models were run using GPU machines containing 16 CPU cores and 3 GPU cards (each with 4 P100 Nvidia GPUs). Each run took approximately 3 days of computer time to simulate a 30-day flood event.

3.2 Data requirement for model configuration

Hydrodynamic models are data intensive. A large amount of temporal and spatial data is required for setting up a hydrodynamic model for flood inundation modelling. While some input data (e.g. stream network, water level, discharge) can be extracted from the secondary sources, most input data are case-specific and need to be prepared before running the model. To configure the MIKE 21 FM model, the data needed for the hydrodynamic model domain includes:

- topography
- surface roughness
- stream network
- inflow/outflow
- water level
- local runoff.

4 Victoria catchment hydrodynamic model calibration

4.1 Physical and hydro-meteorological properties

The Victoria River and its tributaries, the most substantial of which are the Baines, Wickham, Armstrong, Camfield and Angalarri rivers, define a catchment area of 82,400 km^2 (Figure 4-1). The Victoria River itself spans approximately 500 km, from Entrance Island at its mouth to Kalkarindji in the far south of the catchment. Tidal variation at the mouth of the Victoria River is up to 8 m, and these tides propagate upstream to approximately 5 km downstream of Timber Creek (Power and Water Authority, 1987). The catchment is relatively flat, with maximum elevations of around 450 m with respect to the Australian Height Datum (mAHD) in the far south-west. The northern portion of the catchment area is dominated by escarpments, hills and ridges of sedimentary geology. Within this lies a north-east to south-west band of alluvial plain associated with the Baines and Angalarri rivers. Nearly 60% of the catchment consists of dissected hills, outcrops, plateaux and scarps, with rocky and/or shallow soils of little agricultural potential. These higher-relief areas give way to lower sloping land and alluvial plains. The coastal marine plains are seasonally or permanently wet saline soils with potential acid sulfate risks (Hughes et al., 2024a).

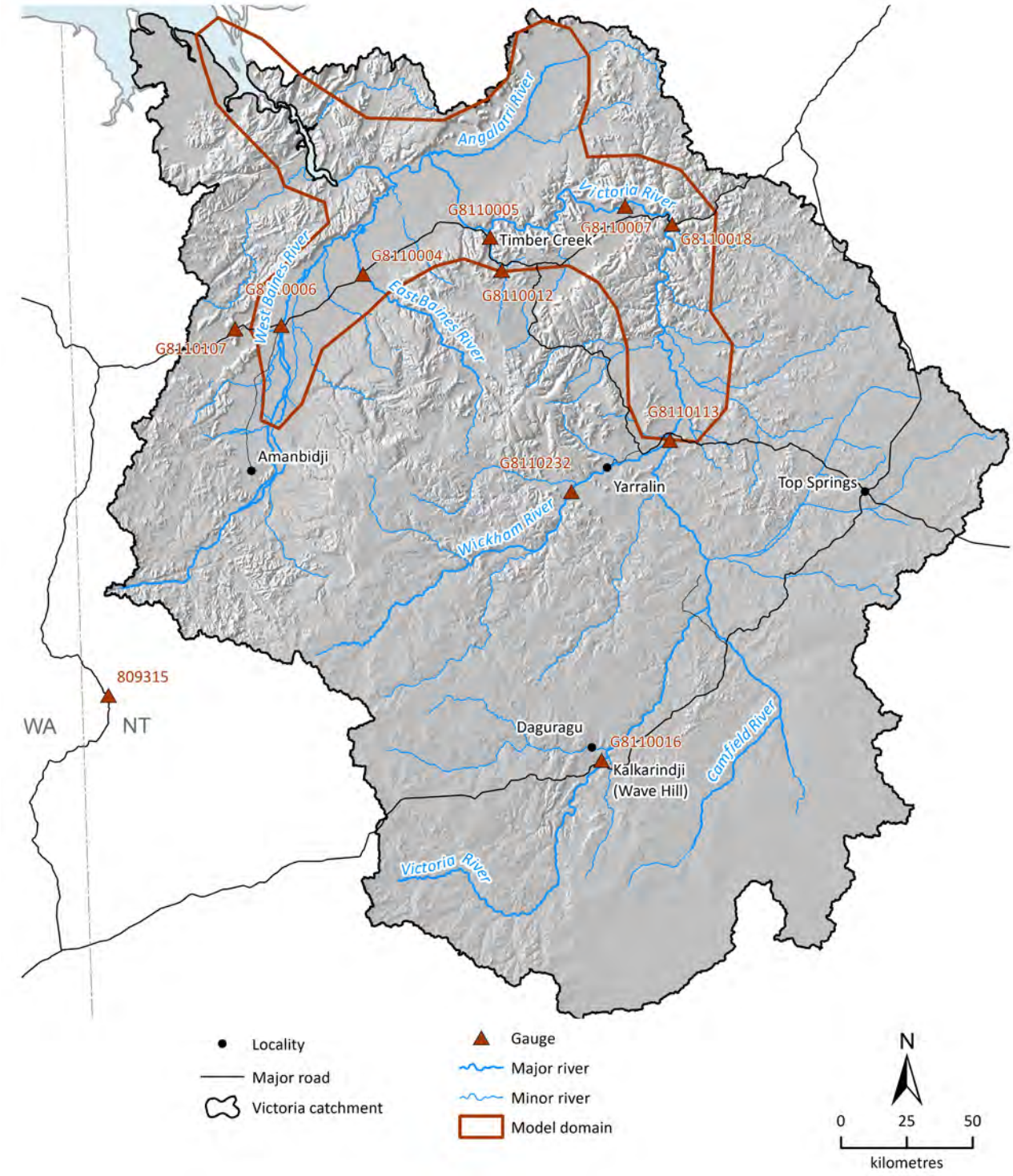

Figure 4-1 Victoria catchment map showing the river network, streamflow monitoring stations and the hydrodynamic model domain

4.1.1 CLIMATE

The Victoria catchment has a highly seasonal climate with an extended dry season (Figure 4-2). It receives a mean of 681 mm of rain per year, 95% of which falls during the wet-season months (November to April). The mean daily temperatures and potential evaporation are high relative to other parts of Australia. The median wet-season rainfall shows a decrease from north to south, but no distinct pattern is observed during the dry season (McJannet et al., 2023). The highest

monthly rainfall totals typically occur during January, February and March (Figure 4-2). Potential evaporation in the Victoria catchment exceeds 1900 mm in most years. Evaporation exhibits a strong seasonal pattern, ranging from over 200 mm per month during the build-up (October to December) down to about 100 mm per month during the middle of the dry season in June. The high mean annual PE and moderate mean annual rainfall result in a large mean annual rainfall deficit across most of the catchment. Consequently, a large proportion of the catchment is semi-arid. Tropical cyclones do not affect the Victoria catchment every year, so their contribution to the total annual rainfall is highly variable from one year to the next. From 1969 to 2022, the Victoria catchment experienced 53 tropical cyclones. Seventy-two percent of seasons experienced no tropical cyclones, 21% one, and 6% two. When a tropical cyclone or a low-pressure system does cross the catchment, typically 200 to 500 mm of rain falls over a 2 to 5-day period, and daily rainfall totals have exceeded 200 mm in the estuary area of the catchment (McJannet et al., 2023).

Approximately a third of global climate models (GCMs) project an increase in mean annual rainfall by more than 5%, a fifth of GCMs project a decrease in mean annual rainfall by more than 5%, and about half project 'little change' (McJannet et al., 2023).

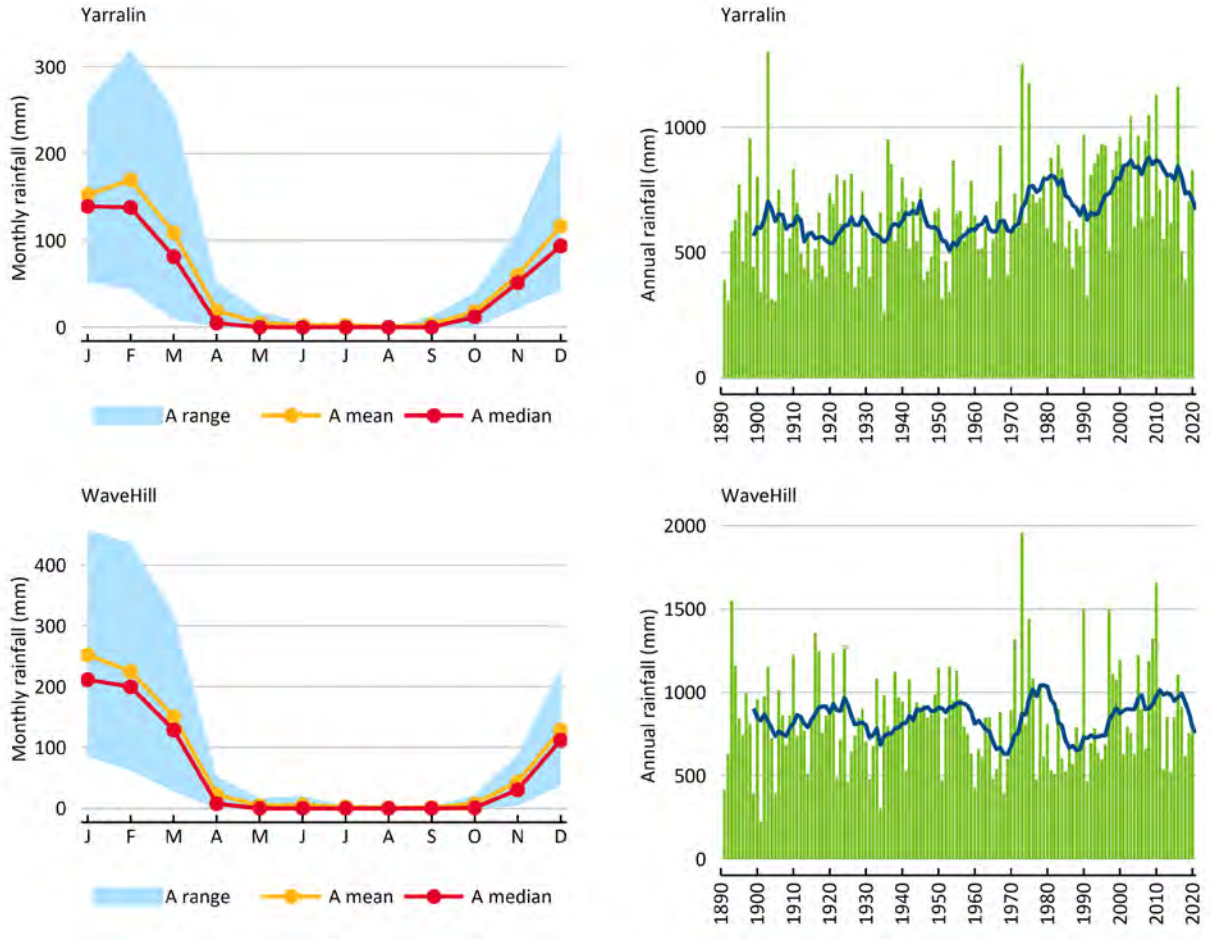

Figure 4-2 Historical monthly rainfall (showing the range in values between the 20% and 80% monthly exceedance rainfall) and annual rainfall at Yarralin on the Wickham River and at Kalkarindji on the Victoria River

The blue line represents the 10-year moving mean.

4.1.2 STREAMFLOW

The reaches of the Victoria catchment exhibit a wide range of flow regimes. While the lower Victoria River is near perennial, streams across most of the catchment are intermittent or ephemeral. Streamflow gauges in the southern portions of the catchment exhibit, in general, fewer days of observed flow per year than streams in the northern areas of the catchment. The mean annual flow at the catchment outlet is estimated to be around 7000 GL/year (see companion technical report on river modelling in the Victoria catchment, Hughes et al., 2024a). Driven by the highly seasonal climate, streamflow in the Victoria River displays very strong seasonal patterns. Figure 4-3 shows the monthly flow distribution at gauge G8110007 on the Victoria River. Approximately 87% of flow occurs in just 3 months, from January to March, and 97% of flow occurs in the wet-season months of December to April.

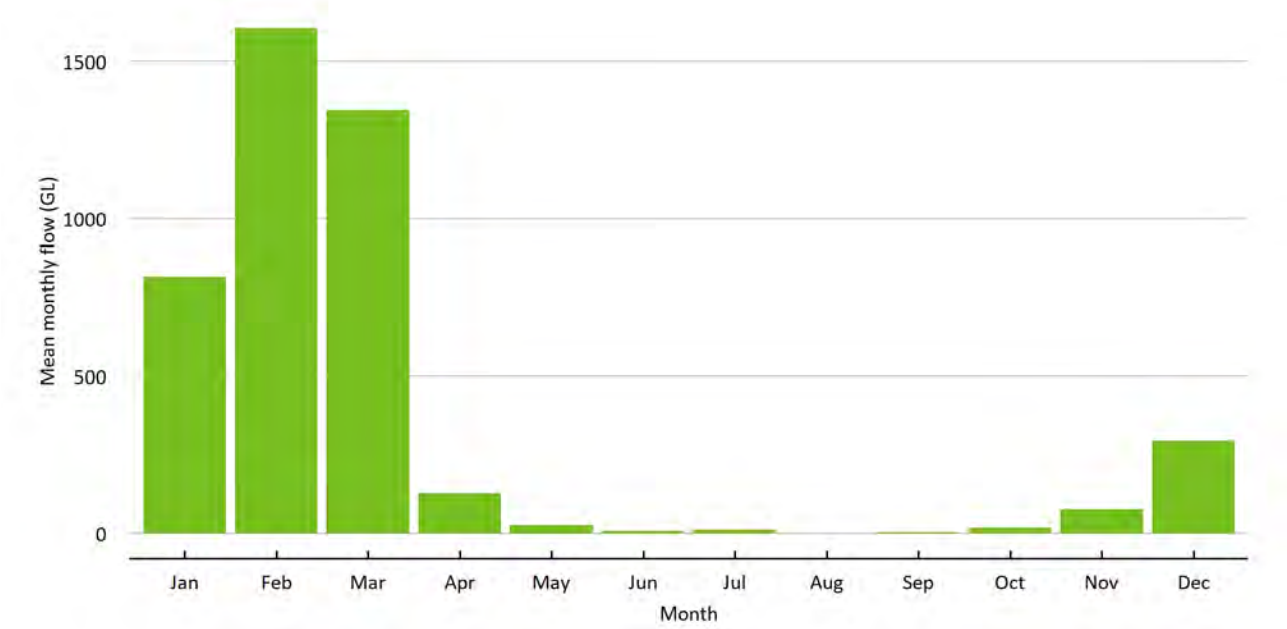

Figure 4-3 Monthly flow distribution at gauge G8110007 (Coolibah Homestead) on the Victoria River, based on the observed data for 1953 to 2023.

4.1.3 FLOODING

Intense seasonal rains from monsoonal bursts and tropical cyclones in the period of December to March create flooding in parts of the Victoria catchment and inundate large areas of floodplains on each side of the Victoria River and its two major tributaries, the Baines and Angalarri rivers (Figure 2-1). This is an unregulated catchment, and its overbank flow is generally governed by the topography of the floodplain. Characterising these flood events is important for a range of reasons. Flooding can be catastrophic to agricultural production in terms of loss of stock, fodder and topsoil, and damage to crops and infrastructure. In addition, it can isolate properties and disrupt vehicle traffic providing goods and services to people in the catchment. However, flood events also provide the opportunity for offstream wetlands to be connected to the main river channel. The high biodiversity found in many unregulated floodplain systems in northern Australia is thought to largely depend on seasonal flood pulses, which allow for biophysical exchanges to occur between rivers and offstream wetlands.

Flooding is widespread at the junction of the Victoria and Baines rivers, downstream of Timber Creek. In the last 70 years (1953 to 2023), there have been 80 floods ranging from small to large in the catchment. This figure was based on an overbank threshold of 1560 m^3/s, which was estimated by obtaining daily streamflow at the Coolibah Homestead on the Victoria River gauge (G8110007) and comparing it against floodplain inundation on the available satellite imagery. For flood events with an AEP of 1 in 2, 1 in 5 and 1 in 10, the peak discharge at the Coolibah Homestead on the Victoria River was 1850, 3210 and 5120 m^3/s, respectively. Figure 4-4 shows the annual maximum daily discharge over the past 70 years (1953 to 2023) at Coolibah Homestead. While floods can occur in any month from November to April, approximately 87% of historical floods have occurred in the period January to March (Figure 4-5). Of the ten largest flood peak discharges at Coolibah Homestead, six events have occurred in March, three in February and one in December. Flood peaks typically take about 2 to 3 days to travel from Dashwood Crossing to Timber Creek, at a mean speed of 3.4 km/hour.

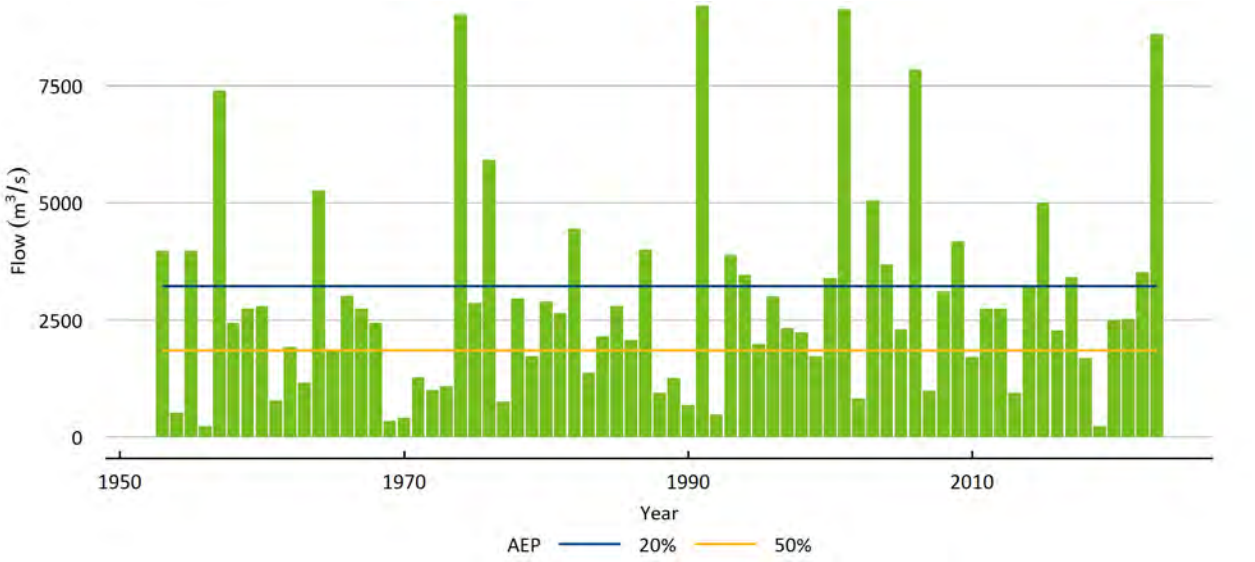

Figure 4-4 Annual maximum daily flow at Coolibah Homestead (G8110007) on the Victoria River from 1953 to 2023

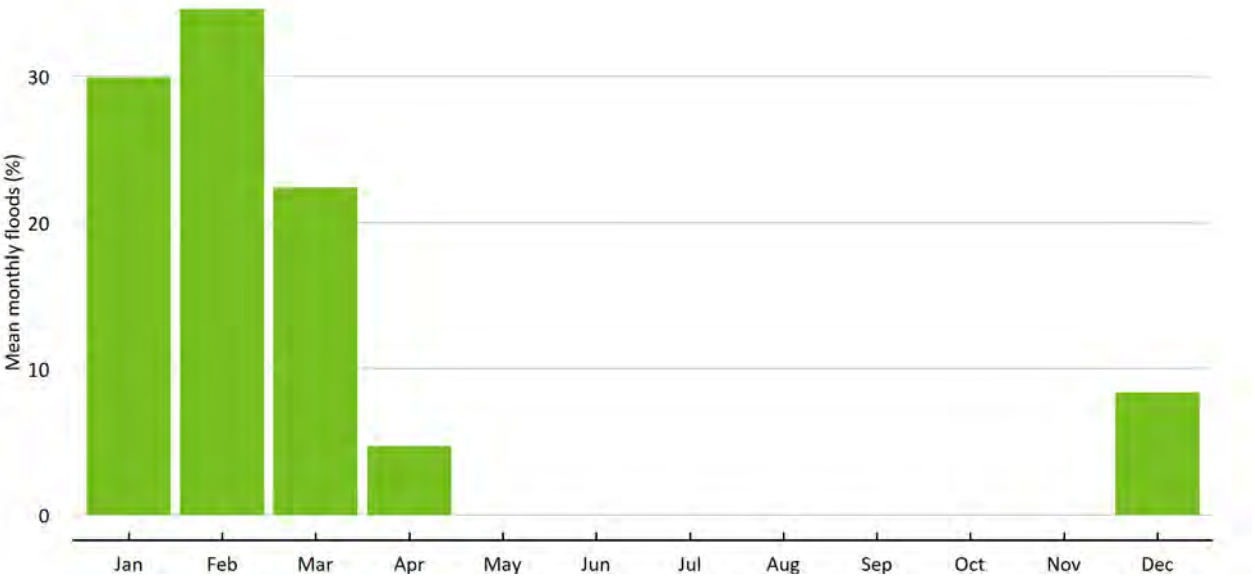

Figure 4-5 Monthly flood frequency in the Victoria catchment (floods defined as an AEP of ≥1 in 1, based on historical records from 1953 to 2023) at Coolibah Homestead (G8110007)

AEP = annual exceedance probability.

4.2 Model configuration

The hydrodynamic model was configured for the proportion of the Victoria catchment encompassing the floodplains of the major rivers and the tidal flats at the mouth of the Victoria River (Figure 4-6). The modelling domain included areas downstream of Amanbidji on the West Baines River and downstream of Dashwood Crossing on the Victoria River and covered an area of 16,730 km^2. The model included eight inflow boundaries across the river network and one water-level boundary at the river mouth (Figure 4-6). The model domain included 53 subcatchment outlets, incorporating local runoff, as described in Section 4.3.4.

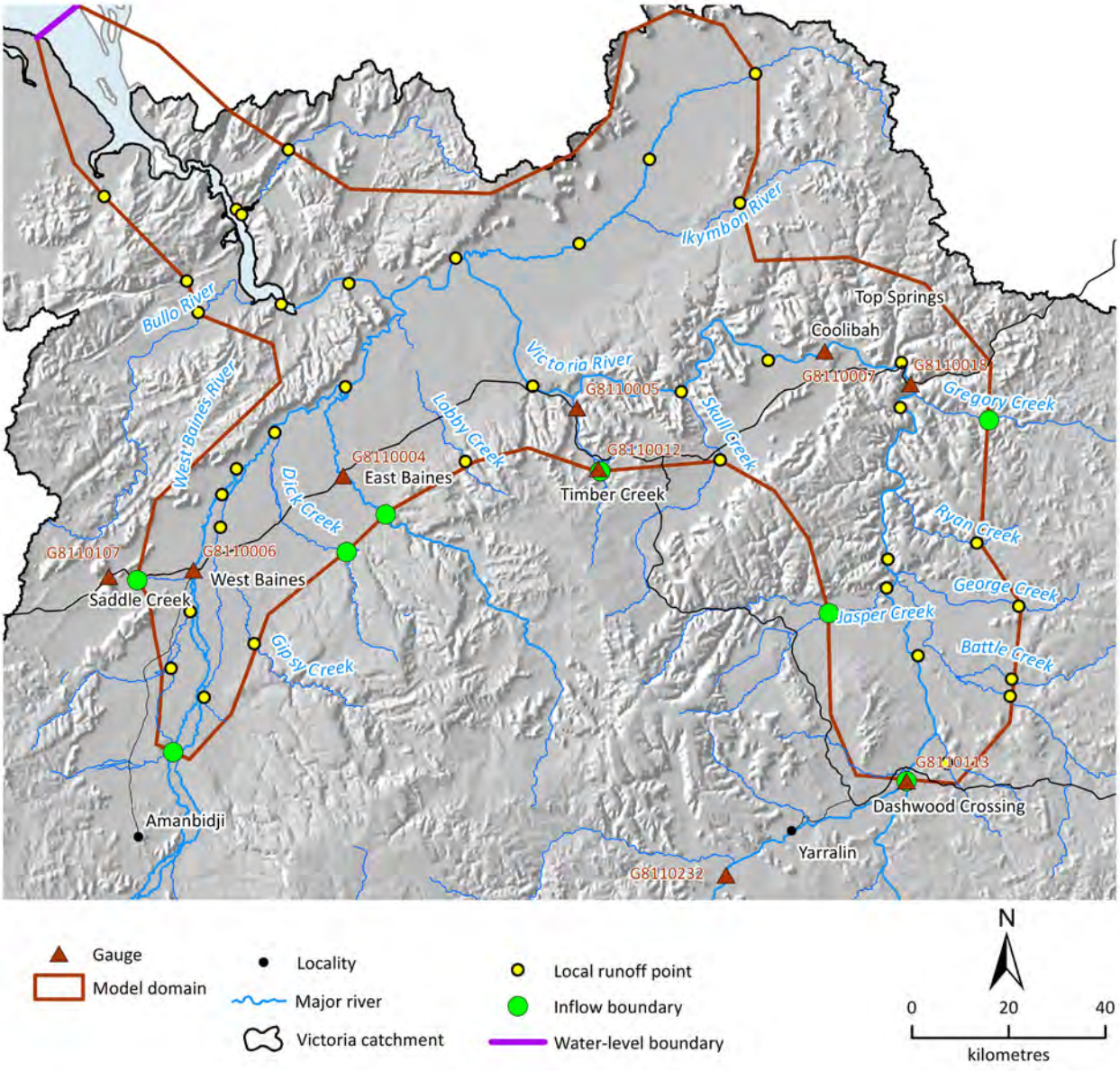

Figure 4-6 Hydrodynamic model configuration of the Victoria catchment, showing boundary inflow and local runoff points in the model domain

4.3 Model input

4.3.1 TOPOGRAPHY

Land surface topography data are essential for flood inundation modelling in addition to hydro-meteorological inputs (Sanders, 2007). The vertical accuracy of these data is critical, since the inundation depths and extents simulated by hydrodynamic models are highly sensitive to such errors, especially on low-gradient floodplains (Horritt and Bates, 2002).

A digital elevation model (DEM) was produced for the Victoria MIKE 21 FM model domain based on a LiDAR 5-m DEM (±0.3 m horizontal and ±0.1 m vertical accuracy) patched with a 30 m Forest And Buildings removed Copernicus digital elevation model (FABDEM). The highest resolution publicly available topographic information that encompasses the whole of the Victoria catchment is based on a 1-second (i.e. ~30 m) Shuttle Radar Topography Mission (SRTM) DEM (Gallant et al., 2011) and a 1-second FABDEM (Hawker et al., 2022). These two global DEMs were compared, and FABDEM was chosen due to its superior vertical accuracy in the Assessment area (Meadows et al., 2024). The FABDEM was used for the hydrodynamic modelling domain to cover areas for which LiDAR data were not available. The final combined DEM was created by resampling the FABDEM to 5 m (to match the original LiDAR resolution) and merging it with the LiDAR data using a methodology described by Gallant (2019). The Gallant method attenuates the difference between the resampled coarse DEM and the LiDAR data at the interface to zero over a distance beyond the LiDAR extent. The LiDAR elevations remain intact, while the coarse DEM elevations are modified by the attenuated difference, resulting in a 'seamless' combination while retaining hydrological connectivity. The final product of the Victoria DEM is a 5 m–grid raster file of size 6.8 GB.

The LiDAR data covers the major proportion of the West Baines and Angalarri rivers and the small proportion of the Victoria River that regularly floods (Figure **4**-**7**). The hydrodynamic modelling domain encompasses an area of 16,730 km^2, and the area covered by LiDAR is 6956 km^2 (i.e. ~41.6% of the model domain).

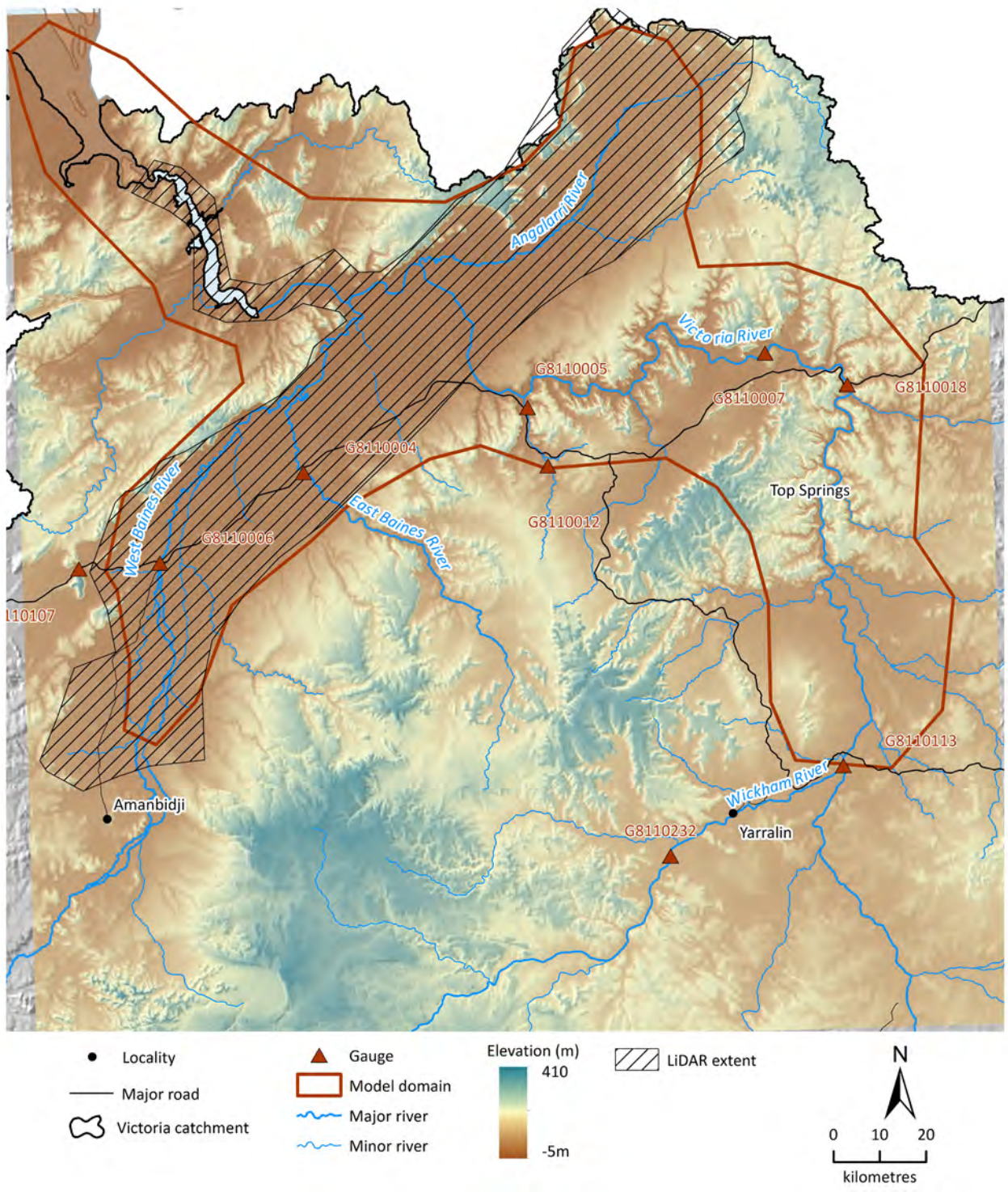

Figure 4-7 LiDAR data coverage in the hydrodynamic model domain of the Victoria catchment

4.3.2 SURFACE ROUGHNESS

The hydraulic roughness coefficients of the land surface were derived from DEA Land Cover, which is a collection of annual land-cover maps for Australia for the period from 1988 to 2020 (Owers et al., 2021) in which Australia's landscapes are classified into six basic land-cover categories (Table 4-1). The categories were represented in the model by Manning's roughness coefficient (*n*), as estimated in the published literature (Arcement and Schneider, 1989; Chow, 1959; LWA, 2009)), and a roughness map was produced.

Table 4-1 Manning's roughness coefficient (*n*) for various types of land cover occurring in the Victoria catchment

LAND COVER TYPE	MANNING'S *n* ($s/m^{1/3}$) RECOMMENDED RANGE	MANNING'S *n* ($s/m^{1/3}$) CALIBRATED
Artificial surface	0.035–0.050	0.04
Cultivated terrestrial vegetation	0.035–0.060	0.04
Natural bare surface	0.03–0.035	0.03
Natural aquatic vegetation	0.04–0.060	0.05
Natural terrestrial vegetation	0.04–0.080	0.06
Open water	0.03–0.033	0.03

4.3.3 INFLOW AND OUTFLOW BOUNDARY CONDITIONS

The hydrodynamic model consisted of seven inflow boundaries, but gauge data were available for only one boundary (i.e. Dashwood Crossing on the Victoria River). The upstream river boundary conditions of the hydrodynamic models were obtained from the Australian Water Resource Assessment – River model (AWRA-R) simulations (see the companion technical report on river modelling in the Victoria catchment, Hughes et al., 2024a). The river model discharge gauge nodes used in the hydrodynamic models are shown in

Table 4-2. In addition to these, the tidal sea-level data was used for the downstream water-level boundary. The Quoin Island station was used for the tidal sea-level data as it is the closest to the mouth of the Victoria River. The remaining inflows to the boundary of the hydrodynamic model domain that were not captured by the river model were simulated using the Sacramento rainfall-runoff model (Hughes et al., 2024b).

Table 4-2 List of stream gauges that were used for the Victoria hydrodynamic model configuration and calibration

STATION ID	STATION NAME	CATCHMENT AREA (km^2)	GAUGE RECORD	GAUGE STATUS	DATA USED FOR
G8110004	East Baines River upstream of the Victoria Hwy	2444	1963–2023	Open	Inflow boundary
G8110006	West Baines River at the Victoria Hwy	12,956	1961–2023	Open	Calibration
G8110007	Victoria River at Coolibah Homestead	52,192	1953–2023	Open	Calibration
G8110012	Timber Creek upstream of Victoria Highway	164	1968–2023	Open	Inflow boundary
G8110101	Dick Creek at the Victoria Highway	507	1968–1978	Closed	Inflow boundary
G8110107	Saddle Creek at the Victoria Highway	221	1968–2023	Open	Inflow boundary
G8110113	Dashwood Crossing	40,723	1962–2023	Open	Inflow boundary

4.3.4 LOCALLY GENERATED STREAMFLOW

The hydrodynamic model domain was subdivided into 53 subcatchments, based on the topography and stream network (Figure 4-6). The Sacramento model simulated gridded runoff was averaged for each subcatchment by assigning Scientific Information for Land Owners (SILO) cells to the subcatchments in accordance with the intersecting cells. Streamflow at the outlet (also called the 'pour point') of each subcatchment was calculated by multiplying the runoff by the subcatchment area. This locally generated runoff was added into the hydrodynamic model as a point source of water in the system. Subcatchment boundaries and pour points were generated using ArcGIS tools. The locations of some pour points were manually changed to ensure all subcatchments delivered the local flow directly into a river or creek (Figure 4-6).

4.4 Flood frequency and selected events for model calibration

Flood frequency analysis (FFA) was performed in the Victoria catchment to establish the streamflow thresholds above which a flood event would occur. A flood event was defined as the occurrence of overbank flows that could be identified through satellite imagery. If the flow rate dropped below the overbank flow threshold for five consecutive days, the event was considered to have ended. To determine the number of times each event was exceeded by larger events, events with higher peak discharge and larger total event volume were counted. Flood frequency was estimated for the two major rivers, the Victoria and the West Baines rivers. For the Victoria River, flood frequencies were estimated using streamflow observations from gauging station G8110007 (on the Victoria River at Coolibah Homestead), as this gauge has a long historical record (>50 years). Similarity, for the West Baines River, flood frequencies were estimated using streamflow observations from gauging station G8110006 (on the West Baines River at the Victoria Highway). Based on these observations, a threshold flow rate of 1560 m^3/s was used to identify overbank flow for the G8110007 gauge on the Victoria River, and a threshold flow rate of 180 m^3/s for the G8110006 gauge on the West Baines River. Traditionally, flood frequencies are estimated based on the maximum discharge for an individual event. However, in this Assessment, to help determine the true magnitude of the events, the FFA took into account both the total flow volume and the peak discharge for each event. This was motivated by the knowledge that not only the maximum discharge but the duration of an event can have a great impact on the inundated area. Figure 4-8 displays the relationship between peak flow and AEP for the two gauges, one on the West Baines River and the other on the Victoria River. While flow volume was higher for larger floods, the duration of the flood was a key factor associated with the volume of the flood flow.

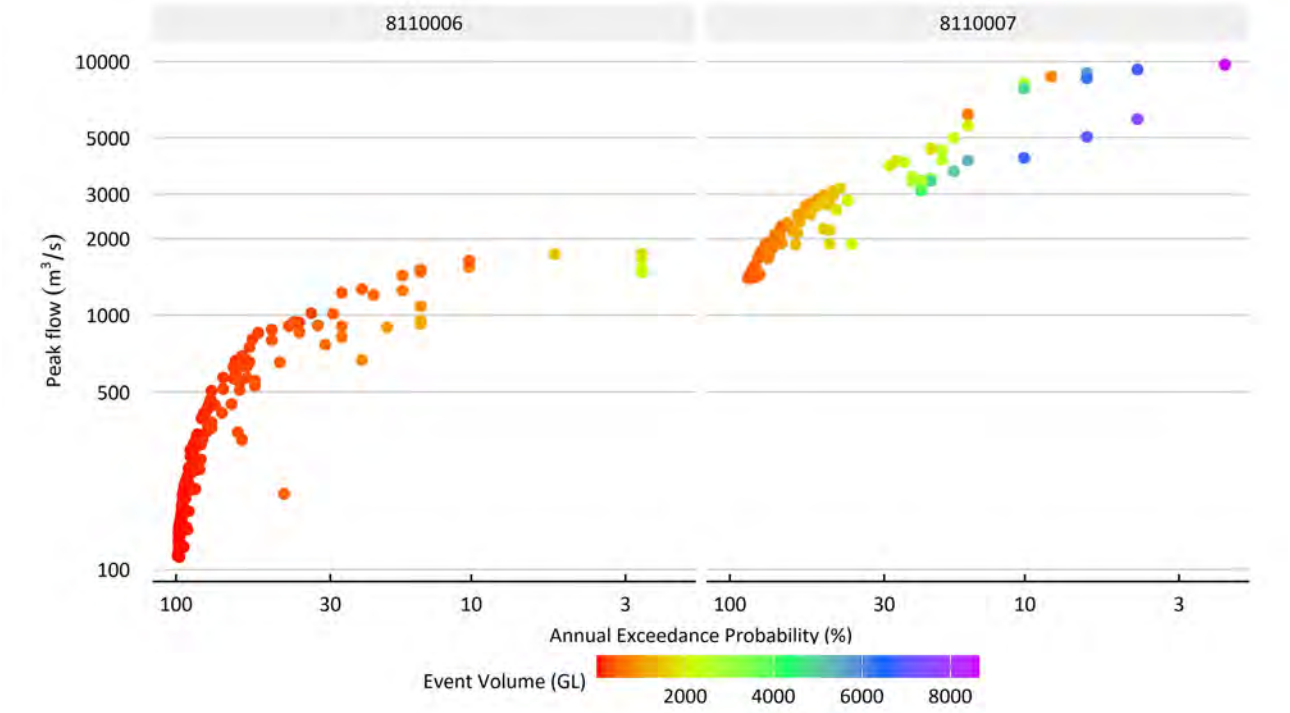

Figure 4-8 Peak flood discharge and annual exceedance probability at: (a) gauge 8110006 (on the West Baines River at the Victoria Highway) and (b) gauge 8110007 (on the Victoria River at Coolibah Station Homestead)

Flood events were selected for the model calibration based on the availability of cloud-free Landsat, MODIS and Sentinel imagery, while ensuring the magnitude of the flood events spanned the AEPs of interest to ecologists and the land suitability analysis. Five events were chosen, with flood magnitudes ranging from an AEP of 1 in 2 to 1 in 18, based on the flow data at Coolibah Homestead on the Victoria River (Table 4-3). The requirement for a large number of simulations, involving all combinations of scenarios and calibration events, necessitated the use of only two flood events (in 2021 and 2023) for scenario modelling.

Table 4-3 Flood events used for calibration

EVENT PERIOD	DURATION (DAYS)	PEAK DATE	PEAK FLOW (m^3/s)	ANNUAL EXCEEDANCE PROBABILITY (YEARS)	PURPOSE
23/03/2001 – 1/04/2001	12	27/03/2001	1964	1 in 2	Calibration, scenario modelling
4/02/2014 – 23/02/2014	20	18/02/2014	3213	1 in 5	Calibration, scenario modelling
24/12/2015 – 8/01/2016	16	27/12/2015	5008	1 in 10	Calibration
14/02/2021 – 1/03/2021	16	22/02/2021	2522	1 in 3	Calibration
18/02/2023 – 16/03/2023	27	7/03/2023	8599	1 in 18	Calibration

4.5 Hydrodynamic model simulation and outputs

The simulations for hydrodynamic models in the calibration and scenario modelling were undertaken with a 1-second time step to satisfy the numerical stability criteria for the biggest flood event in the analysis. Each event was simulated for 30 days (longer than the flood durations) irrespective of the time of flood recession, to ensure the entire rising and falling limbs were included in the simulation. The models were run using GPU machines consisting of 16 CPU cores and 3 GPU cards (each with 4 P100 Nvidia GPUs). For each run, it took about 3 days of computer time to a simulate a 30-day flood event. At the hydrodynamic model boundaries, daily discharges were specified for all inflow boundaries, and hourly tide levels were specified at the seaside boundary. The model used an inbuilt interpolation technique to derive flow variables at each computational time step. The model outputs included the water surface elevation, depth and velocity for each mesh element. While the model has the option of producing output at any time interval, all outputs in this analysis were recorded at 6-hour time intervals. A separate model was configured and simulated for each flood event.

Total water depths and water velocities were obtained from each model run and converted to three-column XYZ format American Standard Code for Information Interchange (ASCII) data. In the post-processing, the two-dimensional triangular flexible-mesh data were converted to 5 m $\times$ 5 m gridded data via an inverse distance weighted interpolation algorithm.

4.6 Hydrodynamic model calibration

The calibration process was constrained by the excessive time required by the hydrodynamic model simulations, which limited the number of iterations possible for tuning. However, the simulations were checked to ensure correct activation of the anabranches and connectivity to the various floodplain water bodies. The duration of the floodplain inundation was tuned by adjusting the floodplain infiltration rates and the surface roughness to ensure inundation patterns were consistent with the satellite/remotely sensed imagery. In addition to evaluation against the satellite imagery, simulated stage height outputs were compared with observed stage heights at two floodplain river gauges, one on the Victoria River at Coolibah Homestead (G8110007) and the other on the West Baines River at the Victoria Highway (G8110006).

The evaluation of hydrodynamic modelled inundation extent was performed using available and suitable Landsat and MODIS inundation maps for the selected flood events (including at least one image for each flood event). To evaluate the performance of the hydrodynamic model using the remotely sensed flood extent observations, two evaluation methods were employed:

- A visual comparison of the spatial inundation areas indicated by the satellite image and the model simulation was undertaken to assess how the main inundation patterns were represented by the hydrodynamic model.
- A quantitative assessment of the spatial inundation metrics (whether the model correctly simulated inundated pixels or not) was undertaken to assess how well the hydrodynamic model captured the overall inundation extent.

Both evaluation methods were performed with resampling of the remotely sensed inundation maps (Landsat 30 m and MODIS 500 m) at 5 m–grid pixel horizontal resolution, to be consistent

with the hydrodynamic model gridded output. The satellite inundation maps were masked so as to only include the modelled area within the hydrodynamic model domain.

In many cases, satellite-derived inundation maps (even for a sensor like MODIS, with a twice-daily satellite overpass frequency) will only capture portions of the hydrodynamic model domain due to the persistent cloud cover that can occur during flood events. Thus, only pixels in the satellite images showing 'inundated' or 'non-inundated' were considered; this meant that all 'cloudy' or 'no data' pixels were removed from the analysis.

4.6.1 CATEGORICAL STATISTICS

Detection metrics were computed for each adjusted hydrodynamic model domain and for each grid cell. For every available satellite inundation map, each grid cell in the model domain was classified as a hit (H, observed inundation correctly detected), miss (M, observed inundation not detected by product), or false alarm (F, inundation detected but none observed) using a contingency table, following Ebert et al. (2007) (Figure 4-9).

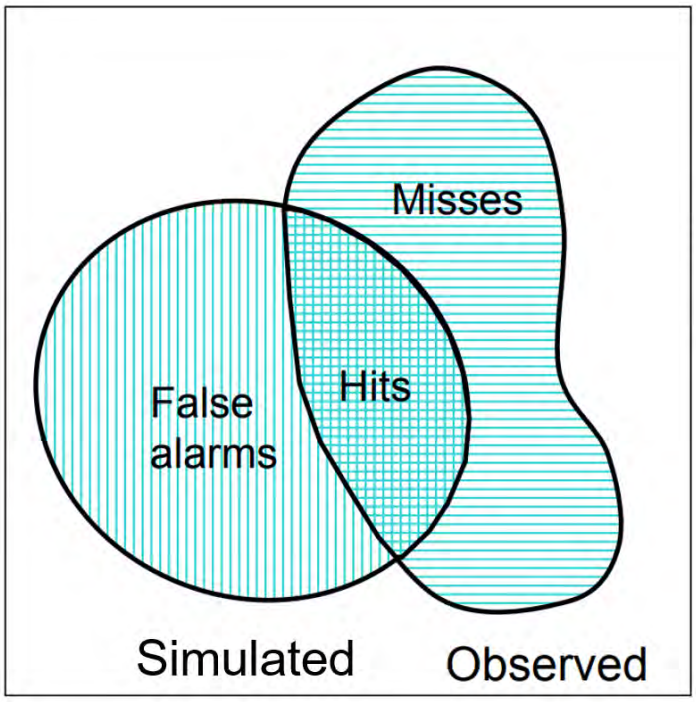

Contingency Table

Simulated \ Observed	yes	no
yes	*hits*	*false alarms*
no	*misses*	*correct negatives*

Figure 4-9 Detection metrics classification at the grid cell level using a contingency table

The following statistics were computed from the contingency table:

- The Probability Of Detection, POD = H/(H + M), gives the fraction of inundated pixels correctly detected (range 0 to 1, 1 indicating a perfect score). It is sensitive to hits, but ignores false alarms, and it should be used in conjunction with the false alarm ratio (see next bullet point).
- The false alarm ratio (FAR) = F/(H + F), gives the fraction of wrongly detected inundated pixels (range 0 to 1, 0 indicating a perfect score). It is sensitive to false alarms, but ignores misses.
- The frequency bias (FB) = (H + F)/(H + M), gives the ratio of the simulated to observed inundated pixels frequency (range 0 to ∞, 1 indicating a perfect score). It measures the ratio of the frequency of the modelled inundated pixels to the frequency of the satellite imagery inundated pixels, and it indicates whether the hydrodynamic model has tended to underestimate (FB < 1)

or overestimate (FB > 1) events. It does not measure how well the modelled inundation extent corresponds to the satellite inundation extents, as it only measures relative frequencies.

- The equitable threat score (ETS), used as an overall performance metric, gives the fraction of the inundated pixels that were correctly detected, adjusted for correct detections (He) that would be expected due to random chance: ETS = (H – He)/(H + M + F – He), where He = (H + M)(H + F)/N and N = the total number of estimates (range –1/3 to 1, 1 indicating a perfect score and 0 indicating no skill). It is sensitive to hits. Because it penalises both misses and false alarms in the same way, it does not distinguish the sources of error.

Although the detection statistics described above are well constrained, there are issues to consider in the interpretation of the results, such as:

- Satellite inundation images may show inundated areas that remain in the landscape as ponded areas in between flood events, because of the gentle topography and the low infiltration rates.
- The results of the grid-to-grid comparison between the hydrodynamic model output and the satellite imagery will be inherently poor where the satellite images (from MODIS in particular) are of a lower spatial resolution than the river channel widths, the river morphology and the resulting inundation dynamics.

The two approaches mentioned above (visual comparison and detection statistics) complement each other – visual comparisons, although labour-intensive and subjective, highlight the sources or nature of the errors and provide diagnostic information regarding necessary changes to the inputs or hydrodynamic model set-up. On the other hand, statistical metrics provide an objective and comparable metric for assessing overall model performance. The calibration is considered successful if the two approaches assess the performance of the model output as reasonable (in terms of overall inundation patterns captured and detection statistics).

4.7 Results and discussion

4.7.1 STAGE HEIGHT

Figure 4-10 shows a typical comparison between simulated and observed stage heights for the different flood events at two gauges, G811007 on the Victoria River and G811006 on the West Baines River. In general, the simulated flood peaks match well with the observed data, especially for the G811006 gauge. While a good match was obtained for the flood peak, there were differences in stage heights for the rising and falling limbs of the flood hydrograph. The arrival times of the peaks differed, and this difference was observed both during the rising and falling stages of the flood. For almost all flood events, the simulated stage heights for the receding flood hydrographs were higher than the observed heights. Also, the results showed overestimation of stage height between the two peaks for the flood event of two or more peaks (e.g. the 2014 and 2021 floods).

The possible reasons for the discrepancies between the simulated and the observed stage heights include: (i) coarse topography data for the major proportion of the Victoria River and (ii) lack of good quality bathymetry data, (iii) lack of observed river flow data, and (iv) poor representation of some river channel. In addition, there are uncertainties in the river model–simulated inflows to the hydrodynamic model domain.

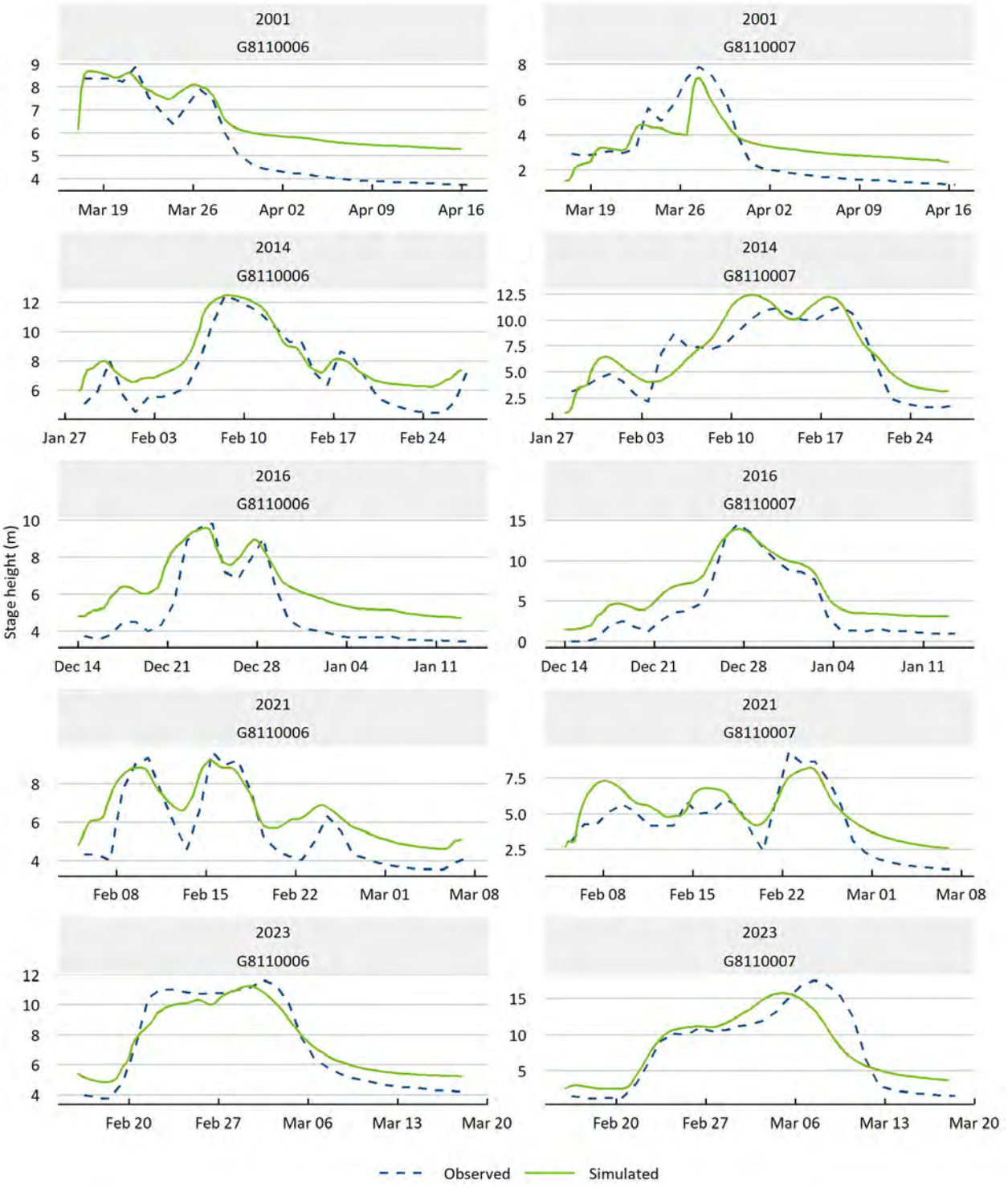

Figure 4-10 Comparison of the model-simulated stage height and the observed stage height at Coolibah Homestead (G8110007) on the Victoria River and at Victoria Highway on the West Baines River (G8110006)

4.7.2 SATELLITE-BASED FLOOD MAPS

The available Landsat (TM, ETM & OLI), MODIS and Sentinel images were processed for the Victoria River hydrodynamic model domain for the calibration periods (Table 4-4). The availability of images and the proportion of cloud/null effects were reported. Due to the large number of MODIS images, only those images containing 80% or less clouds/nulls were processed to obtain

inundation maps. Also, to exclude images with little or no flooding, only images with 5% or more observed inundated area were used for comparison with the hydrodynamic model results.

Table 4-4 Flood event dates and number of satellite images (Landsat (TM, ETM & OLI), sentinel and MODIS) processed for the Victoria catchment hydrodynamic model calibration

START DATE	END DATE	FLOOD MAGNITUDE	NUMBER OF LANDSAT IMAGES	NUMBER OF SENTINEL IMAGES	NUMBER OF MODIS IMAGES
23/03/2001	1/04/2001	1 in 2 AEP	1	0	4
4/02/2014	23/02/2014	1 in 5 AEP	1	0	6
24/12/2015	8/01/2016	1 in 10 AEP	5	0	9
14/02/2021	1/03/2021	1 in 3 AEP	2	3	2
18/02/2023	16/03/2023	1 in 18 AEP	7	1	12

AEP = annual exceedance probability

4.7.3 INUNDATION EXTENT

The results of the hydrodynamic modelling in the Victoria catchment were compared with satellite inundation maps through a direct visual comparison and detection metrics. In the first instance, images that passed the first cloud cover filtering were further scrutinised to identify flood patterns that could be used to inform the calibration of the hydrodynamic modelling. The images within the modelling simulation periods (see

Table 4-4) that showed limited inundation, or images with large cloud cover over the inundated areas, were omitted from further analysis. Generally, at least one image was retained for each flood event to assist in the calibration. Figure 4-11 shows an example of Landsat (TM, ETM, OLI), MODIS and Sentinel inundation maps with corresponding hydrodynamic model inundation maps for the same date.

Table 4-5 presents the detection statistics for selected images considered in the analysis, including images from all five flood events (see Table 4-3 for the flood events). The POD, which gives the fraction of inundated pixels correctly detected, varied within a range of 0.05 to 0.81 (range 0 to 1, 1 indicating a perfect score), with a mean of 0.48. The FAR, which gives the fraction of wrongly detected inundated pixels, varied within a range of 0.15 to 0.95 (range 0 to 1, 0 indicating a perfect score), with a mean of 0.75. This indicates overestimation of inundation by the model compared with satellite imagery. The ETS varied in the range of 0.03 to 0.60 (1 indicating a perfect score and 0 indicating no skill), with a mean of 0.16. This indicates poor overall matching between the simulated and the observed inundation. In general, the simulated inundation was greater than that identified in the satellite images for all flood events (FB > 1). The FB varied within a range of 0.31 to 10.36 (range 0 to ∞, 1 indicating a perfect score), with a mean of 3.39, indicating that there was generally overprediction of inundation by the model, although there was some underestimation as well.

Locations of poor fit generally coincided with complex anabranching networks. Closer inspection of the satellite imagery for these locations revealed that they often did not display flooding of these anabranches. The inability of MODIS to capture inundation in narrow floodplains has been reported for the Fitzroy catchment in WA (Karim et al., 2011) and other catchments in northern

Australia (Ticehurst et al., 2013). Furthermore, MODIS regularly falsely identifies cloud shadow as inundation, which is particularly an issue when using imagery with high (up to 80%) cloud cover.

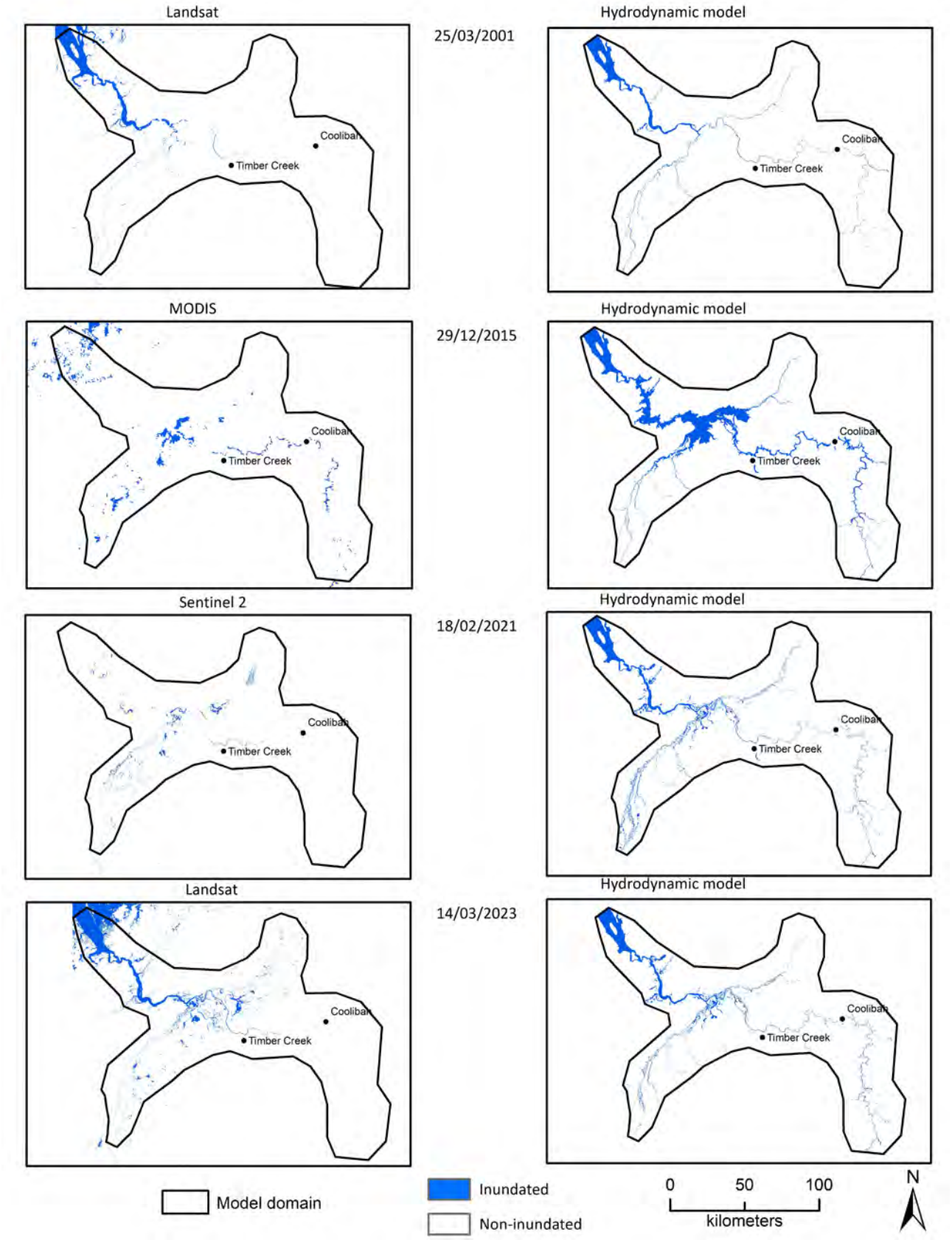

Figure 4-11 Comparison of (Landsat, MODIS, Sentinel) satellite-based inundation maps with hydrodynamic model results for the Victoria catchment

Table 4-5 Detection statistics for the Landsat (TM, ETM & OLI), MODIS and Sentinel images considered in the analysis for the Victoria hydrodynamic model calibration

Percentage available refers to pixels other than cloud/null (including inundated and non-inundated pixels) within the hydrodynamic model domain. ETS stands for Equivalent Threat Score (a measure of overall performance), POD for the Probability Of Detection, FAR for the False Alarm Ratio and FB for Frequency Bias.

SATELLITE	DATE	% AVAILABLE	ETS	POD	FAR	FB
Landsat	25/03/2001	33	0.69	0.15	0.82	0.60
MODIS	29/03/2001	66	0.26	0.81	1.36	0.12
MODIS	30/03/2001	42	0.37	0.79	1.78	0.15
MODIS	19/02/2014	60	0.61	0.86	4.40	0.12
MODIS	20/02/2014	70	0.52	0.93	7.49	0.06
MODIS	21/02/2014	72	0.50	0.88	4.17	0.10
MODIS	22/02/2014	67	0.70	0.91	7.98	0.08
MODIS	31/12/2015	59	0.59	0.68	1.86	0.24
MODIS	1/01/2016	35	0.61	0.82	3.40	0.15
MODIS	2/01/2016	69	0.70	0.84	4.44	0.14
MODIS	3/01/2016	72	0.72	0.79	3.51	0.18
MODIS	4/01/2016	62	0.81	0.91	9.38	0.08
MODIS	5/01/2016	65	0.41	0.93	5.84	0.06
Landsat	6/01/2016	44	0.44	0.33	0.66	0.34
MODIS	9/01/2016	59	0.47	0.93	6.40	0.07
MODIS	11/01/2016	48	0.16	0.95	3.28	0.04
Sentinel	18/02/2021	42	0.15	0.89	1.34	0.07
Landsat	28/02/2021	41	0.05	0.87	0.37	0.03
Landsat	1/03/2021	37	0.09	0.71	0.31	0.07
Sentinel	2/03/2023	45	0.81	0.74	3.09	0.23
MODIS	5/03/2023	29	0.48	0.36	0.76	0.36
MODIS	9/03/2023	50	0.58	0.72	2.04	0.22
MODIS	10/03/2023	66	0.50	0.65	1.43	0.25
MODIS	11/03/2023	45	0.70	0.93	10.36	0.06
MODIS	12/03/2023	70	0.34	0.84	2.06	0.12
MODIS	13/03/2023	63	0.33	0.86	2.35	0.10
Landsat	14/03/2023	50	0.47	0.28	0.65	0.37

Summary

4.8 Summary

The Victoria catchment has large floodplain areas on both sides of the West Baines and Angalarri rivers and parts of the Victoria River, especially at the junction of the Victoria and Baines rivers. Some upstream reaches, such as areas below the Dashwood Crossing and above the Jasper Creek, are quite flat (see Figure 4-6 for land topography) and get inundated during seasonal flooding between the months of December to March (Figure 2-1 and Figure 4-11).

Flood inundation maps were produced using Landsat (TM, ETM, OLI), MODIS and Sentinel imagery. MODIS imagery of 500 m resolution at 1-day intervals was acquired from November 2001 to March 2023 and processed using the OWL algorithm. Landsat imagery of 30 m resolution at 16-day intervals was acquired from 2001 to 2023 and processed using the NDWI algorithm. A total of 14 Landsat images, 47 MODIS images and 13 Sentinel images were selected for processing, based on data quality and relevance to selected flooding events, for the hydrodynamic model calibration. Event-based inundation maps were produced for individual floods, and composite flood maps were produced by combining all images. Cloud cover was a challenge when producing event-based inundation maps. Both Landsat and MODIS show inconsistencies in the spatial flood extent due to the limited number of cloud-free observations. In addition, the inability of MODIS to capture inundation in narrow floodplains has been reported for the Fitzroy catchment (Karim et al., 2011) and for other catchments in Australia (Ticehurst et al., 2013).

Inundations in the floodplains of the Victoria River and its two major tributaries (the Baines and Angalarri rivers), an area of 16,730 km2, were modelled for five flood events ranging from an AEP of 1 in 2 to an AEP of 1 in 18. Inundation is primarily driven by high flows down the Victoria, Baines and Angalarri rivers and to a lesser extent along the East Baines River. Flooding is widespread in parts of the Baines and Angalarri rivers and at the junction of the Victoria and Baines rivers. While the Victoria River is mostly a single-channel river, the Baines and Angalarri rivers consist of a network of braided channels that produce large inundation during floods.

A two-dimensional hydrodynamic model (MIKE 21 FM) was used to simulate flood inundation. The model was calibrated for the 2001, 2014, 2016, 2021 and 2023 flood events using inundation maps derived from satellite imagery. The models were calibrated primarily by adjusting the roughness coefficient and the infiltration rate.

Compared with the Landsat and MODIS inundation maps, the hydrodynamic model captured the overall inundation patterns better along the Victoria River and its major tributaries (e.g. the West Baines and Angalarri rivers). However, the detection statistics showed that the cell-to-cell matching of the model-generated data against the observed satellite data was overall poor, largely due to the inability of MODIS to detect inundation of narrow floodplains. The detection metrics suggest that there is overestimation, especially during receding floods, as well as a general misalignment of inundation patterns. The locations of poor fit generally coincided with complex anabranching rivers. Closer inspection of the satellite imagery in these locations revealed that it often does not display flooding of these anabranches. The inability of MODIS to capture inundation in narrow floodplains has been reported for the Fitzroy catchment in WA (Karim et al., 2011) and for other catchments in northern Australia (Ticehurst et al., 2013). Furthermore, MODIS regularly falsely identifies cloud shadow as inundation, which is particularly an issue when using imagery with high (up to 80%) cloud cover. The hydrodynamic model has some limitations.

However, lack of good-quality satellite images restricts rigorous calibration of the model results. Moreover, there are uncertainties in the river model simulations for inflow boundaries and locally generated runoff.

5 Flood modelling under future climate and development scenarios

5.1 Introduction

Rising global air temperatures are likely to be accompanied by changes in the intensity and patterns of rainfall in Australia. The Australian Academy of Science released a report (Australian Academy of Science, 2021) stating that current emissions trajectories will likely result in Australia experiencing a 3 °C temperature increase by 2100. McJannet et al. (2023) found that GCMs indicated changes in rainfall across the Victoria, Roper and Southern Gulf catchments. These changes in rainfall are usually amplified in runoff. Consequently, increases in global temperatures may be accompanied by changes in the extent and patterns of flood inundation.

In addition, the development of surface water resources for irrigated agriculture in the highly seasonal streamflow regime prevailing in the Victoria catchment is likely to require some degree of storage and river regulation. Surface water storage options have been evaluated at several hypothetical dam locations in the Victoria catchment (Yang et al., 2024). Flood waters stored during the wet season and their gradual release during the dry season will modify the timing and magnitude of floods and the subsequent inundation of floodplains. The impacts of water harvesting during high-flow events were also evaluated during the flood study.

To explore how flood characteristics may change under projected future climate and hypothetical development scenarios, a series of simulation experiments for various scenarios were devised. Due to the long run times of the hydrodynamic model, it was only possible to explore a limited number of scenarios. Hence scenarios were selected to enable general conclusions about likely impacts on floodplain inundation. A summary of the future climate and development scenarios undertaken in the Assessment area is presented in Table 5-1.

Table 5-1 Summary of selected future climate and development scenarios

ASSESSMENT AREA	SCENARIO NAME	FLOOD START DATE (DURATION OF SIMULATION IN DAYS)	EXCEEDANCE PROBABILITY (YEARS)
Victoria catchment, NT	Scenario B Historical climate and hypothetical future development (Dam and Water Harvesting)	5/02/2021 (30)	1 in 3
		16/02/2023 (30)	1 in 18
	Scenario C Projected future climates (dry and wet) and current levels of development	5/02/2021 (30)	1 in 3
		16/02/2023 (30)	1 in 18
	Scenario D Projected future climates (dry and wet) and hypothetical future development (Dam and Water Harvesting)	5/02/2021 (30)	1 in 3
		16/02/2023 (30)	1 in 18

5.2 Future climate scenarios

GCMs are an important tool for simulating global and regional climate. To assess the level of uncertainty in the range of future runoff projections, future climate projections from a large range of archived GCM simulations were downloaded from the Coupled Model Intercomparison Project Phase 6 (CMIP6) website (https://pcmdi.llnl.gov/CMIP6/). Of the 92 available GCMs, 32 included the rainfall, temperature, solar radiation, and humidity data required for the Australian Water Resource Assessment Landscape model (AWRA-L) and AWRA-R hydrological modelling. The Intergovernmental Panel on Climate Change (IPCC) in its Sixth Assessment Report (AR6) presented five different climate scenarios based on a Shared Socioeconomic Pathway (SSP) for the future (IPCC, 2022). For the Assessment, SSP2-4.5 was used to investigate the sensitivity of changes in rainfall and PE on streamflow at approximately the year 2060 (McJannet et al., 2023). Under SSP2-4.5, emissions rise slightly before declining after 2050, but they do not reach net zero by 2100. At approximately 2060, SSP2-4.5 is representative of a 1.6 °C temperature rise relative to a time slice centred around 1990.

GCMs provide information at a resolution that is too coarse to be used directly in catchment-scale hydrological modelling. Hence, an intermediate step is generally performed: the broad-scale GCM outputs are transformed to catchment-scale variables. For this reason, and due to the scale of the catchments being assessed (which makes it resource-intensive to undertake dynamic or statistical downscaling), a simple scaling technique – the pattern scaling (PS) method (Chiew et al., 2009) – was adopted. The seasonal PS method employed used output from the 32 GCMs to scale the 133-year historical daily rainfall, temperature, radiation and humidity sequences (i.e. SILO climate data) to construct the 32 by 133-year sequences of future daily rainfall, temperature, radiation and humidity. The method is described in the companion technical report on future climate across the Victoria, Roper and Southern Gulf catchments (McJannet et al., 2023).

The percentage changes in rainfall and PE spatially averaged across the Victoria catchment under SSP2-4.5 are shown in Figure 5-1. As outlined by McJannet et al. (2023), scenarios Cwet and Cdry for the Victoria catchment were selected representing 10% (3rd) and 90% (29th) exceedance of the 32 GCM-PS shown in Figure 5-1. Seasonal scaling factors from the selected GCMs (i.e. GFDL-ESM4 and INM-CM5-0) were then uniformly applied to each SILO climate grid cell sequence to transform the historical climate variables to the corresponding Cdry and Cwet future climate projection. The scaling factors for the Cdry and Cwet future climate scenarios are listed in Table 5-2. The calibrated river model was used to simulate the river flow at the boundary of the Victoria catchment hydrodynamic model domain under Cdry and Cwet scenarios (Hughes et al., 2024b).

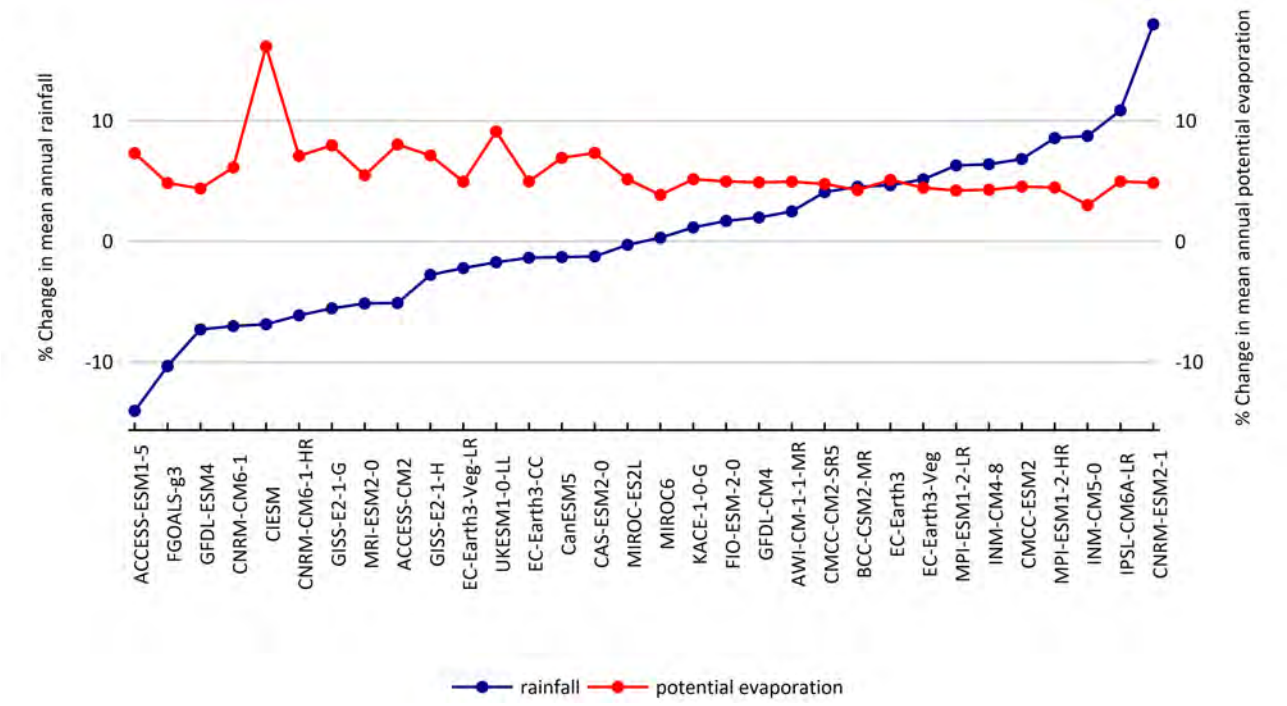

Figure 5-1 Percentage change in mean annual rainfall and mean annual potential evaporation under Scenario C relative to Scenario A (Baseline)

Simple scaling of rainfall and potential evaporation have been applied to global climate model output. GCMs are ranked by increasing rainfall.

Table 5-2 Scaling factors for the selected future climate scenarios

FUTURE CLIMATE SCENARIO	SELECTED GLOBAL CLIMATE MODEL	VARIABLE	ANNUAL SCALING FACTOR	DECEMBER. JANUARY AND FEBRUARY SCALING FACTOR	MARCH, APRIL AND MAY SCALING FACTOR	JUNE, JULY AND AUGUST SCALING FACTOR	SEPTEMBER, OCTOBER AND NOVEMBER SCALING FACTOR
Cdry	GFDL-ESM4	Precipitation	0.927	0.933	0.693	1.122	1.257
		Evaporation	1.044	1.031	1.066	1.055	1.032
Cwet	INM-CM5-0	Precipitation	1.087	1.153	0.887	1.004	1.043
		Evaporation	1.030	1.023	1.032	1.042	1.028

Figure 5-2 shows simulated monthly streamflow (catchment mean runoff, used as an input to the hydrodynamic model) under scenarios A, Cdry and Cwet from 2000 to 2023 (the hydrodynamic model was calibrated for flood events within this period). Under Scenario Cwet, the mean annual catchment streamflow increased by 31%, and the mean wet-season (December to March) streamflow increased by 33% at the G8110113 gauge on the Victoria River. These increases were 25% and 27%, respectively, at the G110006 gauge on the West Baines River. Under Scenario Cdry, the mean annual catchment streamflow decreased by 24% and the mean wet-season streamflow by 26% at the G8110113 gauge. The changes were 16% and 20%, respectively, for the G110006 gauge.

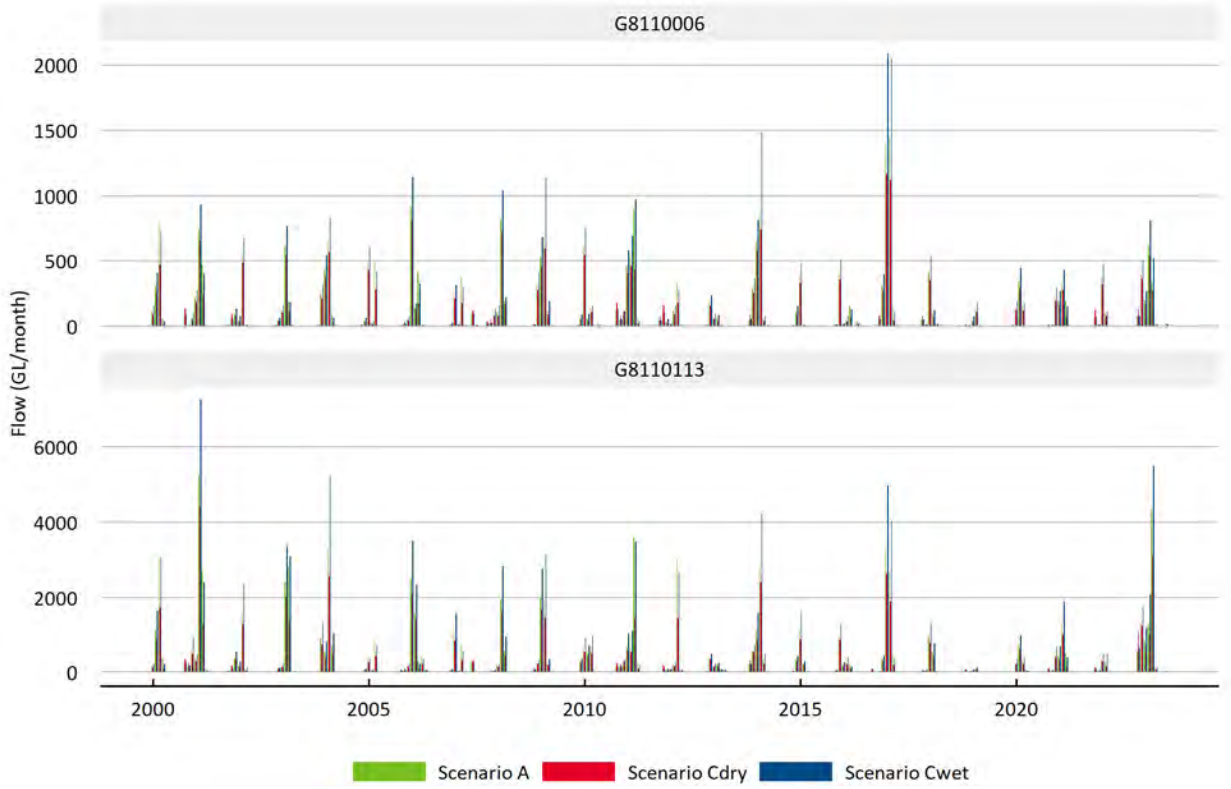

Figure 5-2 Cdry and Cwet river flow scenarios as compared with current climate (for 2000 to 2023) at the boundary of the hydrodynamic model for the Victoria catchment

Figure 5-3 compares the river flow under the current and future climate for the Victoria River system, used as inflows in the hydrodynamic model for the 2021 and 2023 flood events (Section 4.4). It shows relatively large changes in peak and total discharge under scenarios Cwet and Cdry compared with Scenario A for each event. Under Scenario Cdry, the peak streamflow at gauge G8110113 decreased by 26% and 31% for the 2021 and 2023 flood events, respectively. For the gauge G8110006, these changes were 13% and 18% for the 2021 and 2023 flood events, respectively. For both gauges, the increases under Cwet were higher than the decreases under Cdry.

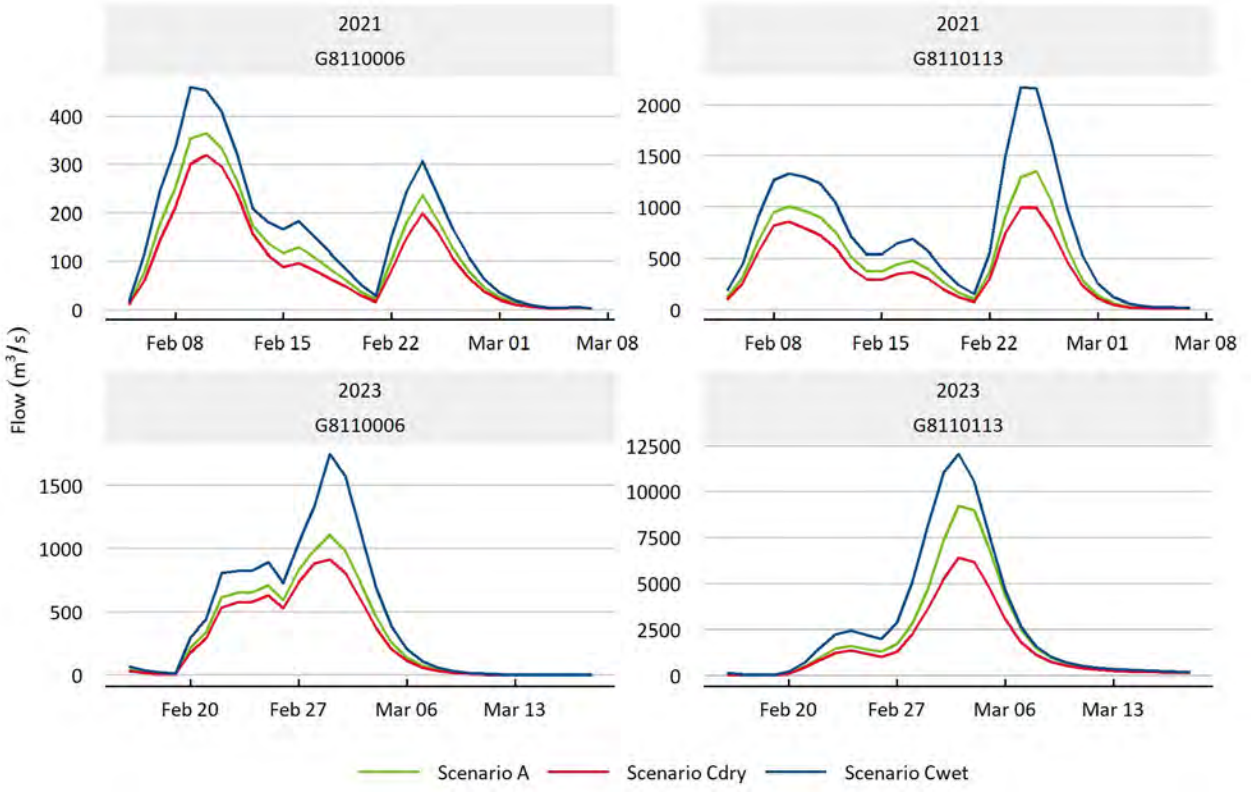

Figure 5-3 Simulated aggregated streamflow used as inflows in the hydrodynamic model (at G8110006 on the West Baines River and at G8110113 on the Victoria River) for two different flood events (in 2021 and 2023) under scenarios A (Baseline), Cdry and Cwet

5.3 Hypothetical development scenarios

5.3.1 INSTREAM DAMS

The potential dams identified in the companion technical report on surface water storage (Yang et al., 2024) were located outside the hydrodynamic model domain. Hence, to explore the impact of instream dams, river system models were configured for various scenarios (refer to the companion technical report on river model scenario analysis, Hughes et al. (2024b), and the river system model output published in that report for the streamflows at the upstream boundary of the hydrodynamic model domain). Only streamflows at the upstream boundaries of the hydrodynamic model domain were updated; the remaining input datasets and boundary conditions in the calibrated hydrodynamic models remained unchanged.

Several potential dam sites were investigated in the Victoria catchment for irrigation and hydro-electric power generation (Yang et al., 2024). However, only three instream dams were considered for inundation impact assessment (Figure 5-4). These were Dam 131 on the Leichhardt Creek, Dam 134 on the Victoria River and Dam 230 on the Gipsy Creek. The capacities of these dams at full supply level are 128, 5899 and 82 GL, respectively. At the beginning of each flood event, the dams were set to 50% full.

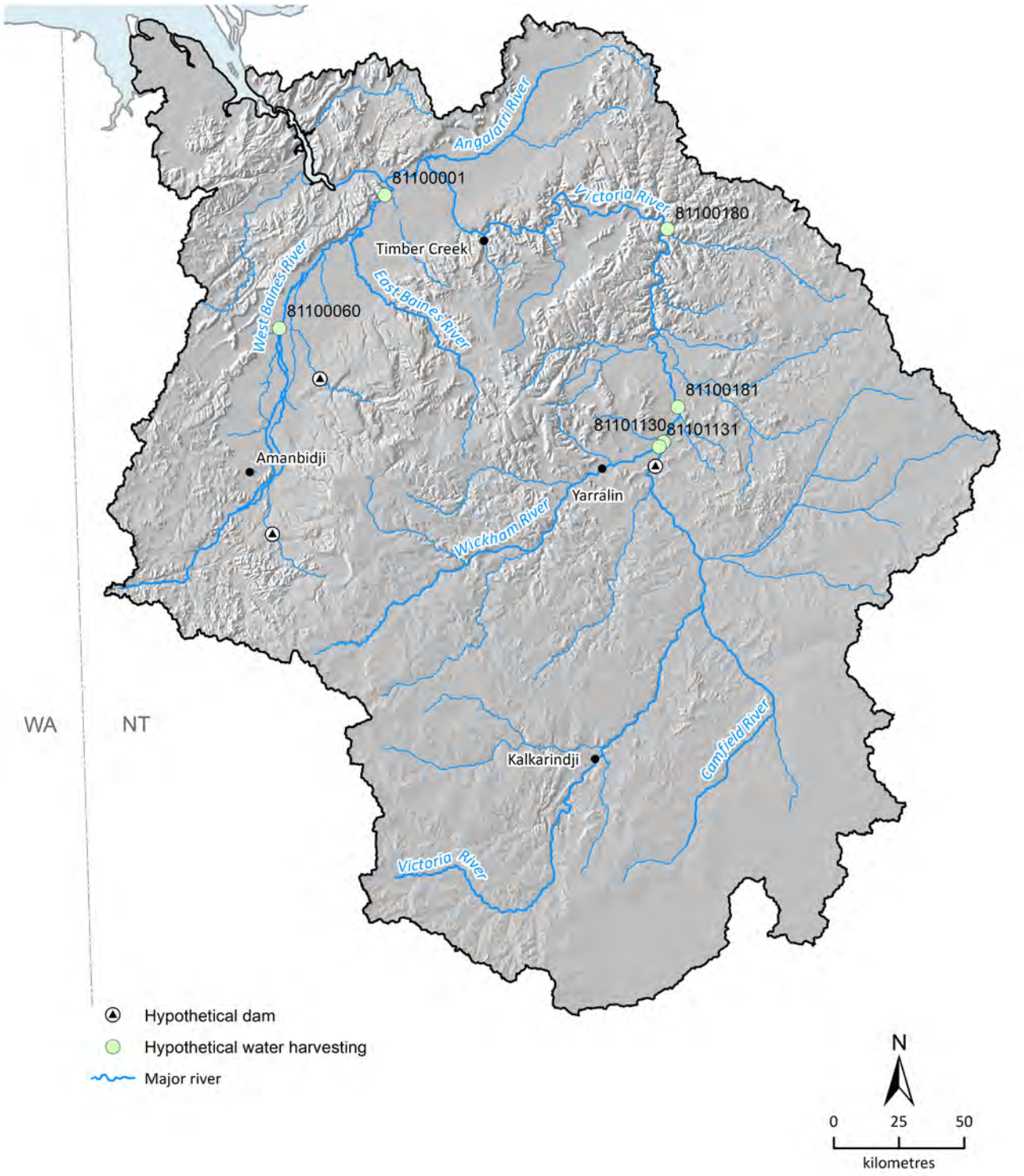

Figure 5-4 Potential dam and water harvesting sites in the Victoria catchment for impact assessment

Reservoir storages are at the specified full supply levels.

The Victoria catchment features a highly seasonal climate, with the majority of streamflow occurring in the months January to March (Hughes et al., 2024a). The effects of instream dams on river flow were simulated in the catchment at various locations for 133 years (1890 to 2022). One characteristic of the dams used for simulated irrigation supply was the annual cycle of filling across the wet season and of emptying across the dry season due to irrigation diversion and evaporation from the dams. This pattern can be seen in the plot of mean monthly dam storage at dam site 134, located centrally on the Victoria River (Figure 5-5).

Figure 5-5 Mean monthly dam storage (as a percentage of total dam capacity) at dam site 134 in the Victoria catchment

As a percentage of total dam capacity, dam storage approaches 100% full in March, and empties across the dry season with irrigation diversion. With regard to floods, this means that, generally, there could be very little mitigation of flood events later in the wet season, particularly during March and April, whereas maximum flood mitigation would be expected to be possible for events in the late dry/early wet season (November and December). The implementation of transparent flows, largely for environmental amelioration, would reduce the mean dam storage at any time of the year, thereby increasing the potential for flood mitigation.

These patterns of storage have consequences for hydrodynamic simulation of instream dam scenarios. In particular, simulated flood events later in the wet season are less likely to generate substantial change in the estimated flooded area due to the antecedent storage. Ideally hydrodynamic models would be run for the entire 133-year period, as for the Victoria catchment model. This would give a better understanding of the effects of dams on flood mitigation. However, due to the very high computational demand of hydrodynamic models, only selected flood events can be simulated. To counter this, two approaches were taken. First, for each simulated event, the reservoir storage was reduced to 50% immediately prior to the event. Second, a regression between the river flow at multiple locations and the estimated flooded area was derived. This was then used to estimate the total flooded area for various scenarios across the entire time series of the river model. This was denoted the flood 'emulator' and allowed for a more balanced assessment of the relative effects of each scenario on the flooded area, since it enabled a daily estimate of the flooded area that took into account any antecedent effects. More detailed information on the emulator can be found in Section 5.5.

5.3.2 WATER HARVESTING

Water harvesting was modelled for six locations on the West Baines and Victoria rivers (Figure 5-4). The total annual withdrawal limit of these sites was set at 680 GL, with a pump rate of 200 ML/day. Within the Victoria catchment, the availability of soils suitable for irrigation within a

reasonable distance of surface water is relatively limited. For this reason, soil-limited water harvesting scenarios were investigated using the flood inundation models. The soil-limited water harvesting scenario represented an annual diversion of 680 GL at 75% annual reliability with no end-of-system requirement (Hughes et al., 2024b). Where water harvesting occurred within the hydrodynamic model domain, distributed extractions were introduced along the relevant river sections. Water harvesting outside the hydrodynamic model domain was incorporated into the model through the changes in inflow to the model domain. Water harvesting within the hydrodynamic model domain was incorporated into the model using water sinks at the relevant locations. Refer to the companion technical report on river model calibration and scenario analysis, Hughes et al. (2024b), for further details about the instream dam and water harvesting scenarios.

5.4 Floodplain inundation scenario analysis

Evaluation of the hydrodynamic modelled scenarios was undertaken by comparing future development (Scenario B), future climate (Scenario C) and future climate and development (Scenario D) scenarios with the baseline simulation (Scenario A). Two types of evaluation were performed across the hydrodynamic model domain for each scenario (Table 5-1):

- a spatial comparison using maps of percentage inundation frequency (the ratio of the number of times a pixel was inundated to the entire duration of the simulation), maximum inundation extent, and inundated depth at maximum inundation extent
- a time-series comparison of inundated area.

5.4.1 SCENARIO B CURRENT CLIMATE AND INSTREAM DAM

Figure 5-6 shows the maximum inundation extent as well as the spatial variation in inundation frequencies for the 2021 (AEP of 1 in 3) and 2023 (AEP of 1 in 18) flood events. The three dams decreased the inundation extent and frequency, but the effects were relatively small in the model domain. Similarly to inundation frequency, the effects on spatial inundation depth were also small (Figure 5-7). However, changes in inundation area due to the dams were noticeable for both the 2021 and 2023 flood events (Figure 5-8). The maximum inundated area for the 2021 event (AEP of 1 in 3) was 321.9 km^2 under Scenario A (Baseline) and 298.2 km^2 under Scenario B (3-dams). This represents a decrease in inundated area of approximately 7.4%. The maximum inundated area for the 2023 event (AEP of 1 in 18) was 1562.4 km^2 under Scenario A (Baseline) and 1405.6 km^2 under Scenario B (3-dams), representing a decrease of approximately 10%. The larger relative impact found for the 1 in 18 AEP event during 2023 was due to the different antecedent conditions at the beginning of the two events, in combination with the decision to reduce the dam storage to 50% immediately prior to the flood event. This can perturb the scenario effect, depending upon the nature of the flood hydrograph. For example, the 2021 flood had one minor peak before the main peak, which filled the dam partially before the second peak.

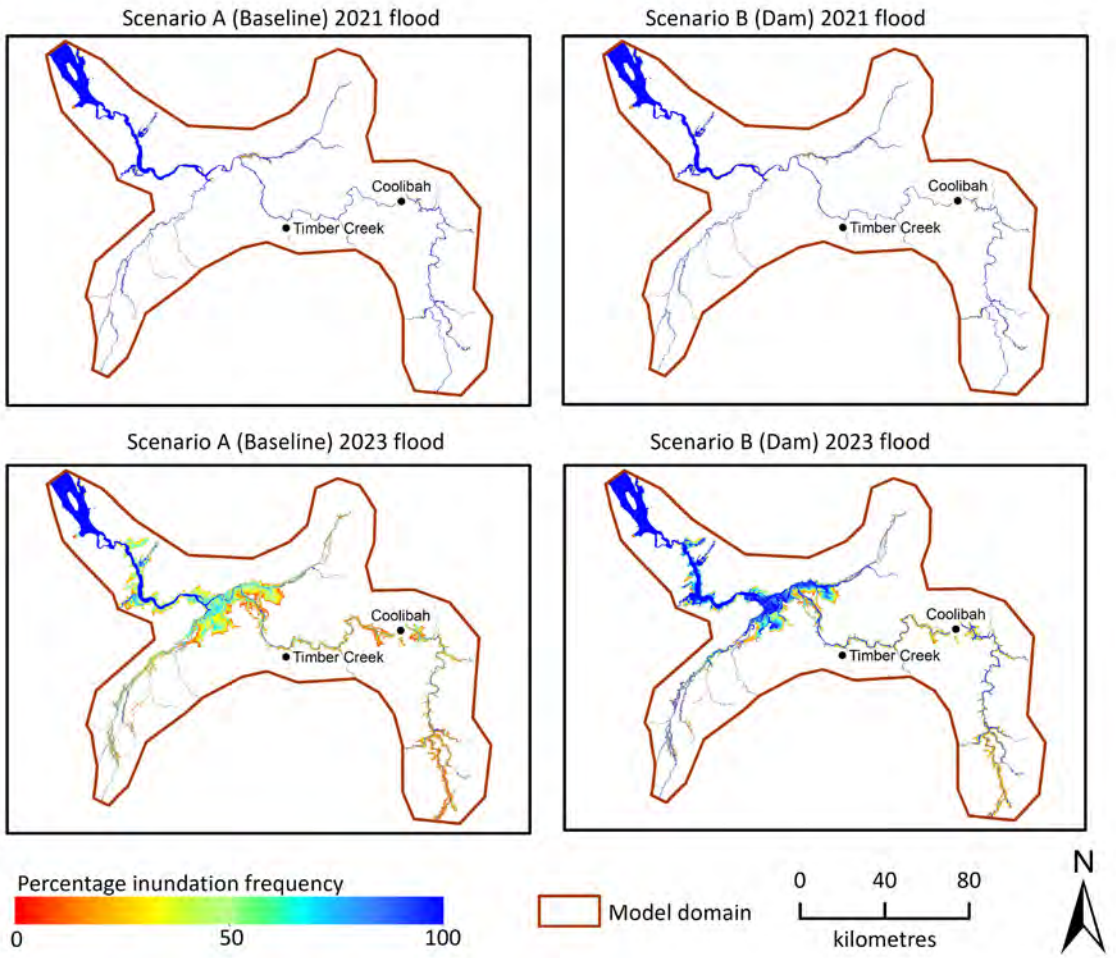

Figure 5-6 Percentage inundated frequency in the Victoria hydrodynamic model domain under scenarios A (Baseline) and B (3-dams)

The 2021 flood event had an AEP of 1 in 3, and the 2023 flood event had an AEP of 1 in 18.

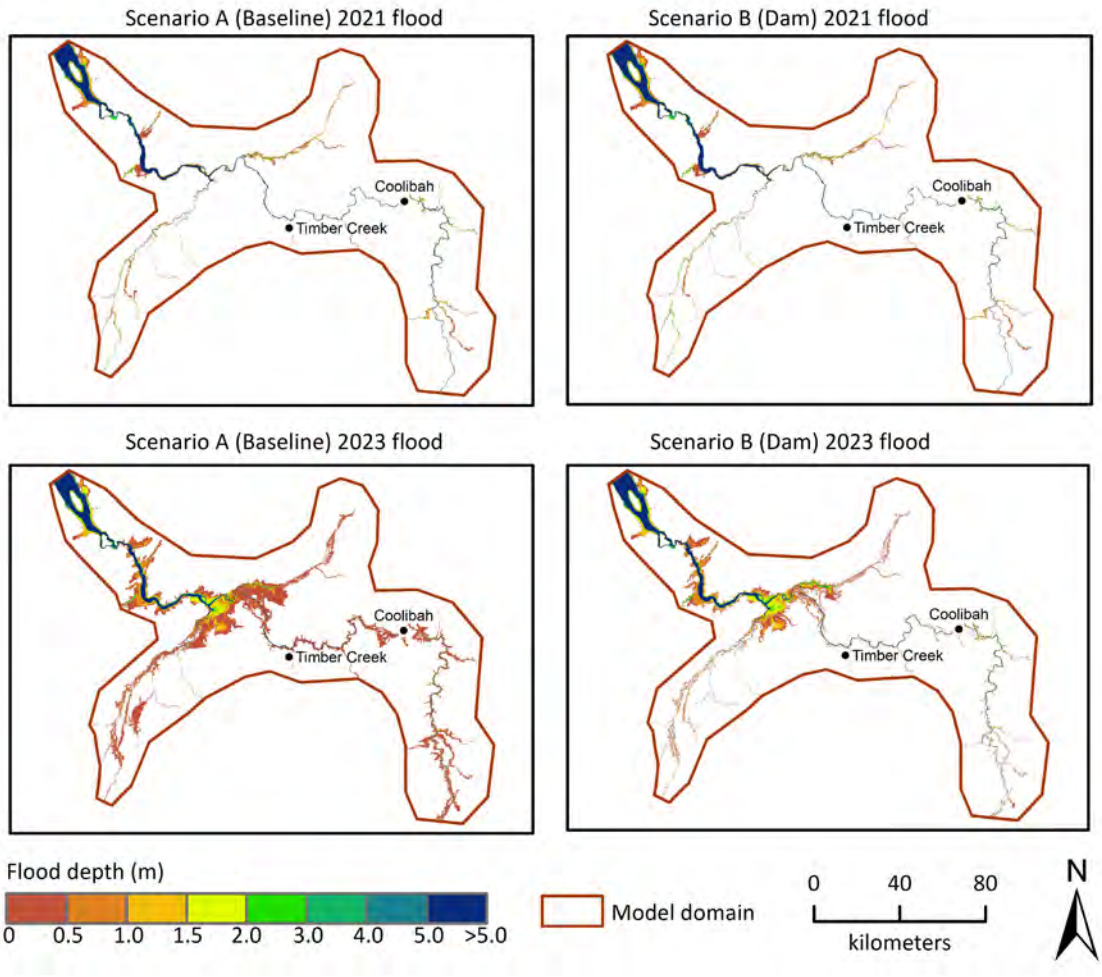

Figure 5-7 Depth at maximum inundation extent in the Victoria catchment hydrodynamic model domain under scenarios A (Baseline) and B (3-dams)

The 2021 flood event had an AEP of 1 in 3, and the 2023 flood event had an AEP of 1 in 18.

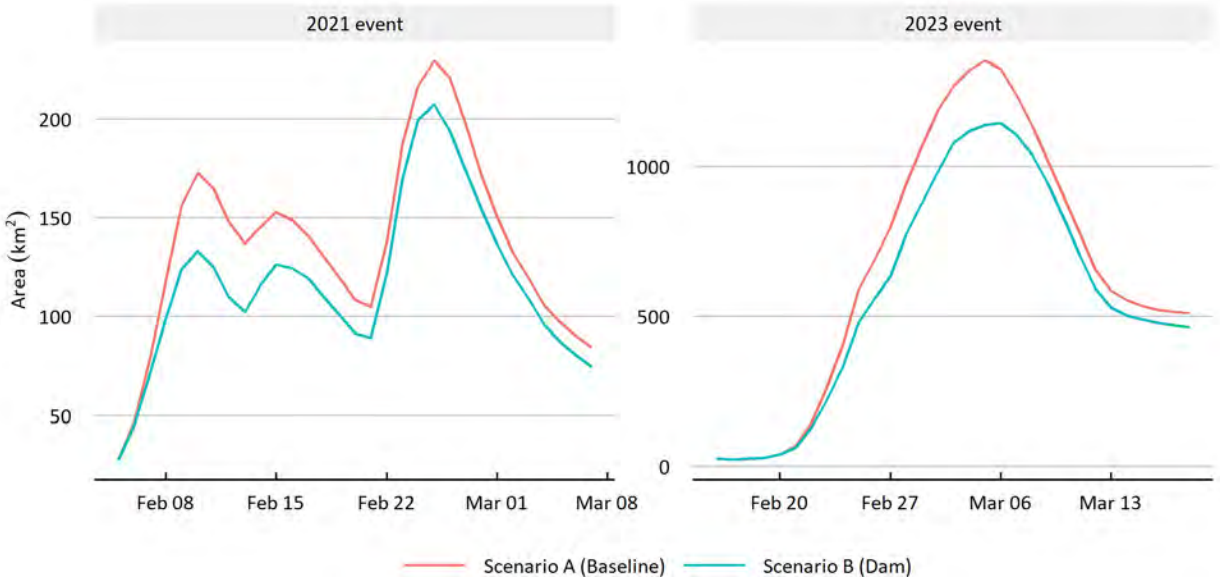

Figure 5-8 Comparison of inundated area (in square kilometres) under scenarios A (Baseline) and B (3-dams)

The 2021 flood event had an AEP of 1 in 3, and the 2023 flood event had an AEP of 1 in 18.

5.4.2 SCENARIO B CURRENT CLIMATE AND WATER HARVESTING

Figure 5-9 shows the maximum inundation extent as well as the spatial variation in inundation frequencies for the 2021 (AEP of 1 in 3) and 2023 (AEP of 1 in 18) flood events. Water extraction reduces the flow in the river and produces less inundation. In general, the effect of the water harvesting is small for the maximum inundation extent as well as inundation frequency. As for inundation frequency, the effect on inundation depth is small (Figure 5-10). However, changes in inundation areas due to water harvesting are noticeable for both the 2021 and 2023 flood events (Figure 5-11). The impacts of water harvesting on flood characteristics over the hydrodynamic model domain are larger for the smaller event relative to those for the larger events. The maximum inundated area under Scenario A (Baseline) for the 2021 event (AEP of 1 in 3) was 321.9 km^2, and 301.3 km^2 under Scenario B (Water Harvesting of 680 GL). This represents a decrease in inundated area of approximately 6.4%. The maximum inundated area for the 2023 event (AEP of 1 in 18) was 1562.4 km^2 under Scenario A (Baseline) and 1525.5 km^2 under Scenario B (Water Harvesting), representing a decrease of approximately 2.4%. As expected, the impacts were larger for the smaller flood event, because the same amount of water is extracted for both flood events. It is important to note that the 2021 flood event had two peaks and that water extractions were implemented during the larger peak.

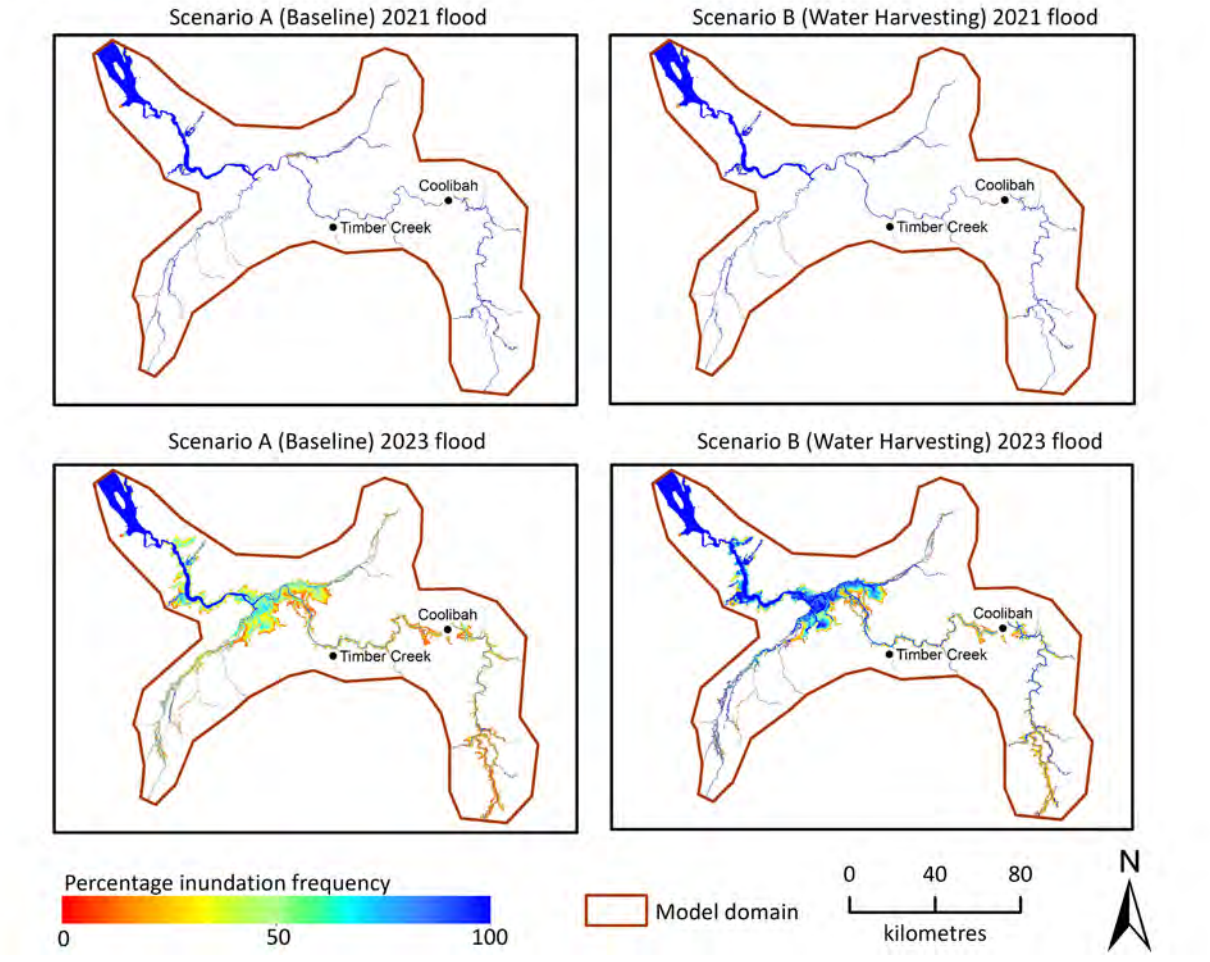

Figure 5-9 Percentage inundated frequency in the Victoria catchment hydrodynamic model domain under Scenario A (Baseline) and B (Water Harvesting)

The 2021 flood event had an AEP of 1 in 3, and the 2023 flood event had an AEP of 1 in 18.

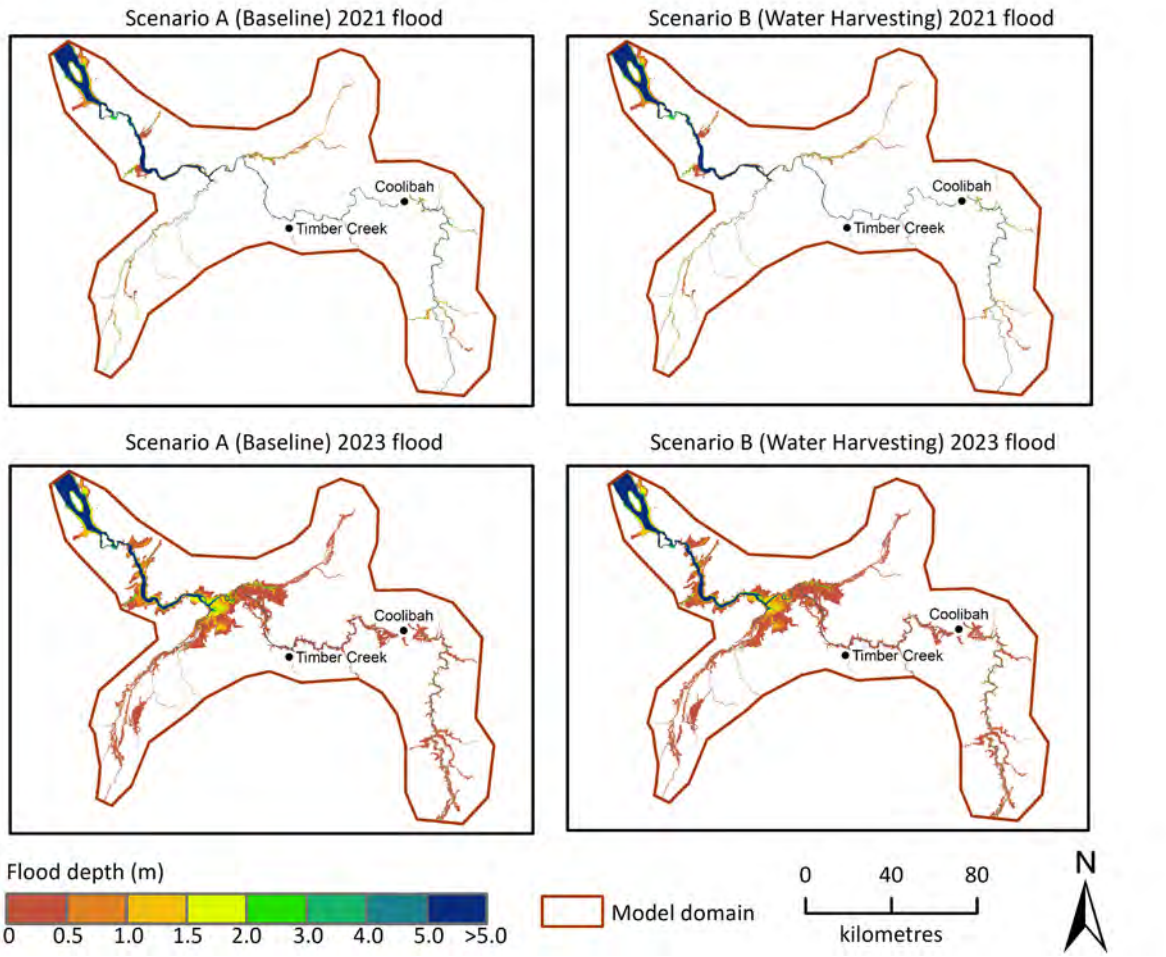

Figure 5-10 Depth at maximum inundation extent in the Victoria catchment hydrodynamic model domain under scenarios A (Baseline) and B (Water Harvesting)

The 2021 flood event had an AEP of 1 in 3, and the 2023 flood event had an AEP of 1 in 18.

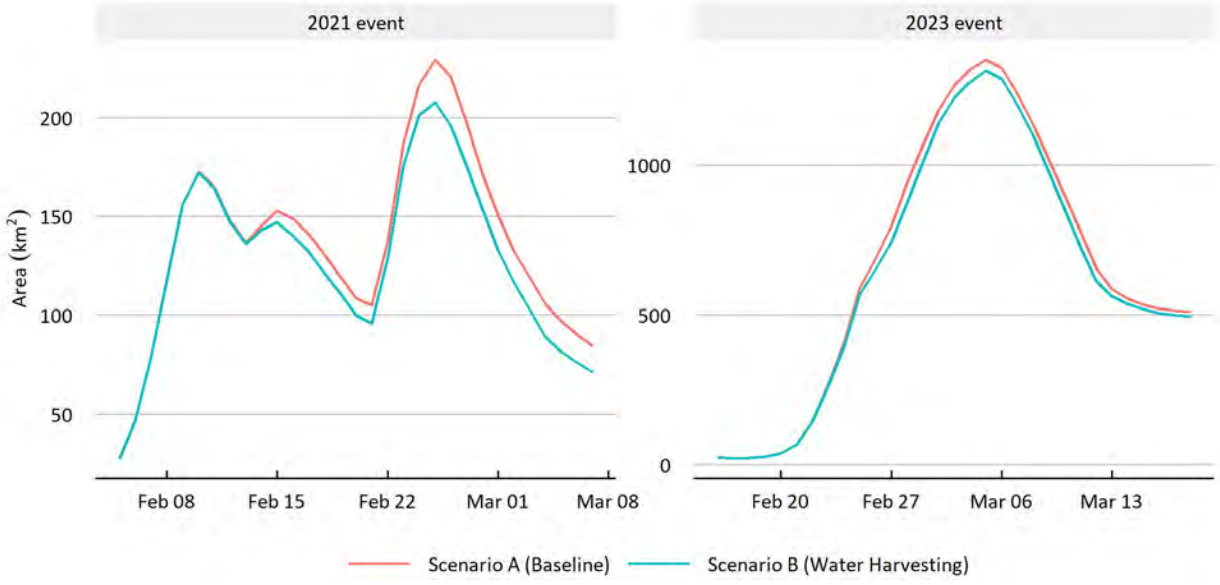

Figure 5-11 Comparison of inundated area (in square kilometres) in the Victoria catchment hydrodynamic model domain under scenarios A (Baseline) and B (Water Harvesting)

The 2021 flood event had an AEP of 1 in 3, and the 2023 flood event had an AEP of 1 in 18.

5.4.3 SCENARIO C FUTURE CLIMATE SCENARIOS

Figure 5-12 shows the difference between scenarios A, Cdry and Cwet in terms of percentage inundated frequency and maximum inundation extent. The results show decreases in percentage inundated frequency and inundation extent for Scenario Cdry compared with Baseline scenarios. Conversely, a significant increase can be seen in Scenario Cwet compared with Scenario A (Baseline). Similar changes are noticed for spatial inundation depth (Figure 5-13). The maximum inundated areas under scenarios Cdry and Cwet for the 2021 event (AEP of 1 in 3) were 279.1 km^2 and 591.3 km^2, respectively, a reduction of 13.3% for Cdry and an increase of 83.7% for Cwet. For the 2023 event (AEP of 1 in 18), the maximum inundated areas under scenarios Cdry and Cwet were 1206.8 km^2 and 2050.1 km^2, respectively, indicating a reduction of 22.8% for the Cdry scenario and an increase of 31.2% for the Cwet scenario. Although the relative increase for the 2021 was higher (83.7%) than for the 2023 event (22.8%), the absolute increase in inundation area was higher for the 2023 event (487.7 km^2) than for the 2021 event (269.4 km^2).

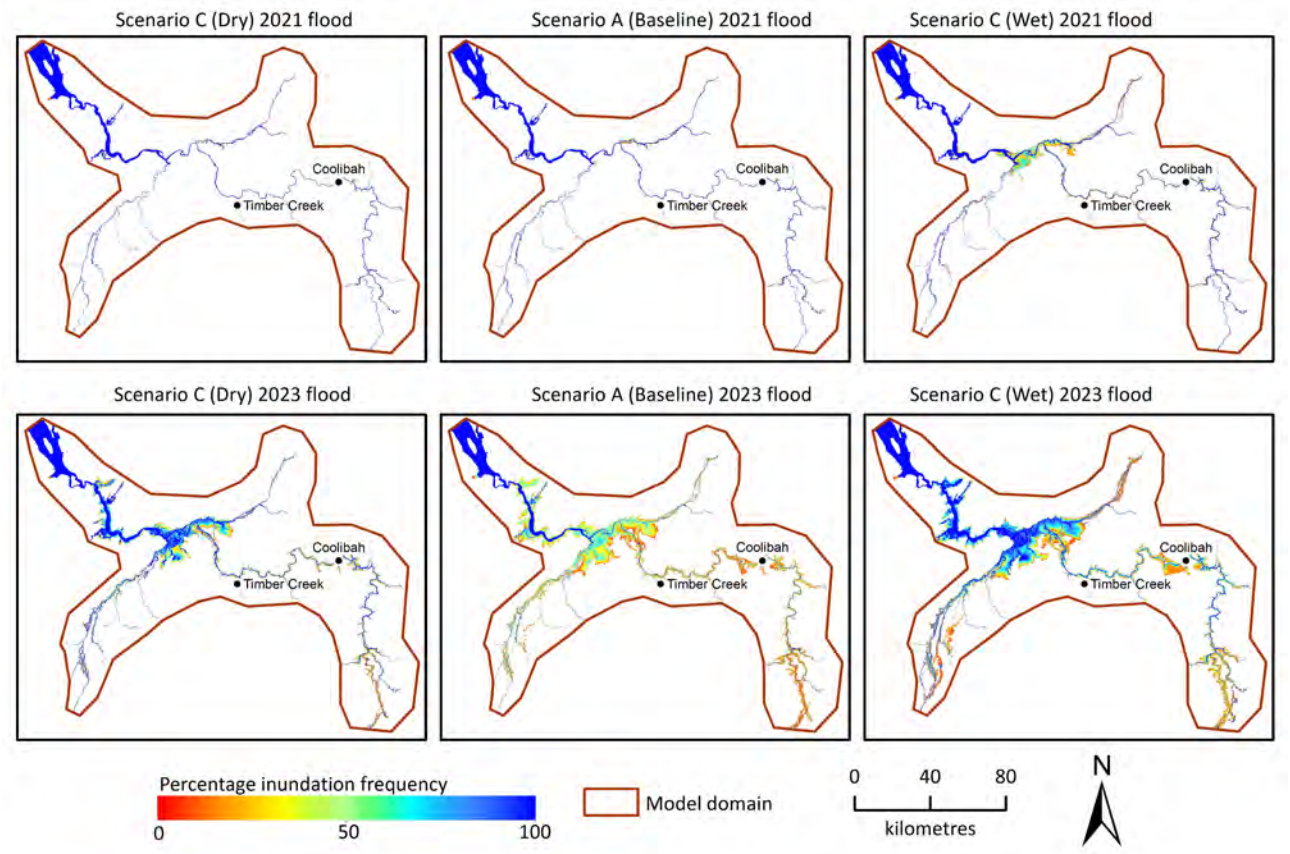

Figure 5-12 Percentage inundated frequency in the Victoria catchment hydrodynamic model domain under scenarios A (Baseline) and C (Future climate)

The 2021 flood event had an AEP of 1 in 3, and the 2023 flood event had an AEP of 1 in 18.

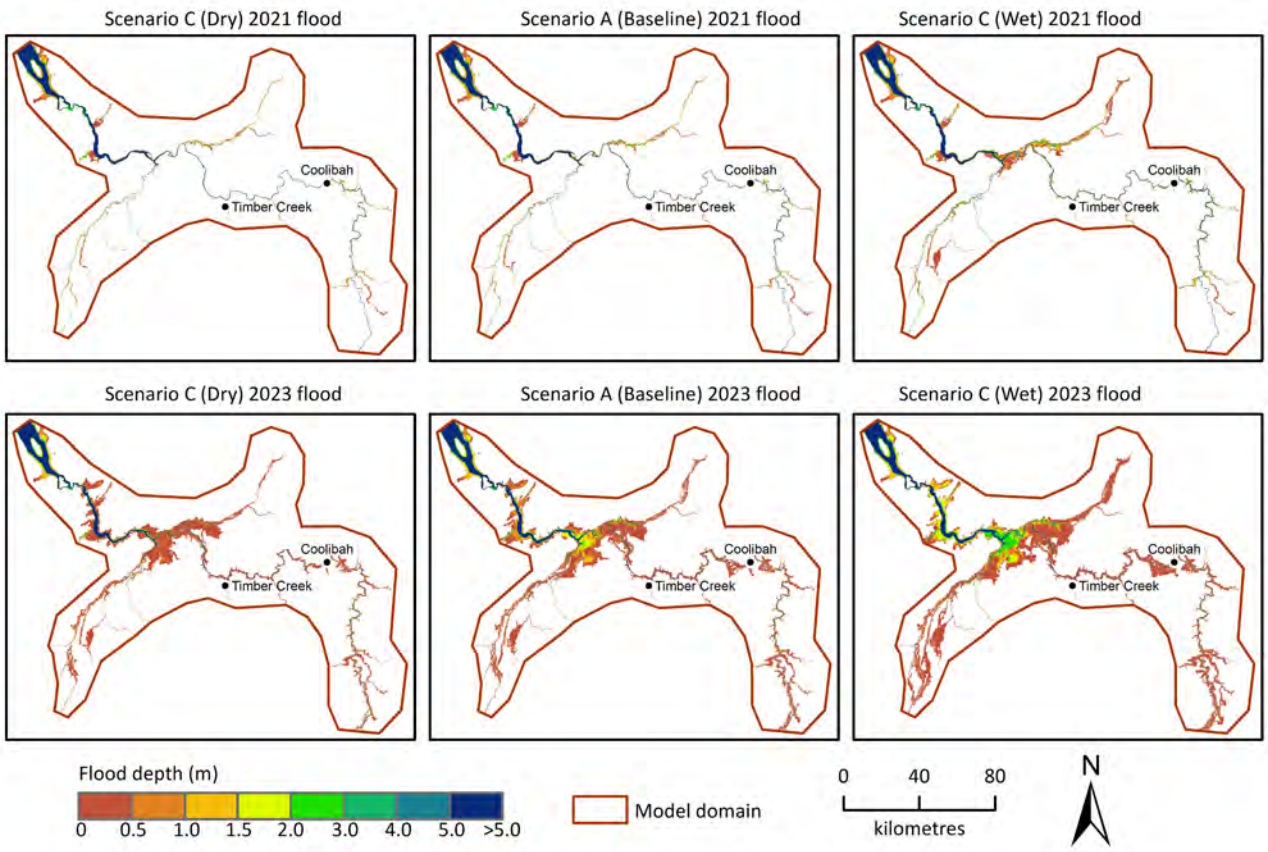

Figure 5-13 Depth at maximum inundation extent in the Victoria hydrodynamic model domain under scenarios A (Baseline) and C (Future climate)

The 2021 flood event had an AEP of 1 in 3, and the 2023 flood event had an AEP of 1 in 18.

The time series in Figure 5-14 shows large differences between the climate scenarios in the inundated area that occurred under scenarios Cdry and Cwet, compared with under Scenario A for both events. The differences were largest at the times of peak inundation, particularly during Scenario Cwet. Under Scenario Cdry, the peak in the inundated area decreased by approximately 13.1% and 22.9% for the 2021 and 2023 flood events, respectively. Under Scenario Cwet, the peak in inundated area increased by approximately 83.2% and 30% for the 2021 and 2023 flood events, respectively. Table 5-3 summarises the inundated area under Scenario C and the changes in maximum and mean inundation areas compared with Scenario A (Baseline).

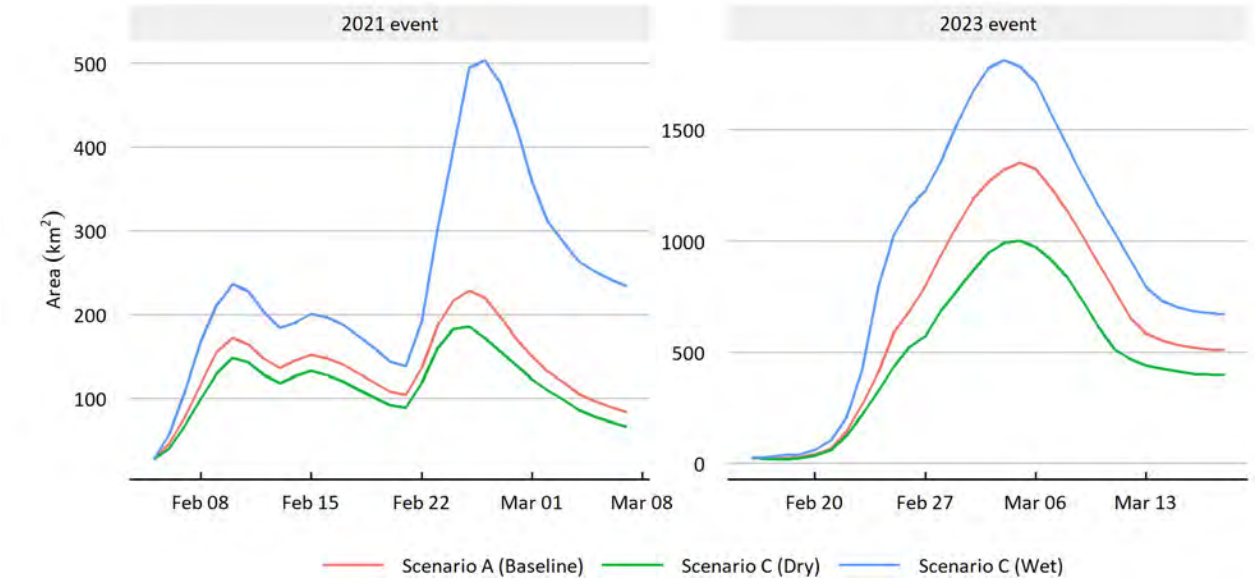

Figure 5-14 Comparison of inundated area (in square kilometres) in the Victoria catchment hydrodynamic model domain under scenarios A (Baseline) and C (Future Climate)

The 2021 flood event had an AEP of 1 in 3, and the 2023 flood event had an AEP of 1 in 18.

Table 5-3 Comparison of the inundated area and associated changes under Scenario C (Future Climate) relative to Scenario A (Baseline)

The 2021 flood event had an AEP of 1 in 3, and the 2023 flood event had an AEP of 1 in 18.

	2021 FLOOD Cdry	2023 FLOOD Cdry	2021 FLOOD Cwet	2023 FLOOD Cwet
Maximum inundated area (km²)	279.1	1206.8	591.3	2050.1
% change in maximum inundated area	−13.3	−22.8	83.7	31.2
Mean inundated area (km²)	215.1	671.0	344.2	1098.4
% change in mean inundated area	−9.2	−20.3	45.3	30.4

5.4.4 SCENARIO D DRY CLIMATE AND INSTREAM DAM

The maps of percentage inundated frequency (Figure 5-15) and depth at maximum inundation (Figure 5-16) show that the three instream dams combined with the future dry climate decreased inundation (frequency, extent and depth) for both the 2021 (AEP of 1 in 3) and 2023 (AEP of 1 in 18) flood events. The combined impacts of dry climate and three dams on inundation extent and frequency were significant, although the climate appears to have been the main driver of the differences. The maximum inundated area under scenarios A (Baseline) and D (Dry Climate and Dam) for the 2021 event were 321.9 km^2 and 260.9 km^2, respectively (Figure 5-17). This represents a decrease in inundated area of approximately 19%. The maximum inundated area under scenarios A (Baseline) and D (Dry Climate and Dam) for the 2023 event were 1562.4 km^2 and 992.5 km^2, respectively, representing a decrease of approximately 36.5%.

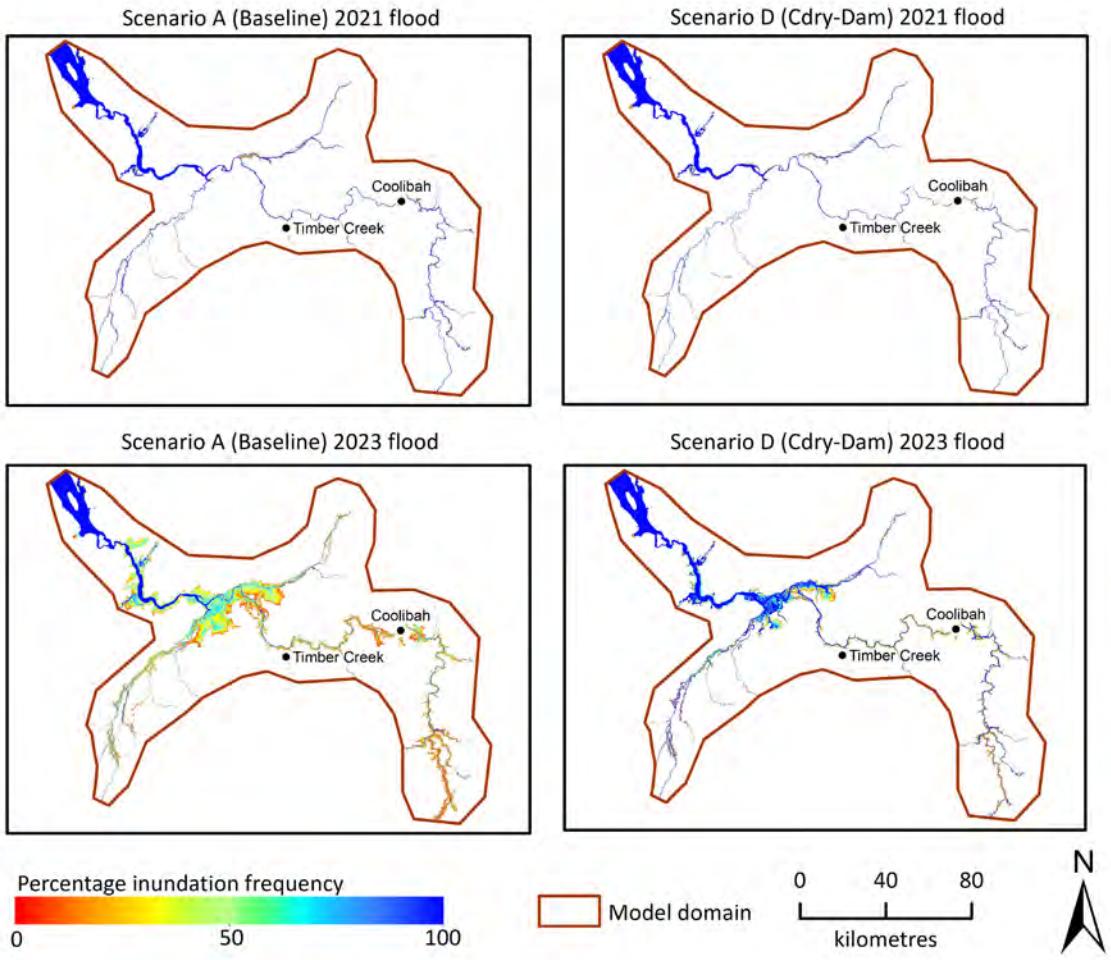

Figure 5-15 Percentage inundation frequency in the Victoria catchment hydrodynamic model domain under Scenario A (Baseline) and D (Cdry-Dam)

The 2021 flood event had an AEP of 1 in 3, and the 2023 flood event had an AEP of 1 in 18.

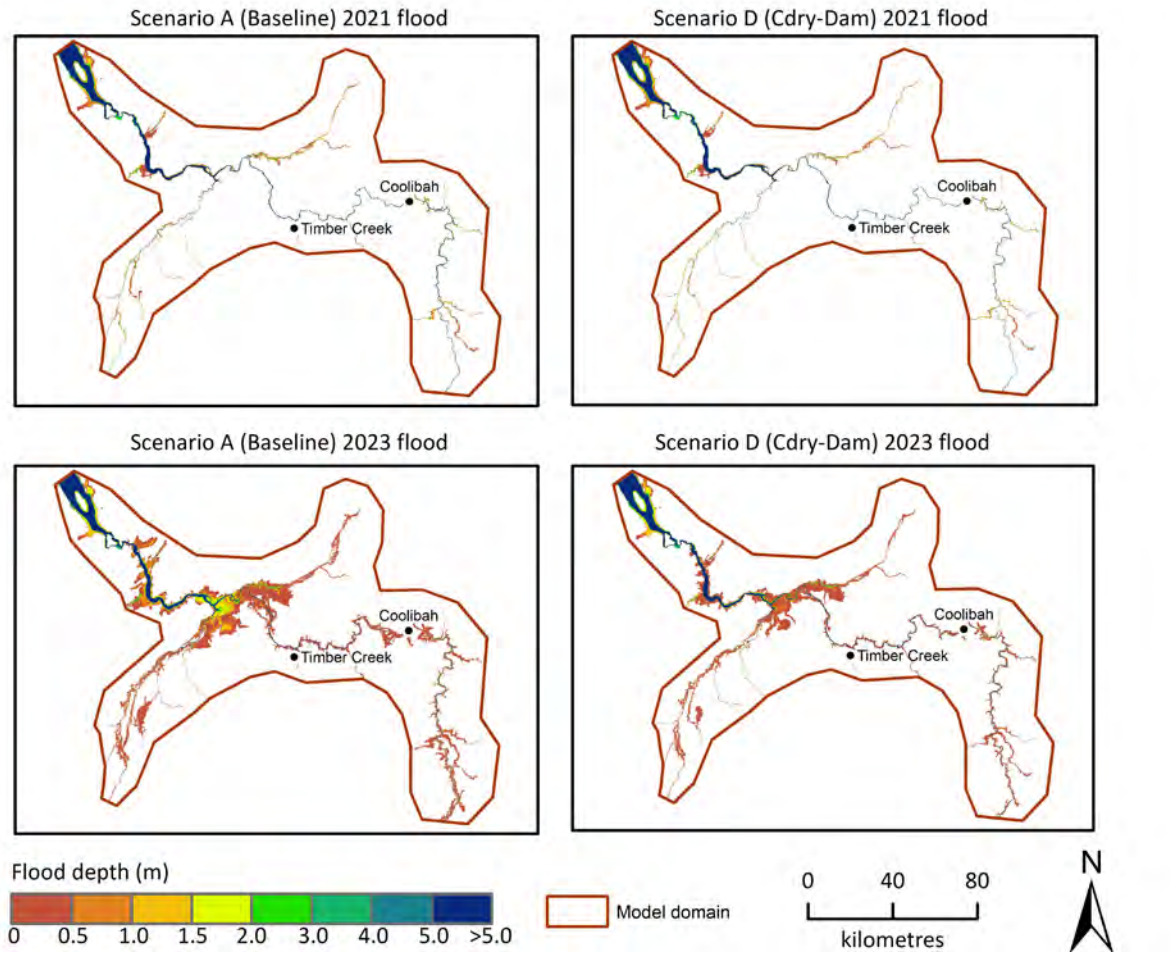

Figure 5-16 Depth at maximum inundation extent in the Victoria catchment hydrodynamic model domain under scenarios A (Baseline) and D (Cdry-Dam)

The 2021 flood event had an AEP of 1 in 3, and the 2023 flood event had an AEP of 1 in 18.

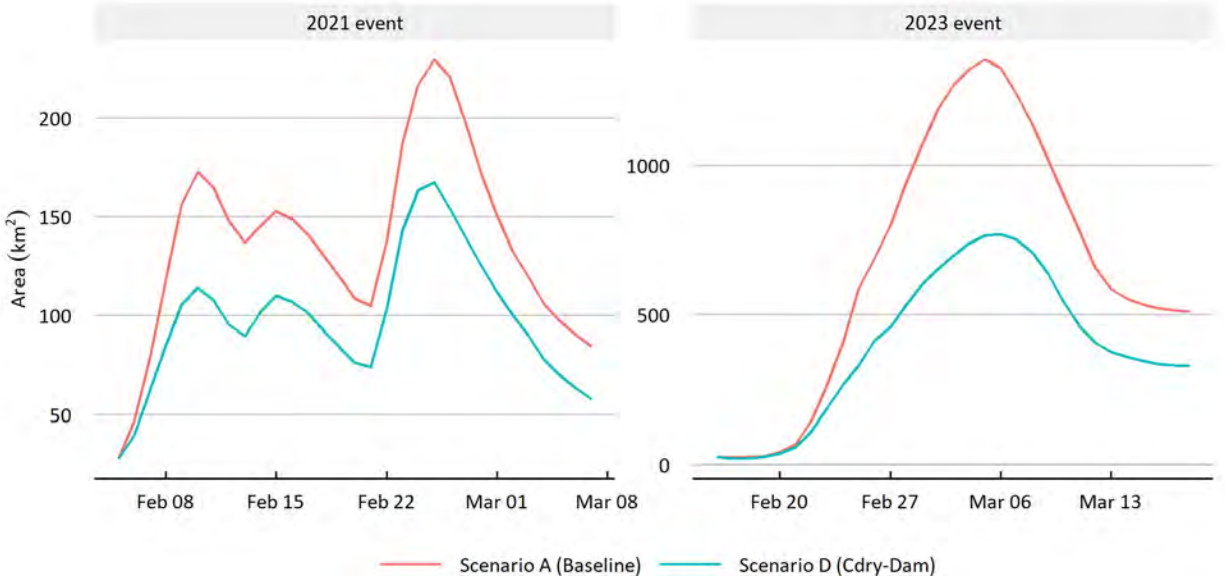

Figure 5-17 Comparison of inundated area (in square kilometres) in the Victoria catchment hydrodynamic model domain under scenarios A (Baseline) and D (Cdry-Dam)

The 2021 flood event had an AEP of 1 in 3, and the 2023 flood event had an AEP of 1 in 18.

5.4.5 SCENARIO D DRY CLIMATE AND WATER HARVESTING

Maps of percentage inundated frequency (Figure 5-18) and depth at maximum inundation (Figure 5-19) show that water harvesting under a future dry climate scenario substantially decreased inundation for the 2021 (AEP of 1 in 3) and 2023 (AEP of 1 in 13) events. The maximum inundated areas under scenarios A (Baseline) and D (Dry Climate and Water Harvesting) for the 2021 event were 321.9 km^2 and 265.9 km^2, respectively. This represents a decrease in inundated area of approximately 17.4%. The maximum inundated areas under scenarios A (Baseline) and D (Dry Climate and Water Harvesting) for the 2023 event were 1562.4 km^2 and 1153.8 km^2, respectively, representing a decrease of approximately 26.1%.

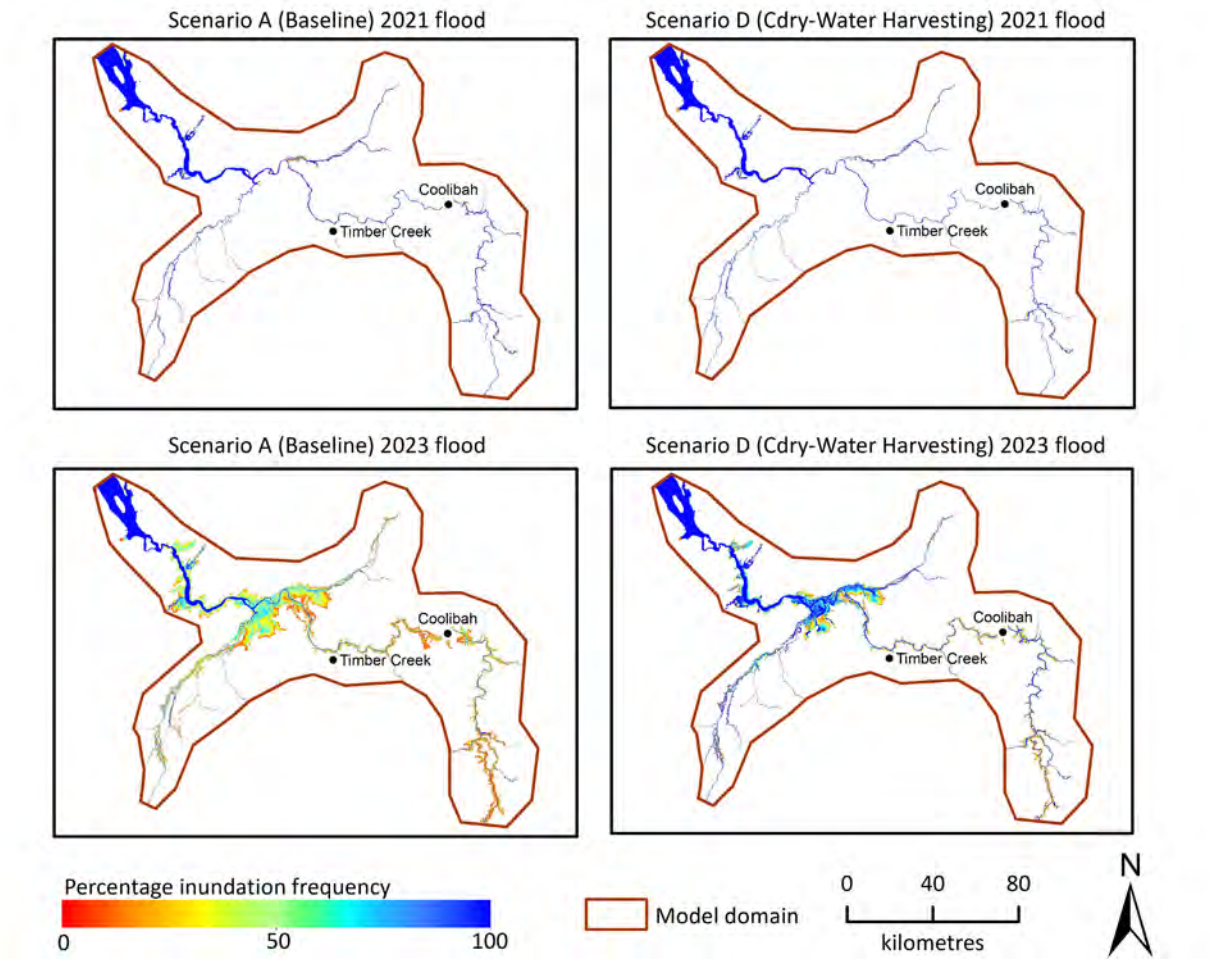

Figure 5-18 Percentage inundation frequency in the Victoria catchment hydrodynamic model domain under Scenario A (Baseline) and D (Cdry-Water Harvesting)

The 2021 flood event had an AEP of 1 in 3, and the 2023 flood event had an AEP of 1 in 18.

The impacts of water harvesting under a future dry climate scenario on flood characteristics over the hydrodynamic model domain are relatively larger for the smaller event (Figure 5-20). The maximum inundated areas under scenarios A (Baseline) and Ddry (Dry Climate and Water Harvesting) for the 2021 event were 545 km2 and 374 km2, respectively. This represents a decrease in inundated area of approximately 31%. The maximum inundated area for the 2023 event was 1697 km2 under Scenario A (Baseline), and 1330 km2 under Scenario D (Dry Climate and Water Harvesting), a decrease of approximately 22%. Figure 5-20 shows the changes in inundation area during the 30-day simulation period. The decreases for peak inundation were 18.4% and 27.3% for the 2021 and 2023 flood events, respectively.

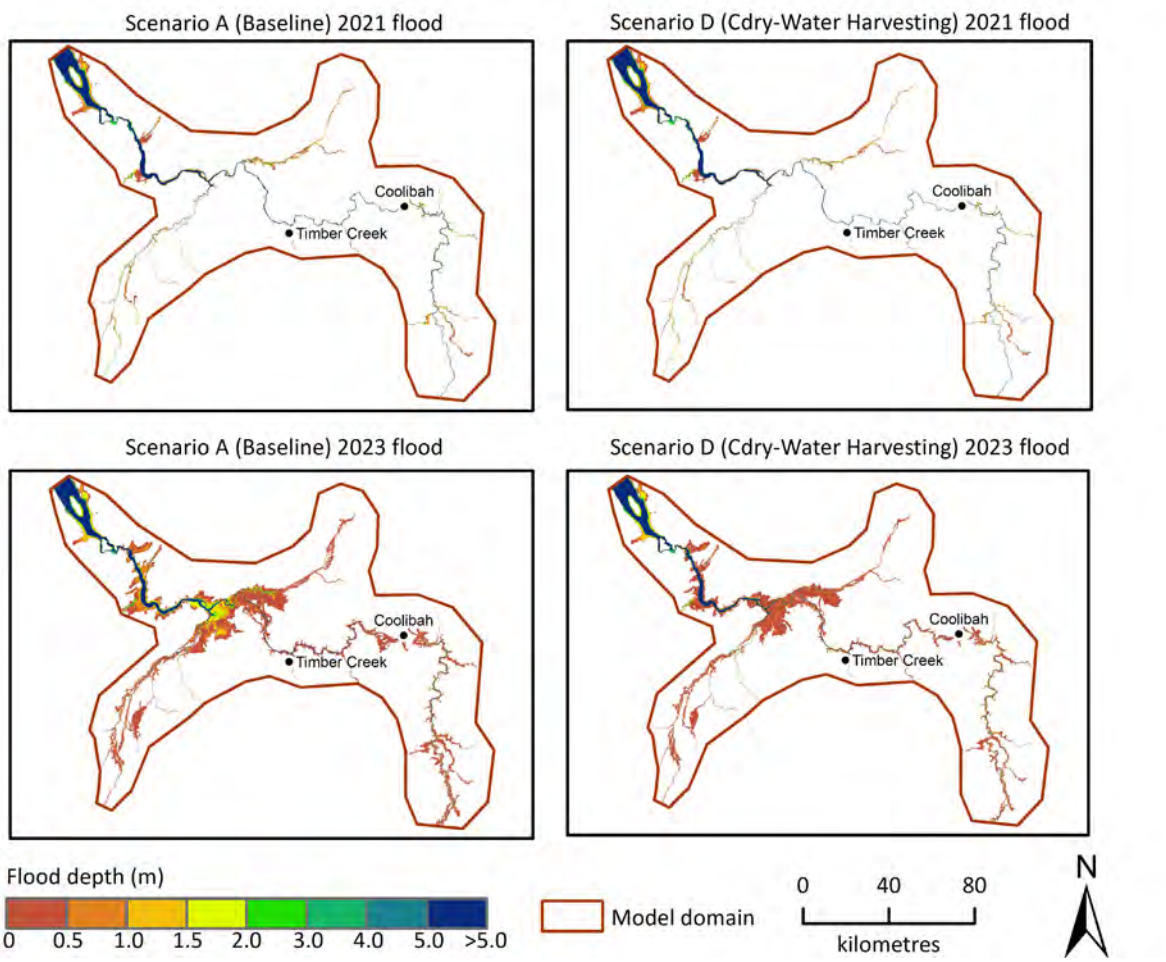

Figure 5-19 Depth at maximum inundation extent in the Victoria catchment hydrodynamic model domain under scenarios A (Baseline) and D (Cdry-Water Harvesting)

The 2021 flood event had an AEP of 1 in 3, and the 2023 flood event had an AEP of 1 in 18.

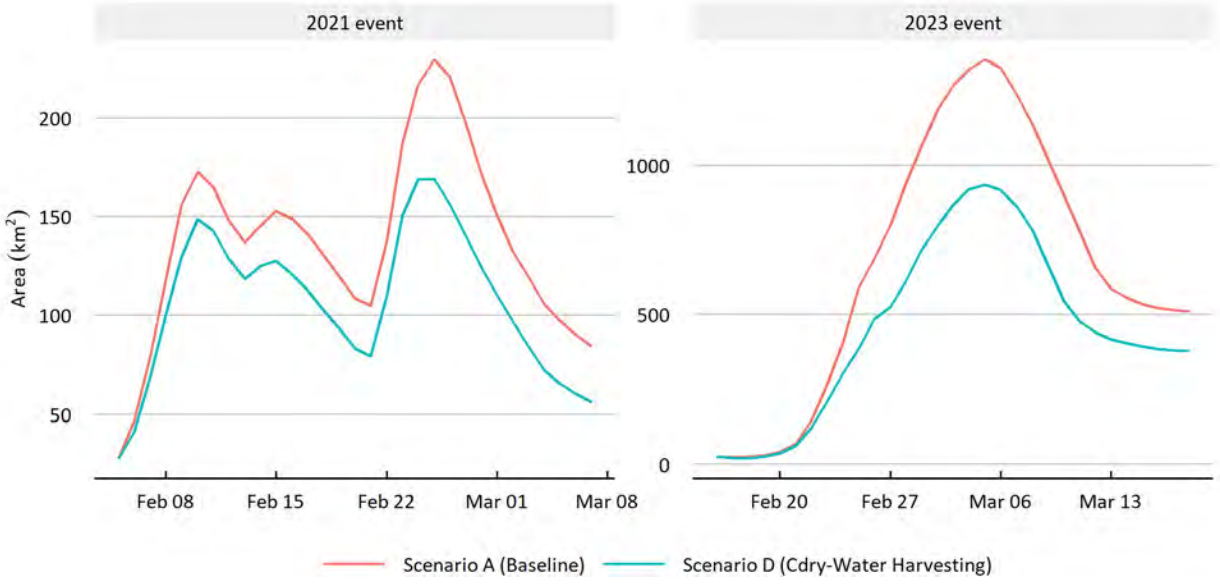

Figure 5-20 Comparison of inundated area (in square kilometres) in the Victoria catchment hydrodynamic model domain under scenarios A (Baseline) and D (Cdry-Water Harvesting)

The 2021 flood event had an AEP of 1 in 3, and the 2023 flood event had an AEP of 1 in 18.

5.5 Floodplain inundation emulator

5.5.1 DEVELOPMENT OF EMULATOR

An emulator was developed for the Assessment area by relating the hydrodynamic model–simulated inundation area to flood discharge through a regression model. Inflows to the hydrodynamic model through the two major rivers (at the 8110006 gauge on the West Baines River and 8110113 gauge on the Victoria River) were aggregated in order to produce a time series of flood discharge. Flow data were examined in relation to the flood extent data. Both event volume and peak inflow were investigated as flood extent covariates. Of the two measures, peak flow during the event period was a more reliable indicator of flood area and was chosen as the measure for use in the regression model. To ensure the calibration data covered a large range, all five calibration events, together with the Scenario Cdry and Scenario Cwet estimates of the flooded area for two events, were utilised.

A power curve in the form of $y = ax^b$ was first tested to calculate the inundation area based on input streamflow. The parameters were estimated during optimisation by minimisation of the following objective function:

$$OF = \frac{\sum_i^n |\hat{A}_i - A_i|}{n} \quad (1)$$

where $\hat{A}_i$ is the estimated flooded area, A_i is the hydrodynamic model–simulated flooded area and n is the number of events.

The calibrated emulator had the following relationship between flow and inundation area:

$$\widehat{\boldsymbol{A}} = 0.4543 * (\boldsymbol{Q}_1 + \boldsymbol{Q}_2)^{0.8739} \quad (2)$$

where $\widehat{\boldsymbol{A}}$ is the estimated time series of the flooded area (km^2), and $\boldsymbol{Q}_1$ and $\boldsymbol{Q}_2$ are the time series of flow (m^3/s) at nodes 81100060 and 81101130.

Overall, the emulator produced a good estimate of the simulated inundation area (Figure 5-21). It can be seen that there are two outliers from the fitted line. These are the calibration events in 2014 and 2016. These values (simulated by the hydrodynamic model) had relatively high FAR values when compared with the MODIS and Landsat images, indicating the possibility of overestimation of the flooded area (Table 4-5).

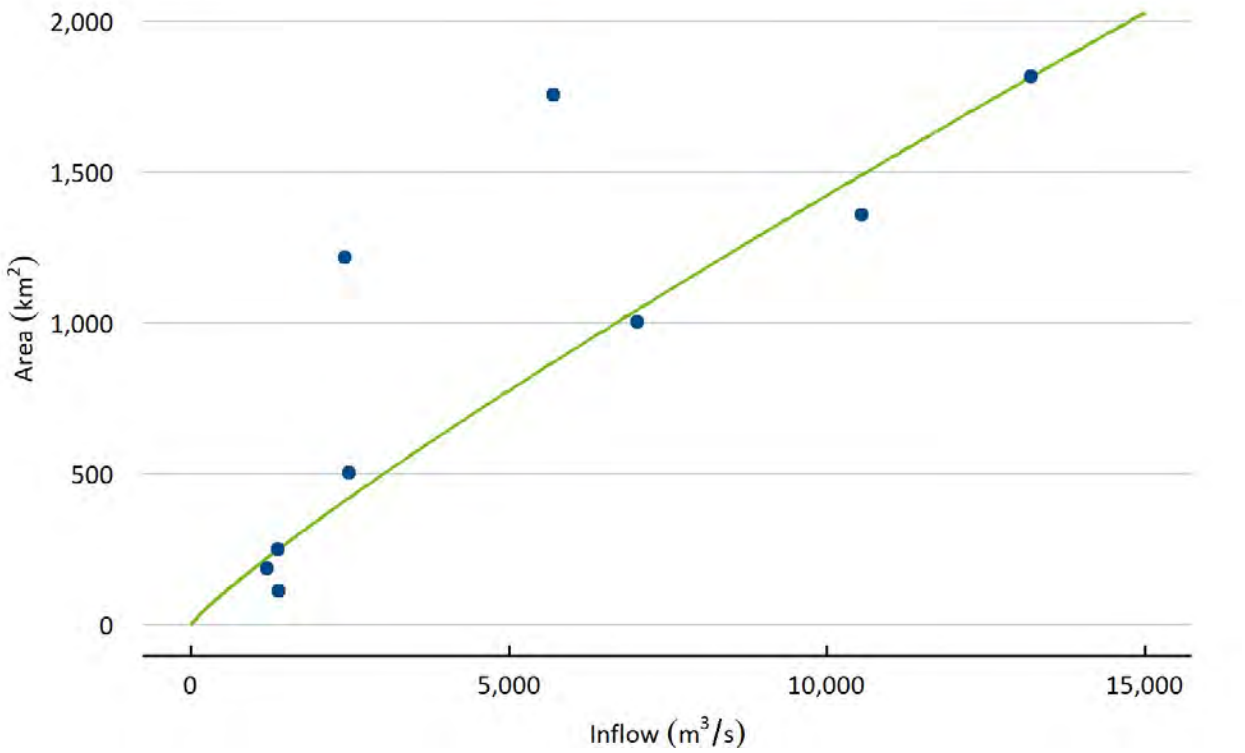

Figure 5-21 Relationship between flood discharge and inundation area for the Victoria catchment

5.5.2 ESTIMATION OF INUNDATION AREA USING THE EMULATOR

The flood emulator was applied to time-series outputs from the river model for a range of scenarios. Figure 5-22 shows the annual maximum inundation area in the period 1890 to 2022 (133 years) for various climate and development scenarios. The Scenario B (Water Harvesting of 680 GL) has little effect on maximum inundation area relative to Scenario A (Baseline), since this method relies on the use of pumps to extract water from streams. Typical pump capacities will be far lower than wet-season peak flows at all water harvesting locations. The effects of instream dams on inundation are relatively high, since dams reduce and delay peak flows by storing water during the high flows, depending upon the antecedent storage capacity of the dam. The dry climate (Cdry) scenarios exhibit large decreases in the flooded area that are related to reduced streamflow rates. Scenario D (Cdry-Dam) for dry climate and3 instream dams has the lowest distribution of the flooded area estimates of all scenarios, essentially combining the effects of the dams and of lower streamflow. It should be noted that the flood area emulator estimate for the Scenario B (Dam) for 3 instream dams) is higher than that for the Cdry scenario, which is somewhat contrary to the situation for the estimates from the two events as modelled by the hydrodynamic model (Table 5-4).

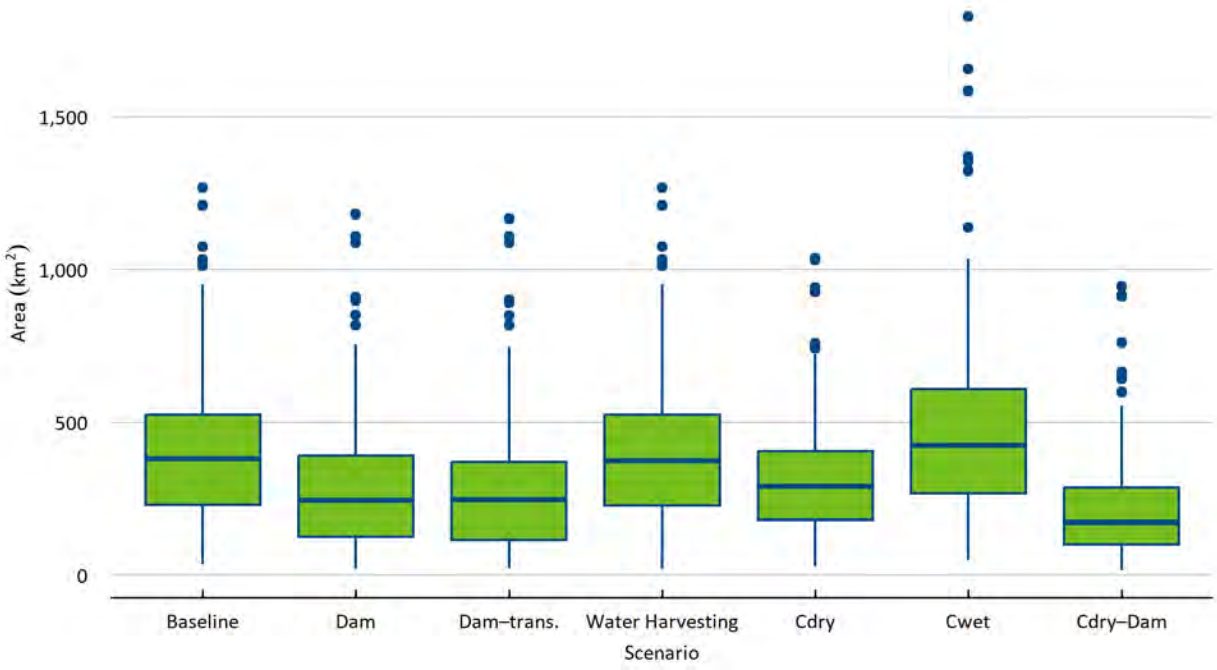

Figure 5-22 Estimated annual maximum flooded area for the various climate and development scenarios for the Victoria catchment across 133 years of simulation

Table 5-4 Emulator estimates of the flooded area for 133 years of simulation

Scenario	Mean annual maximum flooded area (km²)	Maximum flooded area (km²)
A (Baseline)	417	1269
B (Dam)	302	1180
B (Dam-transparent)	300	1167
B (Water Harvesting)	408	1269
Cdry (Dry Climate)	330	1037
Cwet (Wet Climate)	499	1829
D (Dry Climate Dam)	227	946

6 Summary

This part of the Assessment had two major components: calibration of a two-dimensional flexible-mesh hydrodynamic model (MIKE 21 FM), followed by scenario modelling under projected dry and wet future climates (Cdry and Cwet) and hypothetical developments (three instream dams and Water Harvesting). The outputs from the hydrodynamic modelling were used to:

- identify areas susceptible to seasonal flooding under the historical climate and current development scenario
- predict changes in inundation across the floodplains under future dry and wet climate scenarios
- predict how dam storages and water harvesting would alter the inundation dynamics across the floodplain
- assess the combined effects of future climate and future development scenarios (Dams and Water Harvesting) on inundation extent and depth.

Observed daily discharge and stage height data were obtained from the aquatic informatics portal of the NT Government, and tide data were obtained from the Bureau of Meteorology. A flexible-mesh floodplain hydrodynamic model was configured for the middle and lower reaches of the Victoria River and its two major tributaries, the West Baines and Angalarri rivers. Sacramento rainfall-runoff simulations and discharge data from AWRA-R simulations were used as input at the hydrodynamic model boundaries. Flood inundation maps for individual flood events were produced using satellite (Landsat, MODIS and Sentinel) imagery. Composite flood maps were also produced by combining all images to delineate the maximum flood extent in the catchment. These maps and the observed water level at two floodplain gauges (one on the West Baines River and the other on the Victoria River) were used to calibrate the hydrodynamic model. The calibrated hydrodynamic model was used to simulate the impacts of future climate and future developments on inundation extent, frequency and depth.

The hydrodynamic model was calibrated for the 2001 (AEP of 1 in 2), 2014 (AEP of 1 in 5), 2016 (AEP of 1 in 10), 2021 (AEP of 1 in 3) and 2023 (AEP of 1 in 18) flood events, and two of these flood events (2021 and 2023) were used for scenario modelling. The model was calibrated primarily by adjusting the roughness coefficient and the infiltration rate. While a good match was attained for the flood peaks, there were differences in the rising and falling limbs of the flood hydrograph. In general, model predictions were found to be more accurate for large floods.

Comparison with the Landsat, MODIS and Sentinel inundation maps revealed that the hydrodynamic model captured overall inundation patterns along the Victoria, West Baines, East Baines and Angalarri rivers. However, the detection statistics showed that the cell-to-cell matching against the observed satellite data was poor, largely due to the inability of MODIS to detect inundation of narrow floodplains. The model overpredicted inundation area, especially during a receding flood. Locations of poor fit generally coincided with complex anabranching along the West Baines and Angalarri rivers. Closer inspection of satellite imagery in these locations revealed that it often does not display flooding of these anabranches. The inability of MODIS to capture inundation in narrow floodplains has been reported in the Fitzroy catchment in WA (Karim et al.,

2011) and in other catchments in northern Australia (Ticehurst et al., 2013). Furthermore, MODIS regularly falsely identifies cloud shadow as inundation, which is particularly an issue when using imagery with high (up to 80%) cloud cover. The hydrodynamic model has some limitations, and lack of good-quality satellite images restricts rigorous calibration of the model results. Moreover, there are uncertainties in the river model simulations for inflow boundaries and locally generated runoff.

Future climate scenario modelling showed marked changes in inundation areas compared with historical climate and current development, with the major differences being observed under scenarios Cdry and Cwet. For example, the maximum inundation extent increased by 83.7% and 31.2% for the 2021 (AEP of 1 in 3) and 2023 (AEP of 1 in 18) flood events, respectively, under the Cwet scenario. For the Cdry scenario, the maximum inundation extent decreased by 13.3% and 22.8% for the 2021 and 2023 events, respectively.

The reduction in modelled maximum inundation extent under development scenarios (Dam and Water Harvesting) was variable relative to the reduction under Cdry. Under Scenario B (3 instream dams), the reductions in maximum inundation extent were 7.4% and 10%, respectively, for the 2021 and 2023 flood events. However, use of the flood area emulator across the entire river model time series indicated that the mean reduction in flooded area under the Scenario B was higher than under the Cdry scenario. Under Scenario B (Water Harvesting of 680 GL) the reduction in maximum inundation extent for the 2021 (AEP of 1 in 3) event was 6.4%, whereas it was only 2.4% for the 2023 event (AEP of 1 in 18). The flood area emulator also indicated relatively small reductions in flood area under Scenario B (Water Harvesting of 680 GL). The reductions were much higher under the combined Cdry and development scenarios. For example, the reductions were 19.0% and 17.4% for the 2021 flood event under the Cdry-Dam and Cdry-Water Harvesting scenarios, respectively. Instream dams can have a large effect on downstream hydrology, particularly lows flows, depending on dam management and how water is moved from the dam to the site of consumptive supply. One mitigation strategy to reduce potential environmental impacts are transparent releases. For transparent releases, reservoir inflows up to, but not exceeding a pre-defined threshold value are released providing some low flows that would otherwise be stored in the reservoir. For more information regarding transparent flow releases can be found in Hughes et al. (2024b).

References

Arcement GJ and Schneider VR (1989) Guide for selecting Manning's roughness coefficients for natural channels and floodplain. US Geological Survey, Virginia.

Arnell NW and Gosling SN (2016) The impacts of climate change on river flood risk at the global scale. Climatic Change 134(3), 387–401. DOI: 10.1007/s10584-014-1084-5.

Arthington AH, Godfrey PC, Pearson RG, Karim F and Wallace J (2015) Biodiversity values of remnant freshwater floodplain lagoons in agricultural catchments: evidence for fish of the Wet Tropics bioregion, northern Australia. Aquatic Conservation: Marine and Freshwater Ecosystems 25(3), 336–352. DOI: 10.1071/MF12251.

Australian Academy of Science (2021) The risks to Australia of a 3°C warmer world. Australian Academy of Science. Available online: https://www.science.org.au/files/userfiles/support/reports-and-plans/2021/risks-australia-three-deg-warmer-world-report.pdf.

Bayley PB (1991) The flood pulse advantage and the restoration of river–floodplain systems. Regulated Rivers: Research and Management 6, 75–86. DOI: 10.1002/rrr.3450060203.

Bayley PB (1995) Understanding large river floodplain ecosystems. Bioscience 45(3), 153–158. DOI: 10.2307/1312554.

Beighley RE, Eggert KG, Dunne T, He Y, Gummadi V and Verdin KL (2009) Simulating hydrologic and hydraulic processes throughout the Amazon River Basin. Hydrological Processes 23(8), 1221–1235. DOI: 10.1002/hyp.7252.

Bomers A, Schielen RMJ and Hulscher SJMH (2019) The influence of grid shape and grid size on hydraulic river modelling performance. Environmental Fluid Mechanics 19(5), 1273–1294. DOI: 10.1007/s10652-019-09670-4.

Bulti DT and Abebe BG (2020) A review of flood modeling methods for urban pluvial flood application. Modeling Earth Systems and Environment 6(3), 1293–1302. DOI: 10.1007/s40808-020-00803-z.

Bunn SE, Thoms MC, Hamilton SK and Capon SJ (2006) Flow variability in dryland rivers: boom, bust and the bits in between. River Research and Applications 22(2), 179–186. DOI: 10.1002/rra.904.

Chiew FHS, Teng J, Vaze J, Post DA, Perraud JM, Kirono DGC and Viney NR (2009) Estimating climate change impact on runoff across southeast Australia: method, results, and implications of the modeling method. Water Resources Research 45. DOI: 10.1029/2008wr007338.

Chormanski J, Miroslaw-Swiatek D and Michalowski R (2009) A hydrodynamic model coupled with GIS for flood characteristics analysis in the Biebrza riparian wetland. Oceanological and Hydrobiological Studies 38(1), 65–73. DOI: 10.2478/v10009-009-0004-x.

Chow VT (1959) Open channel hydraulics. McGraw-Hill International Edition, Singapore.

CSIRO (2009a) Water in the Fitzroy region. In: CSIRO (ed) Water in the Timor Sea Drainage Division. A report to the Australian Government from the CSIRO Northern Australia Sustainable Yields Project. CSIRO Water for a Healthy Country Flagship, Australia, 61–128.

CSIRO (2009b) Water in the Gulf of Carpentaria Drainage Division. A report to the Australian Government from the CSIRO Northern Australia Sustainable Yields Project. CSIRO Water for a Healthy Country Research Flagship, Australia.

CSIRO (2009c) Water in the Northern North-East Coast Drainage Division. A report to the Australian Government from the CSIRO Northern Australia Sustainable Yields Project. CSIRO Water for a Healthy Country Research Flagship, Australia. xxviii + 116 pp.

DHI (2012) MIKE 21 Flow Model: scientific documentation. Danish Hydraulic Institute, Denmark.

DHI (2016) MIKE 21 flow model FM, Hydrodynamic Module, User Guide. Danish Hydraulic Institute Water and Environment Pty Ltd, Hörsholm, Denmark. <https://manuals.mikepoweredbydhi.help/2017/Coast_and_Sea/MIKE_FM_HD_2D.pdf>.

Dhu T, Dunn B, Lewis B, Lymburner L, Mueller N, Telfer E, Lewis A, McIntyre A, Minchin S and Phillips C (2017) Digital earth Australia – unlocking new value from earth observation data. Big Earth Data, 1(1–2), 64–74. DOI: 10.1080/20964471.2017.1402490.

Doble RC, Crosbie RS, Smerdon BD, Peeters L and Cook FJ (2012) Groundwater recharge from overbank floods. Water Resources Research 48(9). DOI: 10.1029/2011wr011441.

Dottori F, Szewczyk W, Ciscar JC, Zhao F, Alfieri L, Hirabayashi Y, Bianchi A, Mongelli I, Frieler K, Betts RA and Feyen L (2018) Increased human and economic losses from river flooding with anthropogenic warming. Nature Climate Change 8(9), 781–786. DOI: 10.1038/s41558-018-0257-z.

Ebert EE, Janowiak JE and Kidd C (2007) Comparison of near-real-time precipitation estimates from satellite observations and numerical models. Bulletin of the American Meteorological Society 88(1), 47–64. DOI: 10.1175/BAMS-88-1-47.

Ebert EE (2009) Methods for verifying spatial forecasts, 4th International Verification Methods Workshop, Helsinki, 4-6 June 2009.

Frazier P and Page K (2009) A reach-scale remote sensing technique to relate wetland inundation to river flow. River Research and Applications 25, 836–849. DOI: 10.1002/rra.1183.

Frazier P, Page K, Louis J, Briggs S and Robertson AI (2003) Relating wetland inundation to river flow using Landsat TM data. International Journal of Remote Sensing 24(19), 3755–3770. DOI: 10.1080/0143116021000023916.

Gallant J (2019) Merging lidar with coarser DEMs for hydrodynamic modelling over large areas. In: 23rd International Congress on Modelling and Simulation. Modelling and Simulation Society of Australia and New Zealand, 1161–1166.

Gallant J, Wilson N, Dowling T, Read A and Inskeep C (2011) SRTM-derived 1 second Digital Elevation Models Version 1.0 dataset. Geoscience Australia, Canberra. https://data.gov.au/dataset/ds-ga-aac46307-fce8-449d-e044-00144fdd4fa6/details?q=.

Gallardo B, Gascon S, Gonzalez-Sanchis M, Cabezas A and Comin FA (2009) Modelling the response of floodplain aquatic assemblages across the lateral hydrological connectivity gradient. Marine and Freshwater Research 60(9), 924–935. DOI: 10.1071/mf08277.

Gladkova I, Grossberg MD, Shahriar F, Bonev G and Romanov P (2012) Quantitative Restoration for MODIS Band 6 on Aqua. IEEE Transactions on Geoscience and Remote Sensing 50(6), 2409–2416. DOI: 10.1109/Tgrs.2011.2173499.

Guerschman JP, Warren G, Byrne G, Lymburner L, Mueller N and Van-Dijk A (2011) MODIS-based standing water detection for flood and large reservoir mapping: algorithm development and applications for the Australian continent. CSIRO Water for a Healthy Country National Research Flagship Report, Canberra.

Hawker L, Uhe P, Paulo L, Sosa J, Savage J, Sampson C and Neal J (2022) A 30 m global map of elevation with forests and buildings removed. Environmental Research Letters 17(2) 024016. DOI: 10.1088/1748-9326/ac4d4f.

Heiler G, Hein T and Schiemer F (1995) Hydrological connectivity and flood pulses as the central aspects for the integrity of a river–floodplain system. Regulated Rivers: Research and Management 11, 351–361. DOI: 10.1002/rrr.3450110309.

Horritt MS and Bates PD (2002) Evaluation of 1D and 2D numerical models for predicting river flood inundation. Journal of Hydrology 268(1–4), 87–99.

Hughes J, Yang A, Marvanek S, Wang B, Gibbs M and Petheram C (2024a) River model calibration for the Victoria catchment. A technical report from the CSIRO Victoria River Water Resource Assessment for the National Water Grid. CSIRO, Australia.

Hughes J, Yang A, Wang B, Marvanek S, Gibbs M and Petheram C (2024b) River model scenario analysis for the Victoria catchment. A technical report from the CSIRO Victoria River Water Resource Assessment for the National Water Grid. CSIRO, Australia.

IPCC (2022) Climate Change 2022: Impacts, adaptation, and vulnerability. Contribution of Working Group II to the Sixth Assessment Report of the Intergovernmental Panel on Climate Change. [Pörtner HO, Roberts DC, Tignor M, Poloczanska ES, Mintenbeck K, Alegría A, Craig M, Langsdorf S, Löschke S, Möller V, Okem A and Rama B (eds)] Cambridge University Press, Cambridge, UK and New York, NY, USA. https://report.ipcc.ch/ar6/wg2/IPCC_AR6_WGII_FullReport.pdf .

Junk WJ, Bayley PB and Sparks RE (1989) The flood pulse concept in river–floodplain systems. In: Proceedings of the International Large River Symposium. Canadian Special Publications of Fisheries and Aquatic Sciences 106, 110–127. https://publications.gc.ca/site/eng/9.816457/publication.html.

Karim F, Dutta D, Marvanek S, Petheram C, Ticehurst C, Lerata J, Kim S and Yang A (2015) Assessing the impacts of climate change and dams on floodplain inundation and wetland connectivity in the wet–dry tropics of northern Australia. Journal of Hydrology 522, 80–94. DOI: 10.1016/j.jhydrol.2014.12.005.

Karim F, Kinsey-Henderson A, Wallace J, Arthington AH and Pearson RG (2012) Modelling wetland connectivity during overbank flooding in a tropical floodplain in north Queensland, Australia. Hydrological Processes 26, 2710–2723. DOI: 10.1002/hyp.8364.

Karim F, Petheram C, Marvanek S, Ticehurst C, Wallace J and Gouweleeuw B (2011) The use of hydrodynamic modelling and remote sensing to estimate floodplain inundation and flood discharge in a large tropical catchment. In: Chan F, Marinova D and Anderssen RS (eds), 19th International Congress on Modelling and Simulation. Modelling and Simulation Society of Australia and New Zealand, Perth.

Kim B, Sanders BF, Schubert JE and Famiglietti JS (2014) Mesh type tradeoffs in 2D hydrodynamic modeling of flooding with a Godunov-based flow solver. Advances in Water Resources 68, 42–61. DOI: 10.1016/j.advwatres.2014.02.013.

Kron W (2015) Flood disasters – a global perspective. Water Policy 17(S1), 6–24. DOI: 10.2166/wp.2015.001.

Kumar V, Sharma KV, Caloiero T, Mehta DJ and Singh K (2023) Comprehensive overview of flood modeling approaches: a review of recent advances. Hydrology 10(7), 141. DOI: 10.3390/hydrology10070141.

Kvocka D, Falconer RA and Bray M (2015) Appropriate model use for predicting elevations and inundation extent for extreme flood events. Natural Hazards 79(3), 1791–1808. DOI: 10.1007/s11069-015-1926-0.

Liu Q, Qin Y, Zhang Y and Li ZW (2015) A coupled 1D–2D hydrodynamic model for flood simulation in flood detention basin. Natural Hazards 75(2), 1303–1325. DOI: 10.1007/s11069-014-1373-3.

LWA (2009) An Australian handbook of stream roughness coefficients. Land and Water Australia, Canberra.

Mackay C, Suter S, Albert N, Morton S and Yamagata K (2015) Large scale flexible mesh 2D modelling of the Lower Namoi Valley. In: Floodplain Management Association National Conference. Floodplain Management Australia, 1–14.

McJannet D, Yang A and Seo L (2023) Climate data characterisation for hydrological and agricultural scenario modelling across the Victoria, Roper and Southern Gulf catchments. A technical report from the CSIRO Victoria River and Southern Gulf Water Resource Assessments for the National Water Grid. CSIRO, Australia.

Meadows M, Jones S and Reinke K (2024) Vertical accuracy assessment of freely available global DEMs (FABDEM, Copernicus DEM, NASADEM, AW3D30 and SRTM) in flood-prone environments. International Journal of Digital Earth 17(1). DOI: 10.1080/17538947.2024.2308734.

Middleton BA (2002) The flood pulse concept in wetland restoration. In: Middleton BA (ed.) Flood pulsing in wetlands: restoring the natural hydrological balance. John Wiley & Sons, Inc, USA.

Neal J, Villanueva I, Wright N, Willis T, Fewtrell T and Bates P (2012) How much physical complexity is needed to model flood inundation? Hydrological Processes 26(15), 2264–2282. DOI: 10.1002/hyp.8339.

Nicholas AP and Mitchell CA (2003) Numerical simulation of overbank processes in topographically complex floodplain environments. Hydrological Processes 17(4), 727–746. DOI: 10.1002/hyp.1162.

Nobre AD, Cuartas LA, Hodnett M, Rennó CD, Rodrigues G, Silveira A, Waterloo M and Saleska S (2011) Height Above the Nearest Drainage – a hydrologically relevant new terrain model. Journal of Hydrology 404(1–2), 13–29. DOI: 10.1016/j.jhydrol.2011.03.051.

NT Government (2023) Territory Water Plan: A plan to deliver water security for all Territorians, now and into the future. Office of Water Security. Viewed 17 September 2024, https://watersecurity.nt.gov.au/territory-water-plan#:~:text=Priority%20actions%20in%20the%20plan,and%20productivity%20in%20water%20use.

Ogden R and Thoms M (2002) The importance of inundation to floodplain soil fertility in a large semi-arid river. International Association of Theoretical and Applied Limnology, SIL Proceedings, 28(2), 744–749. DOI: 10.1080/03680770.2001.11901813.

Opperman JJ, Galloway GE, Fargione J, Mount JF, Richter BD and Secchi S (2009) Land use. Sustainable floodplains through large-scale reconnection to rivers. Science 326(5959), 1487–1488. DOI: 10.1126/science.1178256.

Otsu N (1979) A threshold selection method from gray-level histograms. IEEE Transactions on Systems, Man and Cybernetics 9(1), 62–66. DOI: 10.1109/TSMC.1979.4310076.

Overton IC (2005) Modelling floodplain inundation on a regulated river: integrating GIS, remote sensing and hydrological models. River Research and Applications 21(9), 991–1001. DOI: 10.1002/Rra.867.

Owers CJ, Lucas RM, Clewley D, Planque C, Punalekar S, Tissott B, Chua SMT, Bunting P, Mueller N and Metternicht G (2021) Implementing national standardised land cover classification systems for Earth Observation in support of sustainable development. Big Earth Data 5(3), 368–390. DOI: 10.1080/20964471.2021.1948179.

Paiva J (1997) Victoria river bridge project, Department of Defence, flood study. Department of Lands, Planning and the Environment, Water Resources Division, Northern Territory Government, Darwin. https://hdl.handle.net/10070/228234.

Peake P, Fitzsimons J, Frood D, Mitchell M, Withers N, White M and Webster R (2011) A new approach to determining environmental flow requirements: sustaining the natural values of floodplains of the southern Murray–Darling Basin. Ecological Management & Restoration 12(2), 128–137. DOI: 10.1111/j.1442-8903.2011.00581.x.

Petheram C, Watson I and Stone P (2013a) Agricultural resource assessment for the Flinders catchment. A report to the Australian Government from the CSIRO Flinders and Gilbert Agricultural Resource Assessment, part of the North Queensland Irrigated Agriculture Strategy. CSIRO Water for Healthy Country and Sustainable Agriculture flagships, Australia.

Petheram C, Watson I and Stone P (2013b) Agricultural resource assessment for the Gilbert catchment. A report to the Australian Government from the CSIRO Flinders and Gilbert Agricultural Resource Assessment, part of the North Queensland Irrigated Agriculture Strategy. CSIRO Water for Healthy Country and Sustainable Agriculture flagships, Australia.

Petheram C, Rogers L, Read A, Gallant J, Moon A, Yang A, Gonzalez D, Seo L, Marvanek S, Hughes J, Ponce Reyes R, Wilson P, Wang B, Ticehurst C and Barber M (2017) Assessment of surface water storage options in the Fitzroy, Darwin and Mitchell catchments. A technical report to

the Australian Government from the CSIRO Northern Australia Water Resource Assessment, part of the National Water Infrastructure Development Fund: Water Resource Assessments. CSIRO, Australia.

Petheram C, Bruce C, Chilcott C and Watson I (eds) (2018a) Water resource assessment for the Fitzroy catchment. A report to the Australian Government from the CSIRO Northern Australia Water Resource Assessment, part of the National Water Infrastructure Development Fund: Water Resource Assessments. CSIRO, Australia.

Petheram C, Chilcott C, Watson I and Bruce C (eds) (2018b) Water resource assessment for the Darwin catchments. A report to the Australian Government from the CSIRO Northern Australia Water Resource Assessment, part of the National Water Infrastructure Development Fund: Water Resource Assessments. CSIRO, Australia.

Petheram C, Watson I, Bruce C and Chilcott C (eds) (2018c) Water resource assessment for the Mitchell catchment. A report to the Australian Government from the CSIRO Northern Australia Water Resource Assessment, part of the National Water Infrastructure Development Fund: Water Resource Assessments. CSIRO, Australia.

Phelps QE, Tripp SJ, Herzog DP and Garvey JE (2015) Temporary connectivity: the relative benefits of large river floodplain inundation in the lower Mississippi River. Restoration Ecology 23(1), 53–56. DOI: 10.1111/rec.12119.

Pinos J and Timbe L (2019) Performance assessment of two-dimensional hydraulic models for generation of flood inundation maps in mountain river basins. Water Science and Engineering 12(1), 11–18. DOI: 10.1016/j.wse.2019.03.001.

Power and Water Authority (1987) Baseflow water quality surveys in the Northern Territory. Volume 5, Fitzmaurice and Victoria Rivers. Report 10/1987. Water Quality Section, Water Resources Group. Northern Territory Power and Water Authority, Darwin.

Rice M, Hughes L, Steffen W, Bradshaw S, Bambrick H, Hutley N, Arndt D, Dean A and Morgan W (2022) A supercharged climate: rain bombs, flash flooding and destruction. Canberra. https://www.climatecouncil.org.au/wp-content/uploads/2022/03/Final_Embargoed-Copy_Flooding-A-Supercharged-Climate_Climate-Council_ILedit_220310.pdf.

Sanders BF (2007) Evaluation of on-line DEMs for flood inundation modeling. Advances in Water Resources 30(8), 1831–1843. DOI: 10.1016/j.advwatres.2007.02.005.

Schumann G, Bates PD, Horritt MS, Matgen P and Pappenberger F (2009) Progress in integration of remote sensing–derived flood extent and stage data and hydraulic models. Reviews of Geophysics 47(4). DOI: 10.1029/2008rg000274.

Shaikh M, Green D and Cross H (2001) A remote sensing approach to determine environmental flows for wetlands of the Lower Darling River, New South Wales, Australia. International Journal of Remote Sensing 22(9), 1737–1751. DOI: 10.1080/01431160118063.

Sims N, Anstee J, Barron O, Botha E, Lehmann E, Li L, McVicar T, Paget M, Ticehurst C, Van-Niel T and Warren G (2016) Earth observation remote sensing: a technical report to the Australian Government from the CSIRO Northern Australia Water Resource Assessment. CSIRO, Canberra.

Symonds AM, Vijverberg T, Post S, van der Spek B, Henrotte J and Sokolewicz M (2016) Comparison between Mike 21 FM, Delft3D and Delft3D FM flow models of Western Port Bay, Australia. Lynett P (ed.) Proceedings of the 35th International Conference on Coastal Engineering. ICCE, Turkey.

Tabari H (2020) Climate change impact on flood and extreme precipitation increases with water availability. Scientific Reports 10(1), 13,768. DOI: 10.1038/s41598-020-70816-2.

Teng J, Jakeman AJ, Vaze J, Croke BFW, Dutta D and Kim S (2017) Flood inundation modelling: a review of methods, recent advances and uncertainty analysis. Environmental Modelling & Software 90, 201–216. DOI: 10.1016/j.envsoft.2017.01.006.

Thoms MC (2003) Floodplain–river ecosystems: lateral connections and the implications of human interference. Geomorphology 56(3–4), 335–349. DOI: 10.1016/S0169-555x(03)00160-0.

Ticehurst C, Dutta D, Karim F, Petheram C and Guerschman JP (2015) Improving the accuracy of daily MODIS OWL flood inundation mapping using hydrodynamic modelling. Natural Hazards 78(2), 803–820. DOI: 10.1007/s11069-015-1743-5.

Ticehurst CJ, Chen Y, Karim F, Dutta D and Gouweleeuw B (2013) Using MODIS for mapping flood events for use in hydrological and hydrodynamic models: experiences so far. In: International Congress on Modelling and Simulation. Modelling and Simulation Society of Australia and New Zealand, 1721–1727.

Tockner K, Bunn SE, Quinn G, Naiman R, Stanford JA and Gordon C (2008) Floodplains: critically threatened ecosystems. In: Polunin NC (ed.) Aquatic ecosystems. Cambridge University Press, Cambridge, UK, 45–61.

Tockner K, Lorang MS and Stanford JA (2010) River flood plains are model ecosystems to test general hydrogeomorphic and ecological concepts. River Research and Applications 26(1), 76–86. DOI: 10.1002/rra.1328.

Townsend PA and Walsh SJ (1998) Modeling floodplain inundation using an integrated GIS with radar and optical remote sensing. Geomorphology 21(3–4), 295–312.

Tuteja NK and Shaikh M (2009) Hydraulic modelling of the spatio-temporal flood inundation patterns of the Koondrook Perricoota Forest Wetlands – The Living Murray. In: 18th World IMACS, MODSIM Congress. Modelling and Simulation Society of Australia and New Zealand, 4248–4254.

Ulubasoglu MA, Rahman MH, Onder YK, Chen Y and Rajabifard A (2019) Floods, bushfires and sectoral economic output in Australia, 1978–2014. Economic Record 95(308), 58–80. DOI: 10.1111/1475-4932.12446.

US Army Corps of Engineers (2016) HEC-RAS River Analysis Svstem: User's Manual. US Army Corps of Engineers, Hydrologic Engineering Center, Davis, California. https://www.hec.usace.army.mil/confluence/rasdocs/rasum/latest/introduction-to-hec-ras.

Wang ZC and Gao ZQ (2022) Dynamic monitoring of flood disaster based on remote sensing data cube. Natural Hazards 114(3), 3123–3138. DOI: 10.1007/s11069-022-05508-3.

Xu HQ (2006) Modification of normalised difference water index (NDWI) to enhance open water features in remotely sensed imagery. International Journal of Remote Sensing 27(14), 3025–3033. DOI: 10.1080/01431160600589179.

Yang A, Petheram C, Marvanek S, Baynes F, Rogers L, Ponce Reyes R, Zund P, Seo L, Hughes J, Gibbs M, Wilson PR, Philip S and Barber M (2024) Assessment of surface water storage options in the Victoria and Southern Gulf catchments. A technical report from the CSIRO Victoria River and Southern Gulf Water Resource Assessments for the National Water Grid. CSIRO Australia

Yu Q, Wang YY and Li N (2022) Extreme flood disasters: comprehensive impact and assessment. Water 14(8), 1211. DOI: 10.3390/w14081211.

Page deliberately left blank

As Australia's national science agency and innovation catalyst, CSIRO is solving the greatest challenges through innovative science and technology.

CSIRO. Unlocking a better future for everyone.

Contact us

1300 363 400
+61 3 9545 2176
csiroenquiries@csiro.au
csiro.au

For further information

Environment
Dr Chris Chilcott
+61 8 8944 8422
chris.chilcott@csiro.au

Environment
Dr Cuan Petheram
+61 467 816 558
cuan.petheram@csiro.au

Agriculture and Food
Dr Ian Watson
+61 7 4753 8606
Ian.watson@csiro.au